Impact of inductors saturation on EMI

N.Femia

Professor of Power Electronics

University of Salerno

President of IPERA S.r.l.

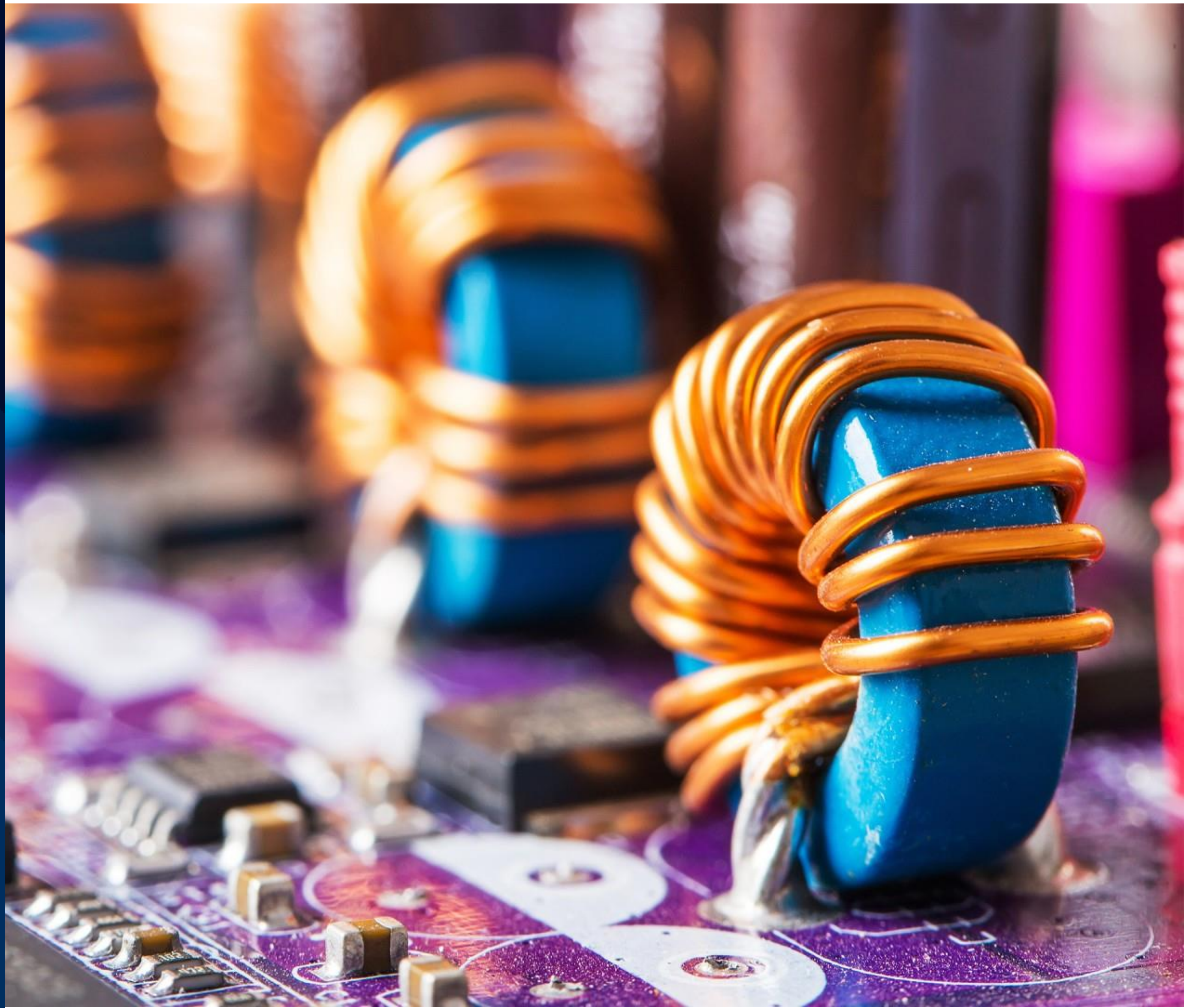

Webinar 1 (Power): conclusions

- power inductors inductance and DC and AC power losses can be easily measured by means of an oscilloscope
- power inductors saturation does not cause ripple increase, losses increase and thermal instability, provided that the inductor is intelligently chosen
- saturating inductors may outperform non-saturating inductors

Webinar 2 (Control): conclusions

- the effects of power inductors saturation on the operation and performance of SMPS control can be mathematically predicted
- SMPS control techniques sensitive to inductors saturation, like hysteretic and peak-current mode, do not undergo performance degradation or instability issues if the saturating inductor is selected and validated under the worst-case OCP, OVP, and UVP conditions
- (de)saturating inductors allow size/weight and switching loss reduction compared to non-(de)saturating inductors

Webinar 3 (EMI): questions

- Can saturable inductors cause EMI issues?
- Can saturable inductors be used in EMI filters design?
- Can saturable inductors provide benefits in EMI reduction?

power inductor = SMPS core

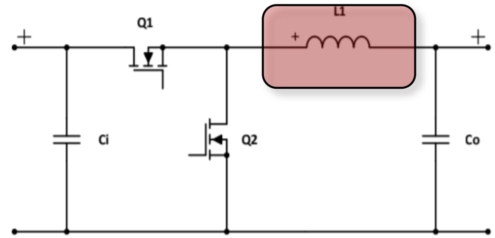

buck

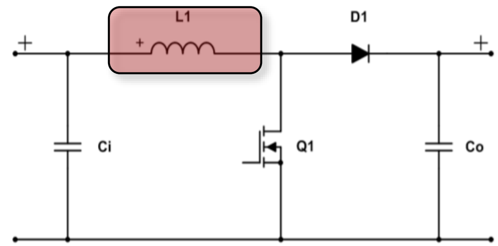

boost

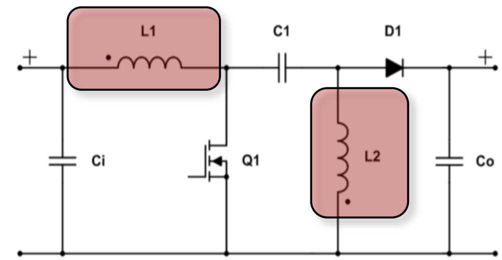

SEPIC

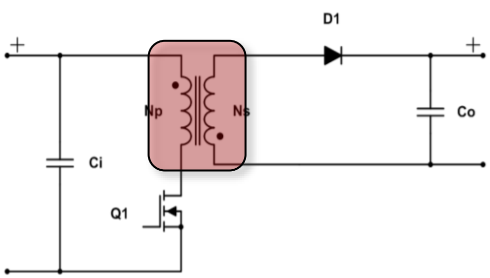

flyback

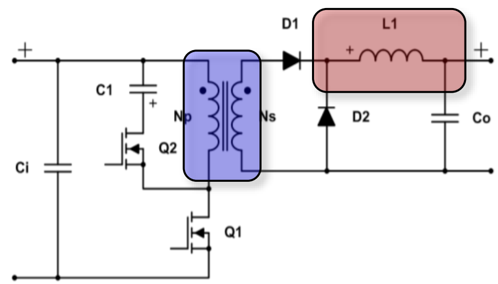

forward

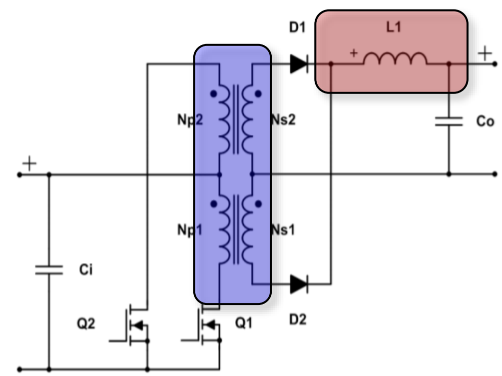

push-pull

reminder: sustainable saturation operation

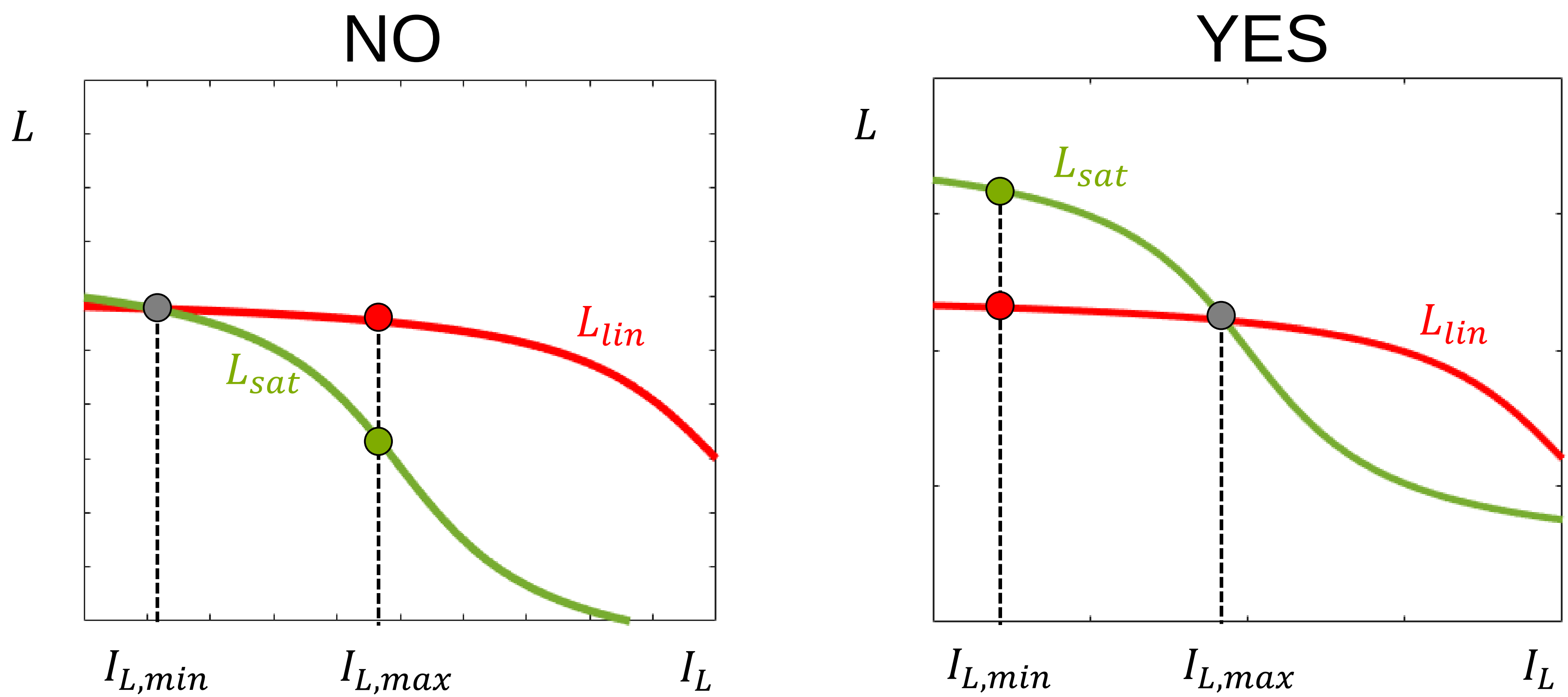

$I_{L,max}$ = DC inductor current under worst-case operating conditions (OCP, UVP, OVP, T_{amax})

$$P_{L@I_{L,max}} < P_{max}, \; T_{core@I_{L,max}} < T_{max}$$

EMI

SMPS design

the good job

EMC certificate

EMI measurements

hardware prototype

design validation

PCB layout design

system design

design decisions

problems analysis

design specifications

the bad job

EMC certificate

EMI measurements

hardware prototype

design validation

PCB layout design

system design

design decisions

problems analysis

design specifications

EMI issues

- EMC regulations
- conducted and radiated EMI
- measurement setup
- noise analysis and understanding
  - sources
  - mechanisms
  - paths
  - boosters
  - mixing

EMI in power converters

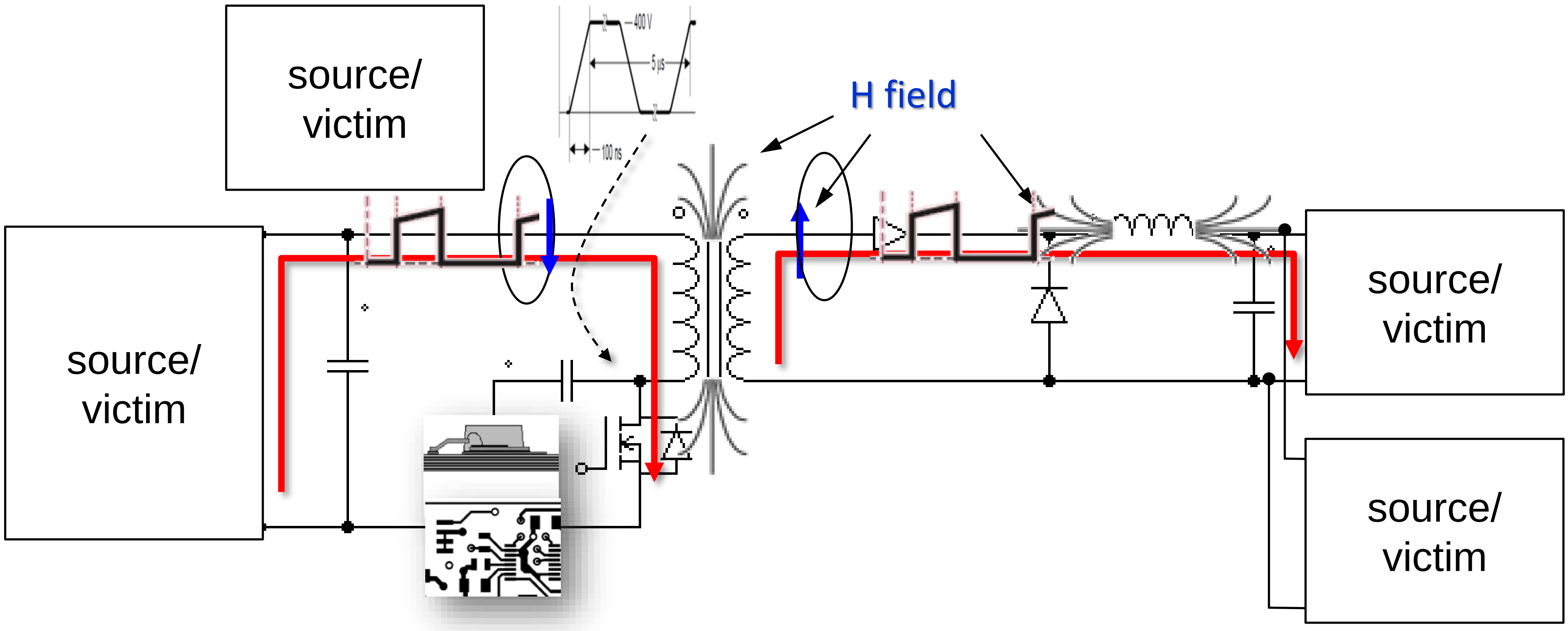

EMI spectrum in power converters

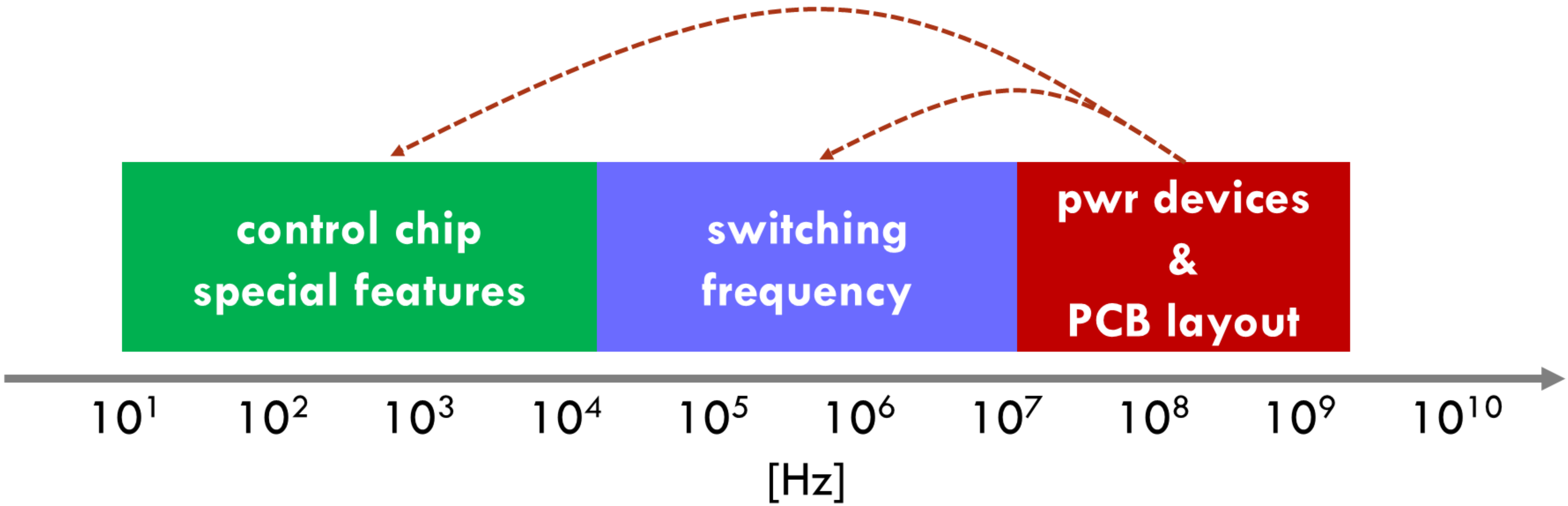

CM-DM conducted EMI

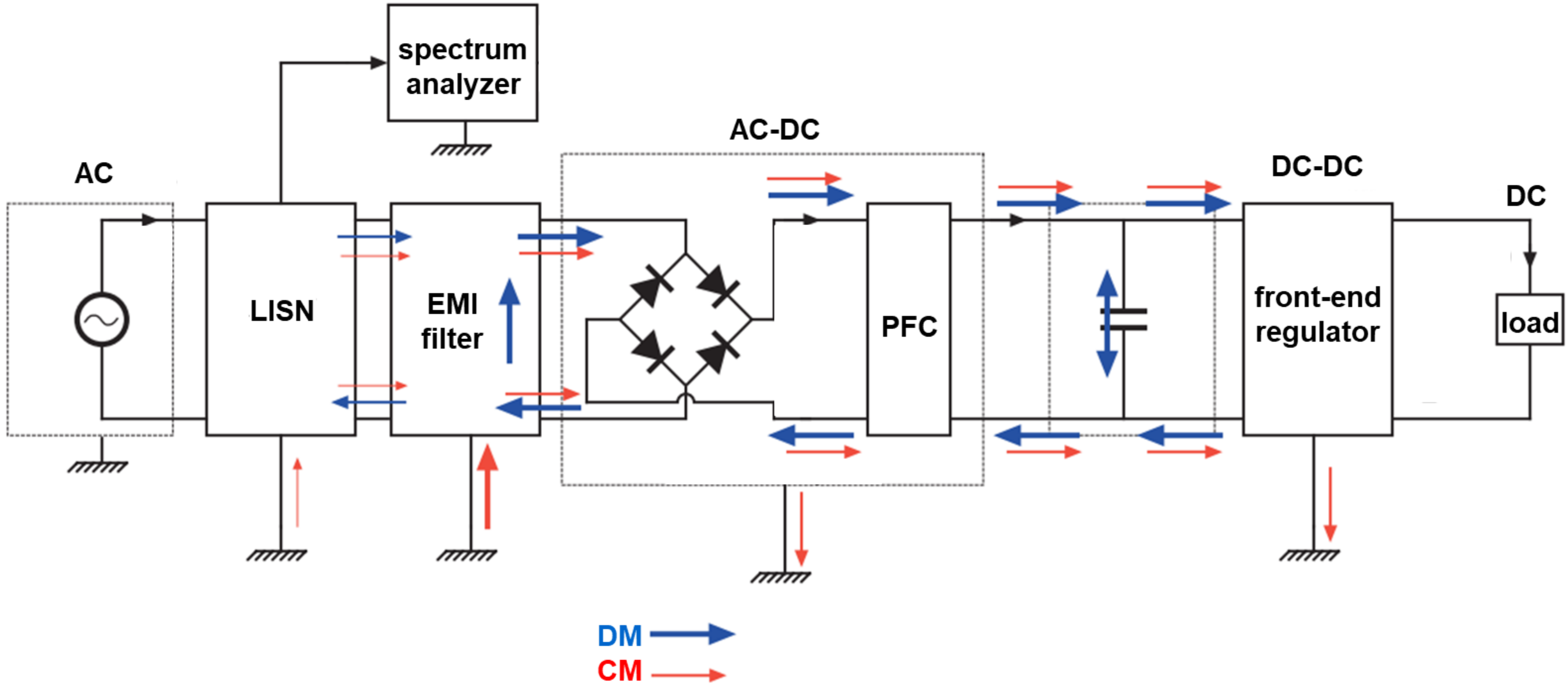

Input Noise

boost regulator

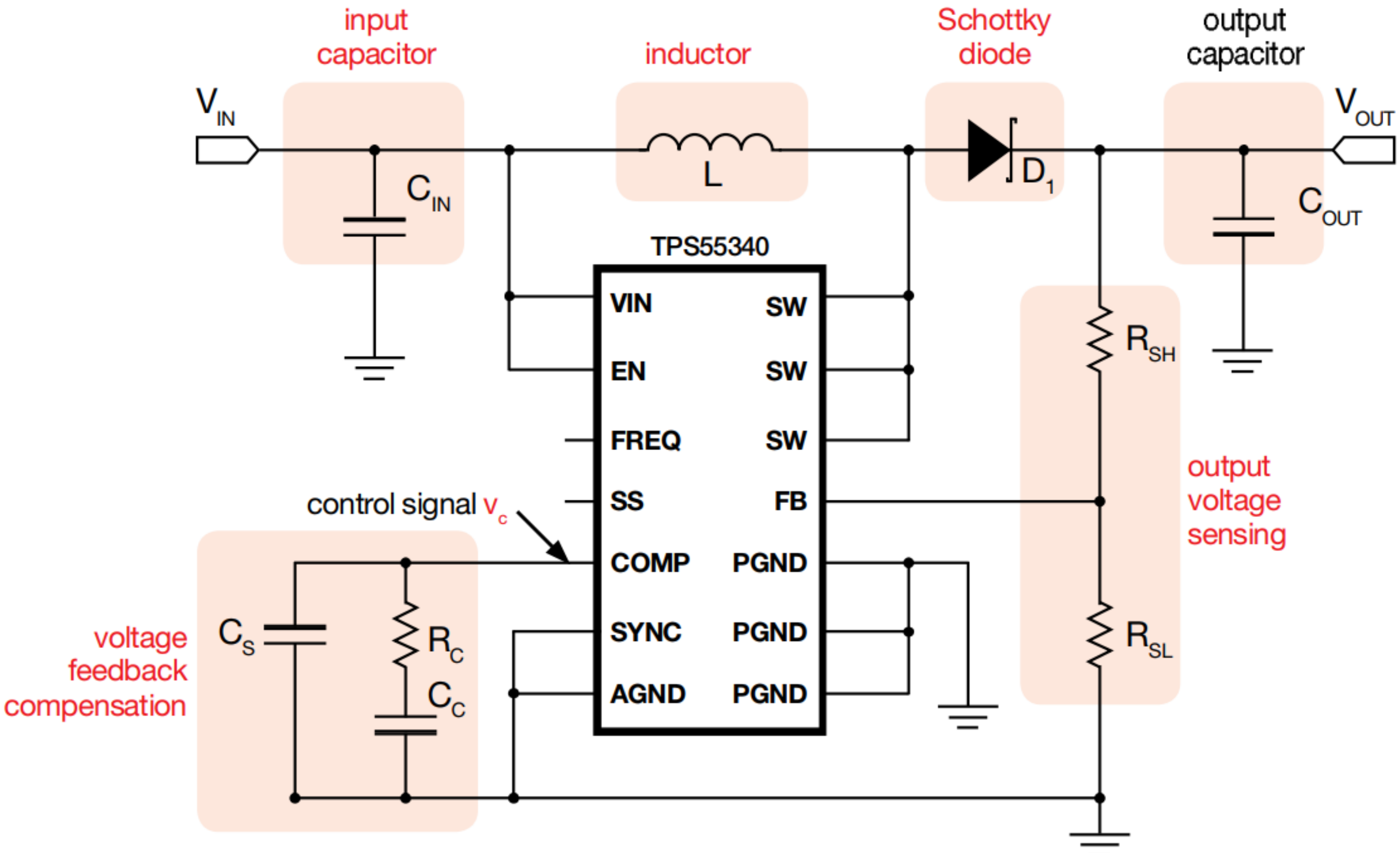

power converters testing tools

https://university.ti.com/en/faculty/teaching-materials-and-classroom-resources/ti-based-teaching-kits-for-analog-and-power-design/power-management-lab-kit-series

TI-PMLK BOOST

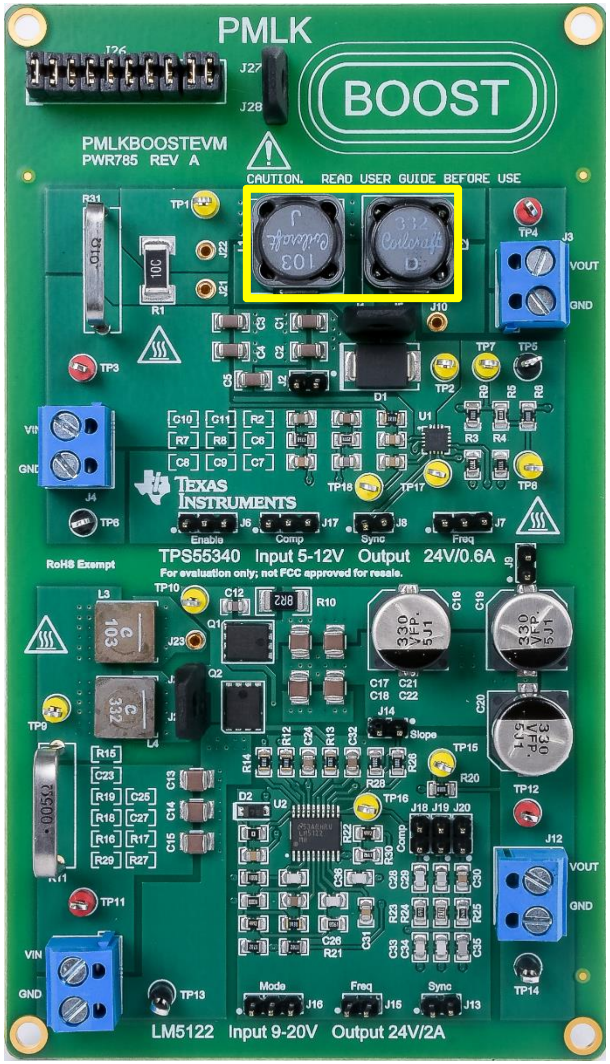

V_{in}=[5,12] V, V_{out}= 24 V , I_{out}=0.6 A, f_s= 300/600 kHz

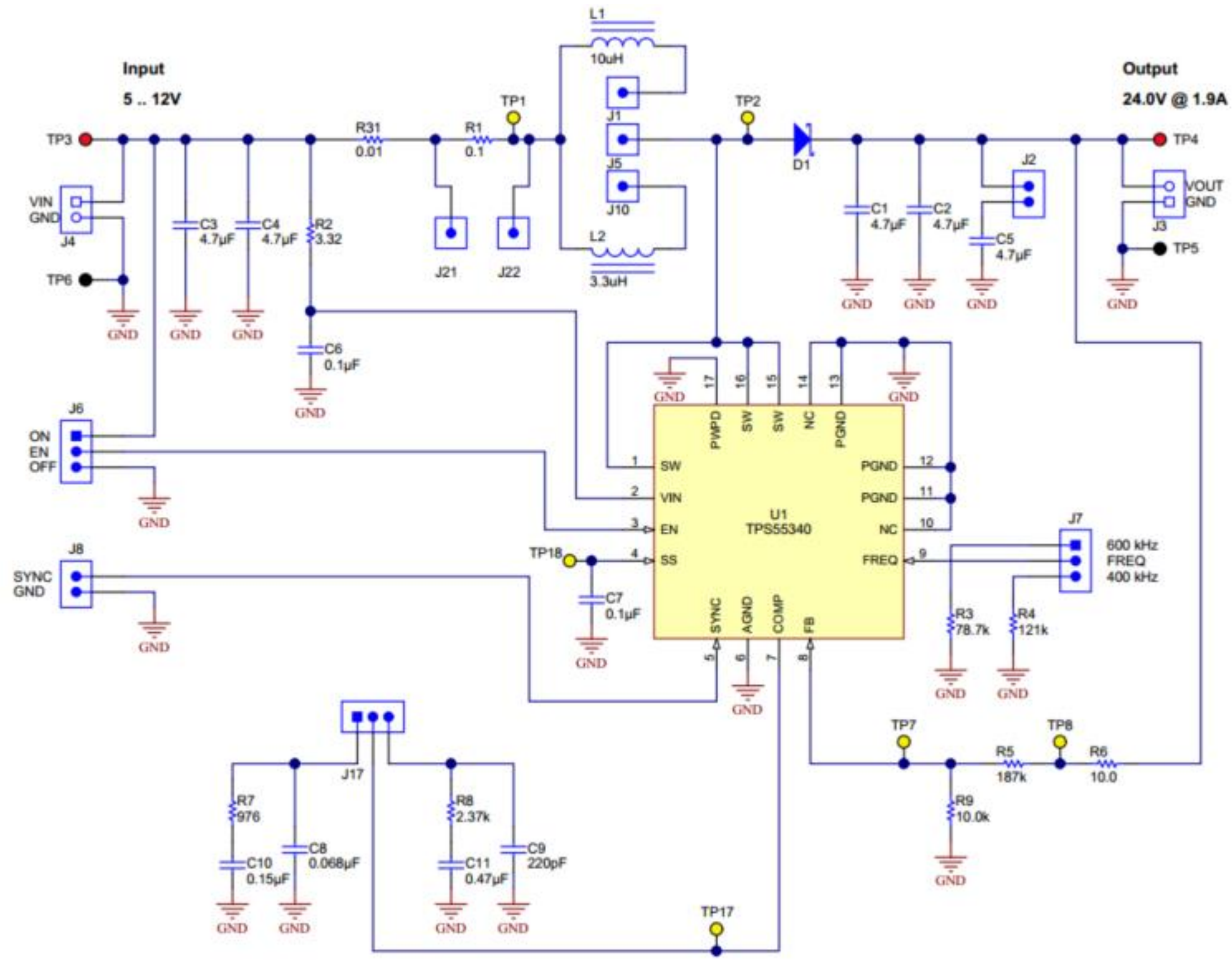

ROHDE&SCHWARZ

TI-PMLK BOOST: de-saturating vs linear inductor test

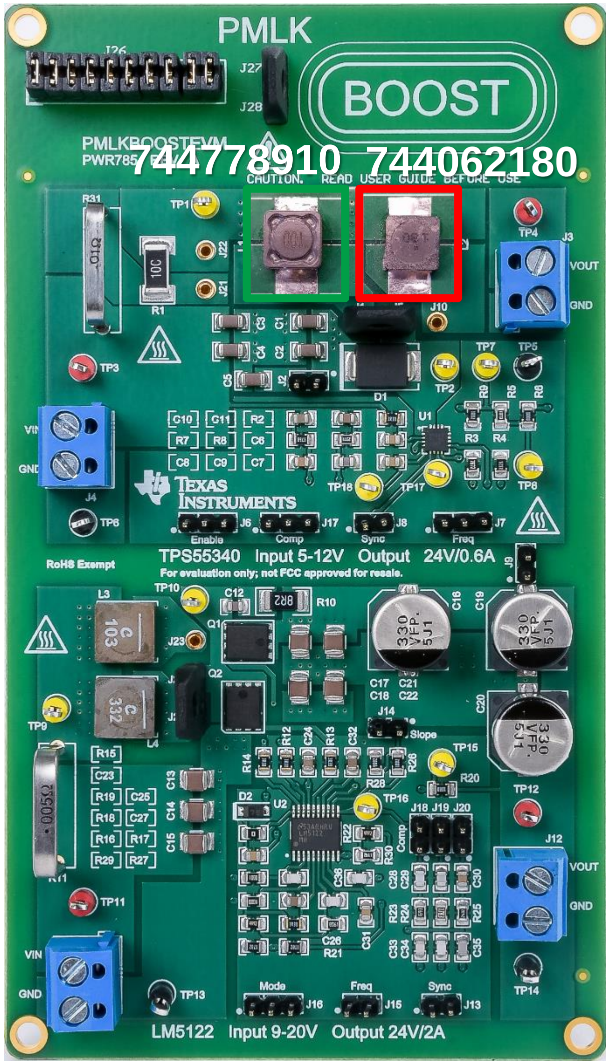

V_{in}= 10 V, V_{out}= 24 V , I_{out}= 0.4/0.2 A, f_s= 300 kHz

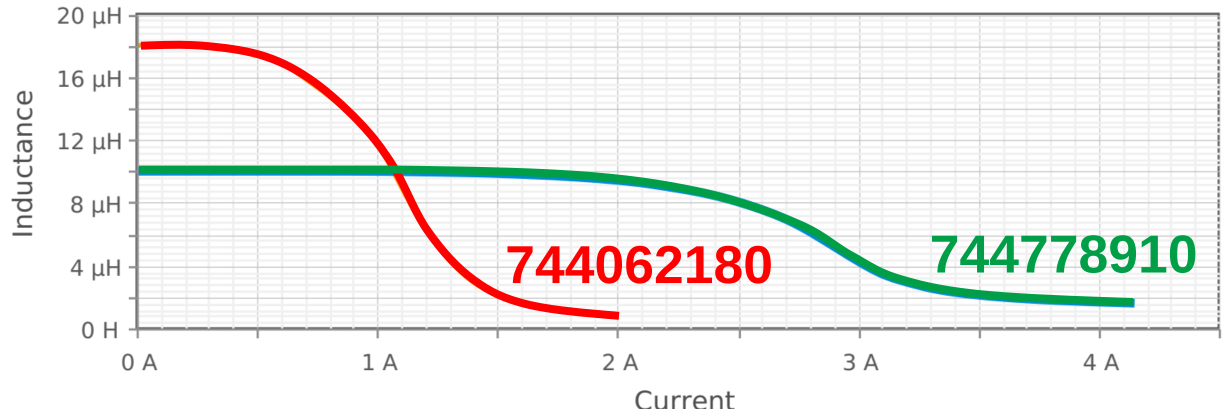

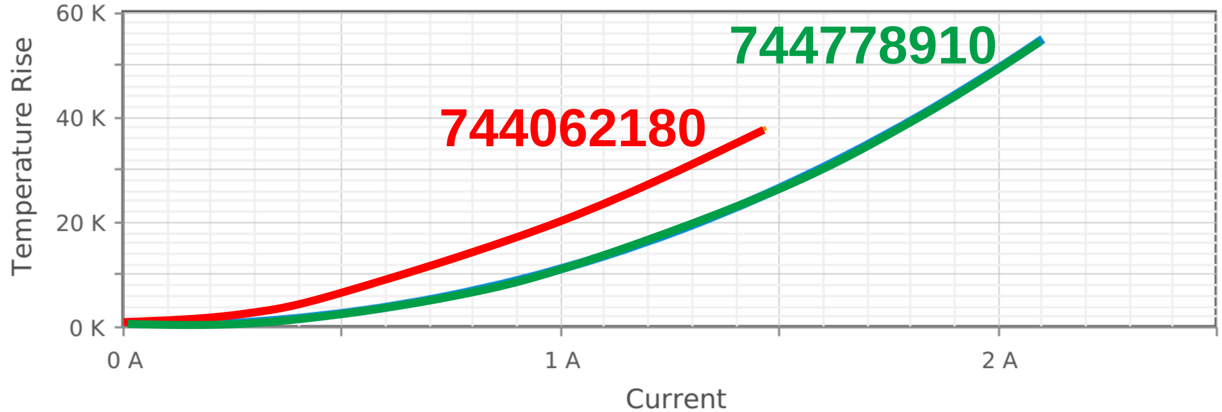

part code	L [uH]	R [mΩ]	Isat [A]	H [mm]	L [mm]	W [mm]	FP [mm²]	Vol. [mm³]
744062180	18	90	1	2.3	7	7	49	113
744778910	10	64	2.2	3.2	7.6	7.6	58	185

TI-PMLK BOOST: test setup

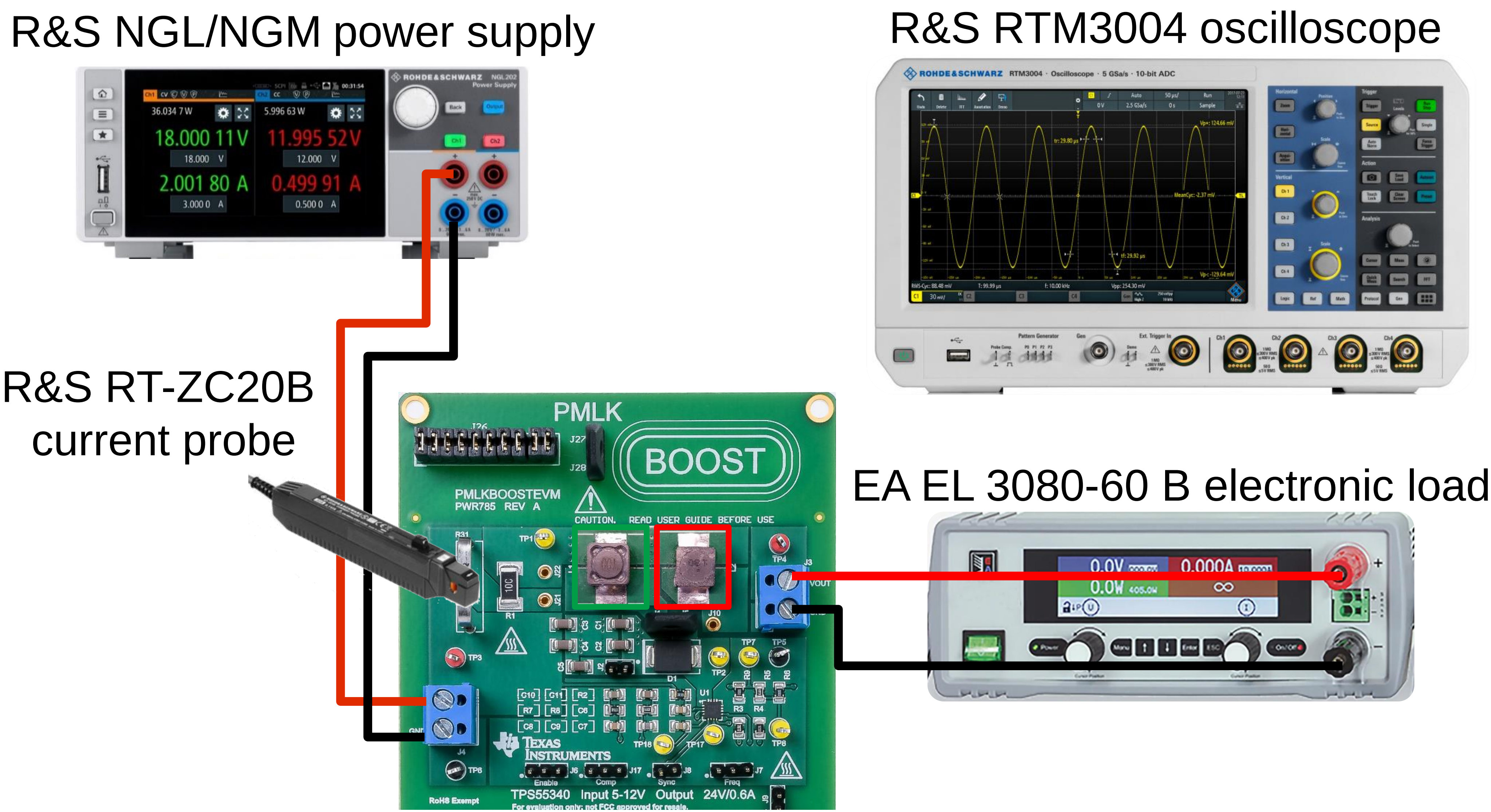

TI-PMLK BOOST: high-current waveforms

V_{in}10V, V_{out}= 24 V , I_{out}=0.4 A, f_s= 300 kHz

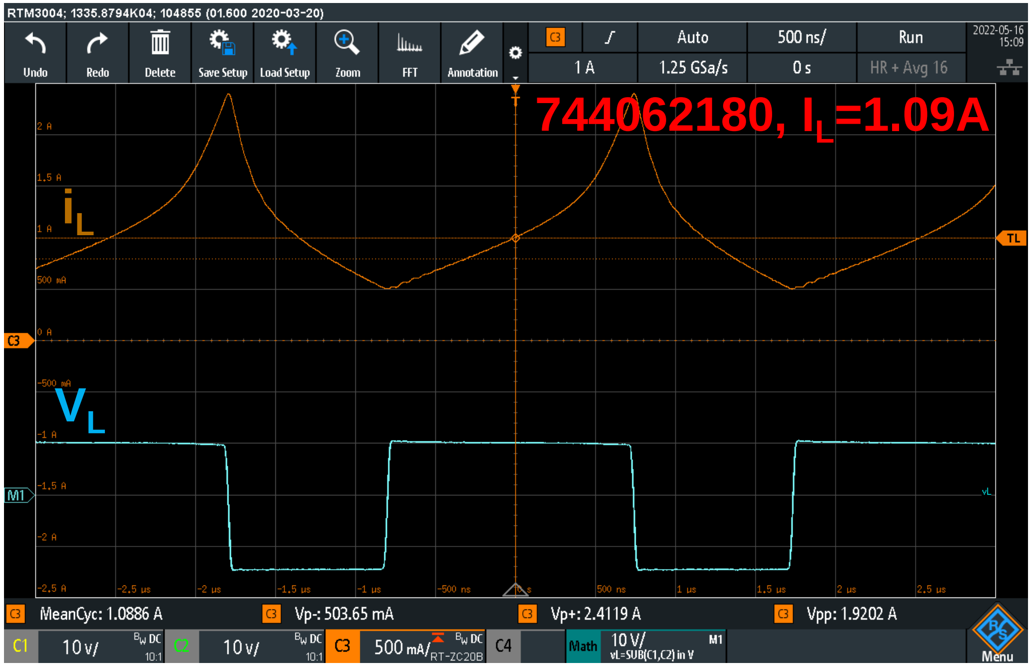

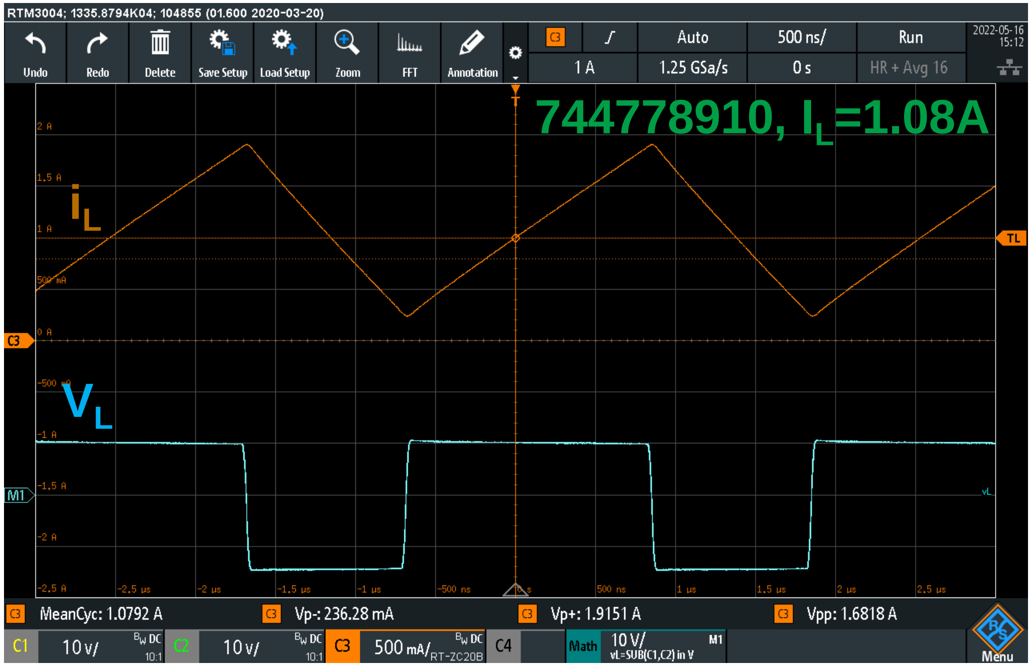

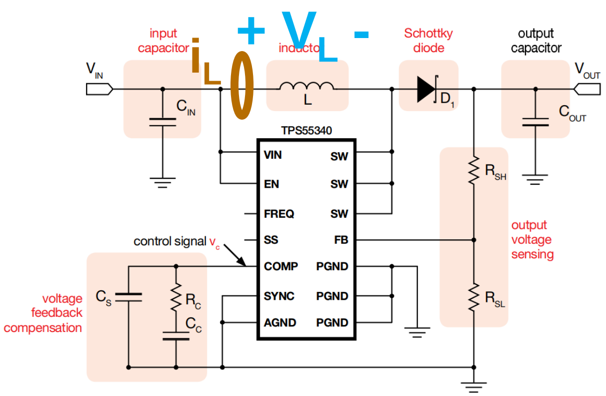

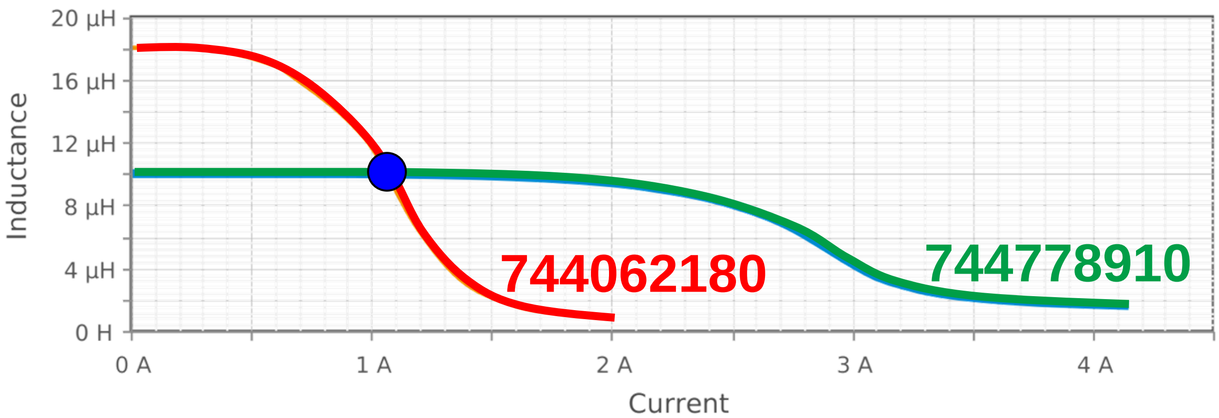

TI-PMLK BOOST: high-current current spectrum

V_{in}10V, V_{out}= 24 V , I_{out}=0.4 A, f_s= 300 kHz

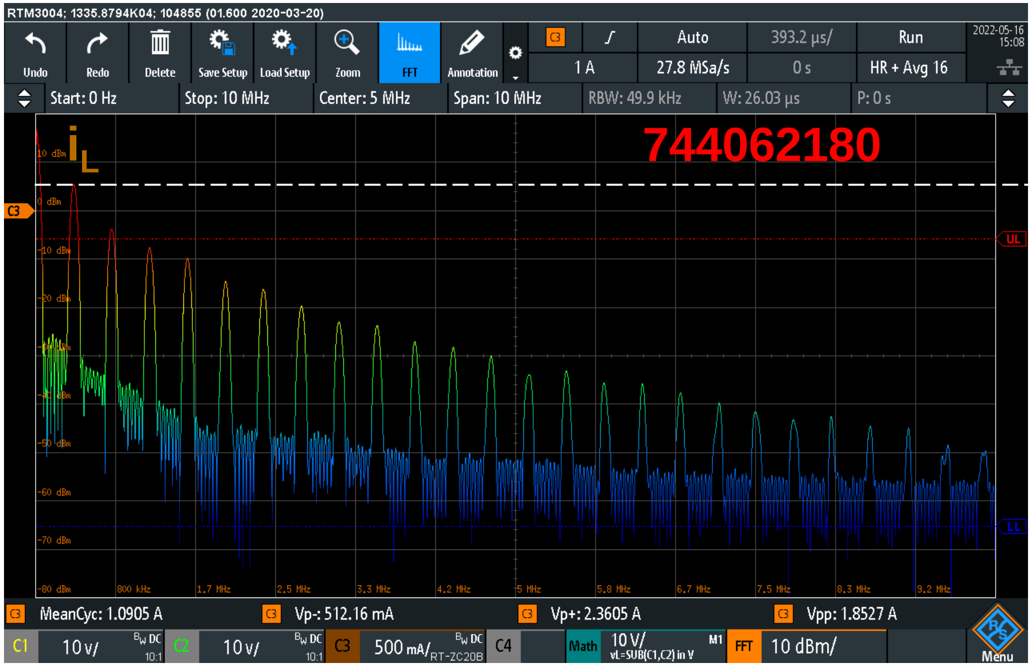

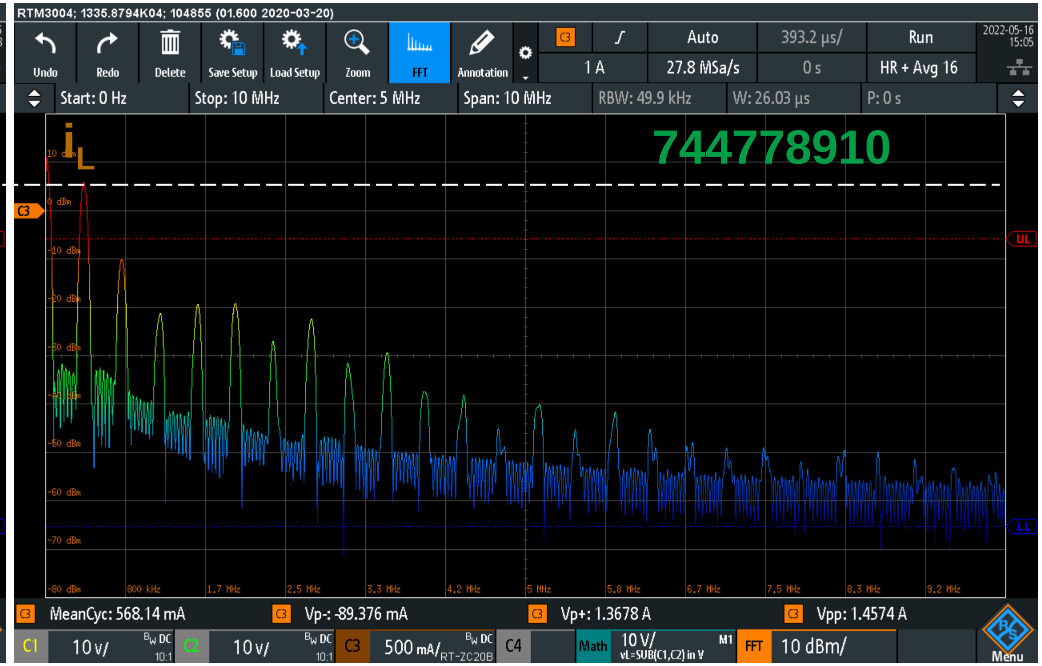

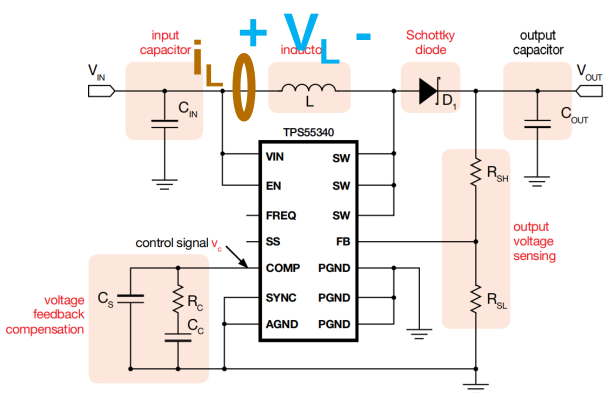

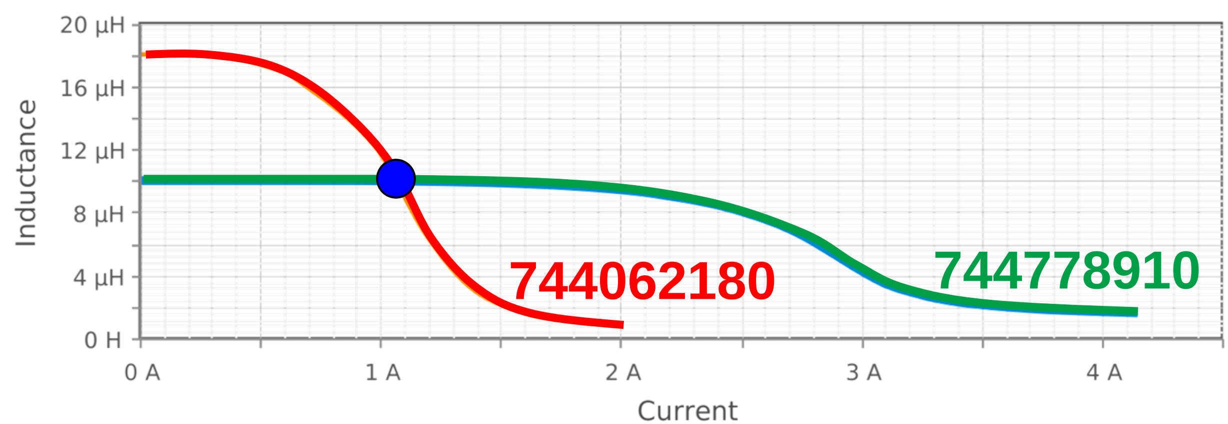

TI-PMLK BOOST: high-current voltage spectrum

V_{in}10V, V_{out}= 24 V , I_{out}=0.4 A, f_s= 300 kHz

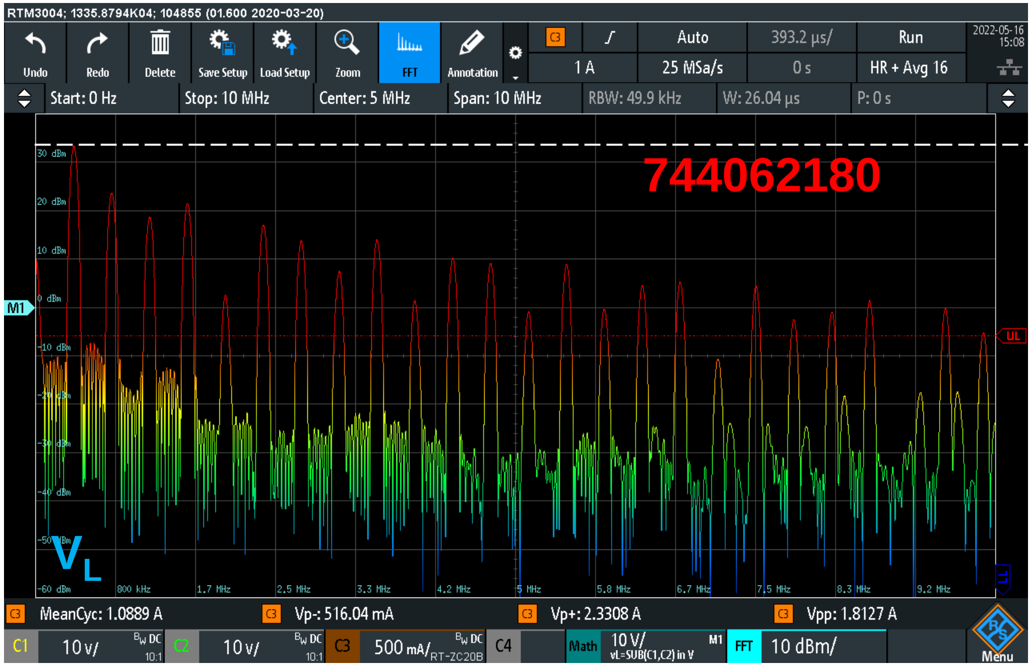

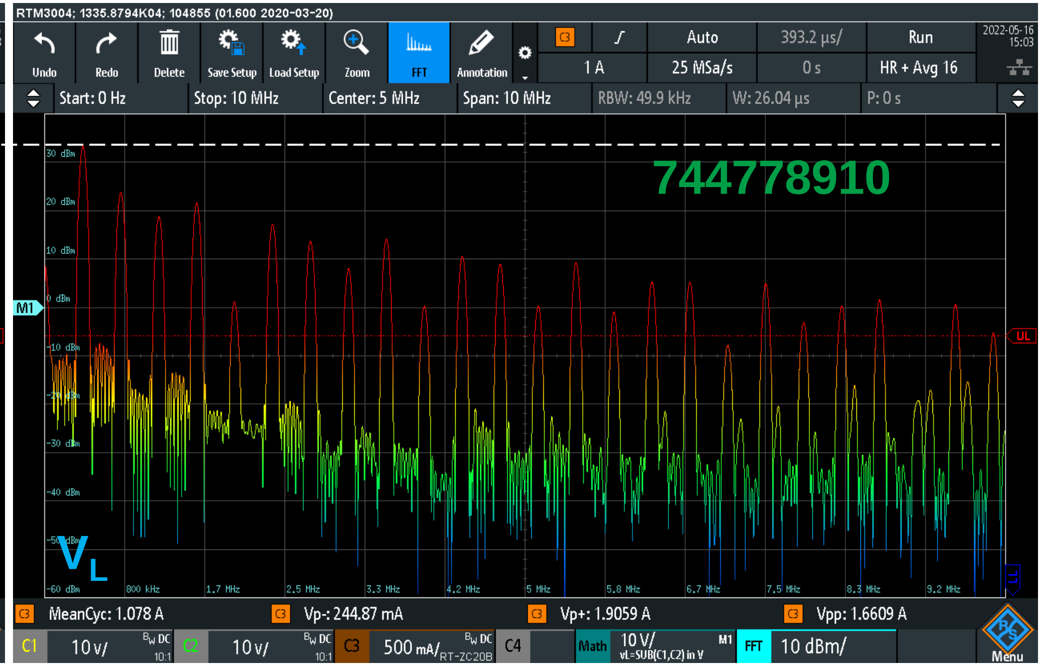

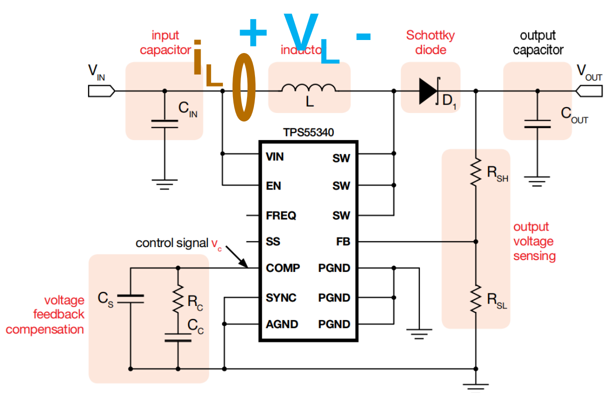

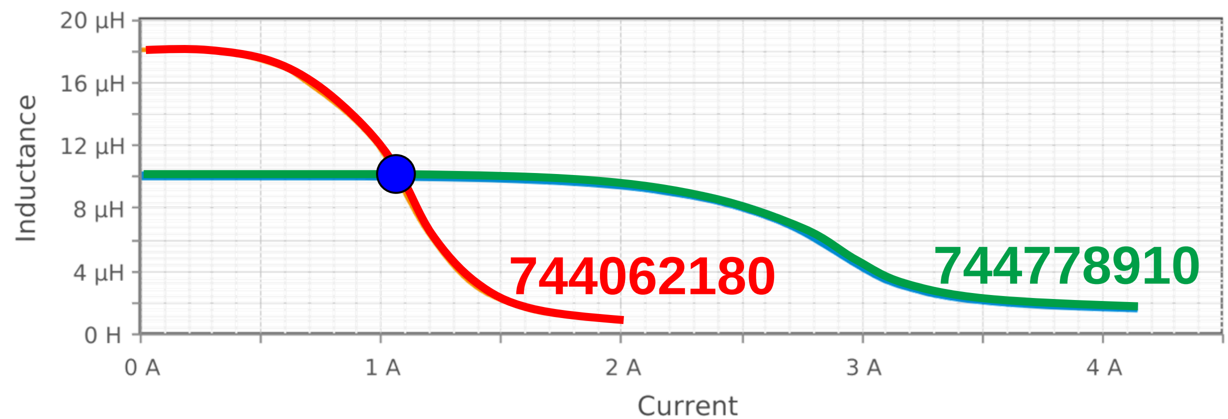

TI-PMLK BOOST: low-current waveforms

V_{in}10V, V_{out}= 24 V , I_{out}=0.2 A, f_s= 300 kHz

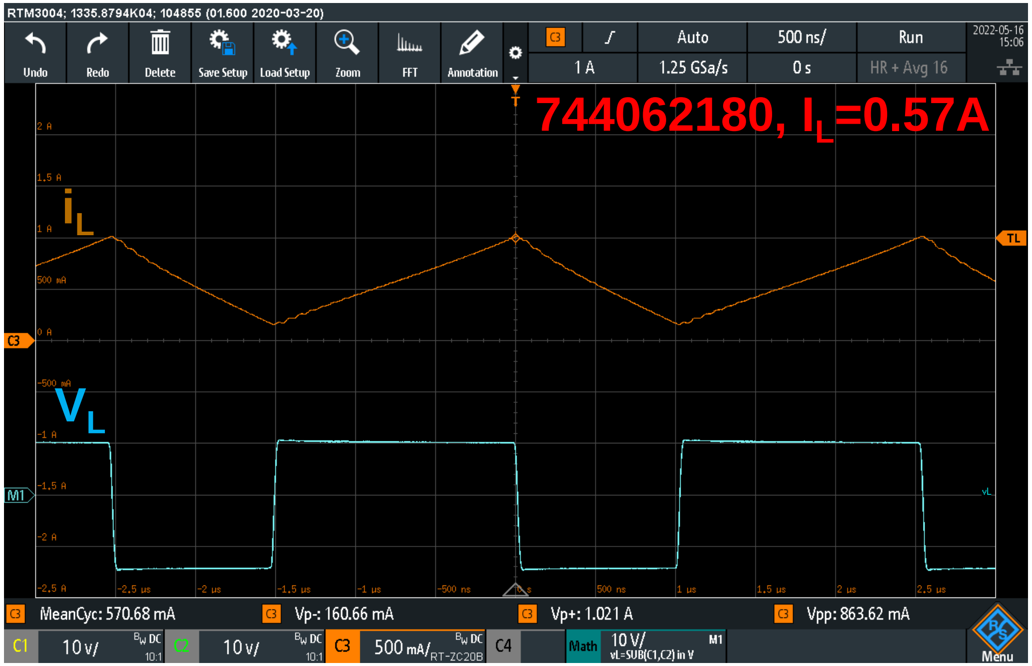

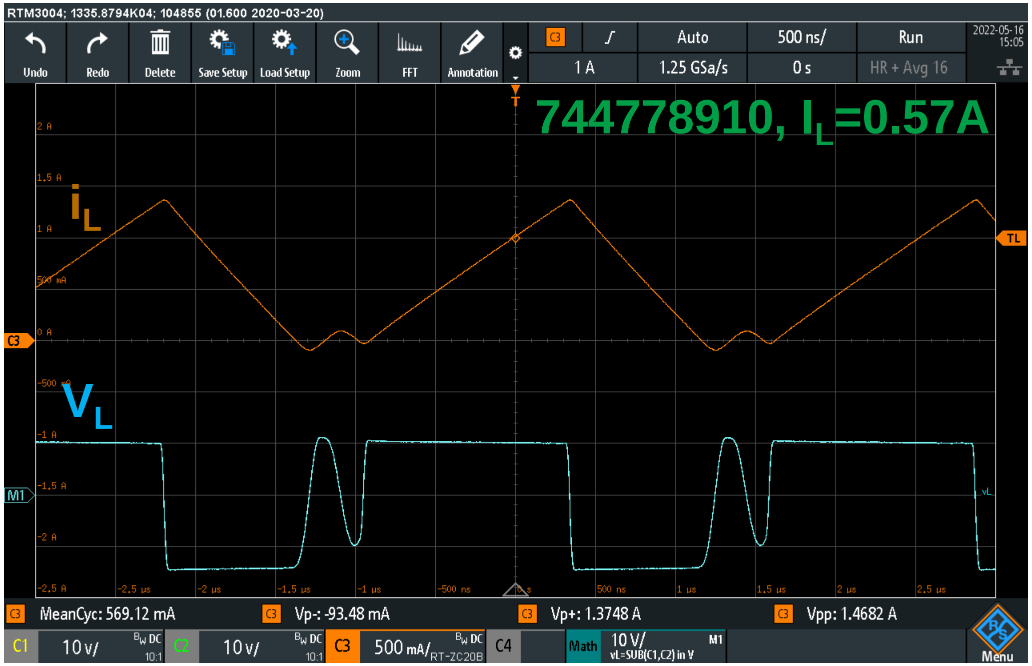

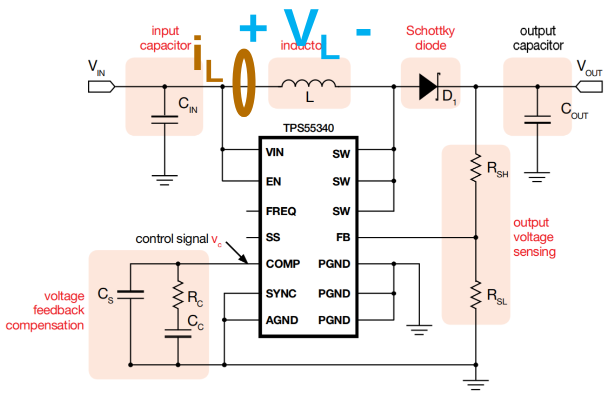

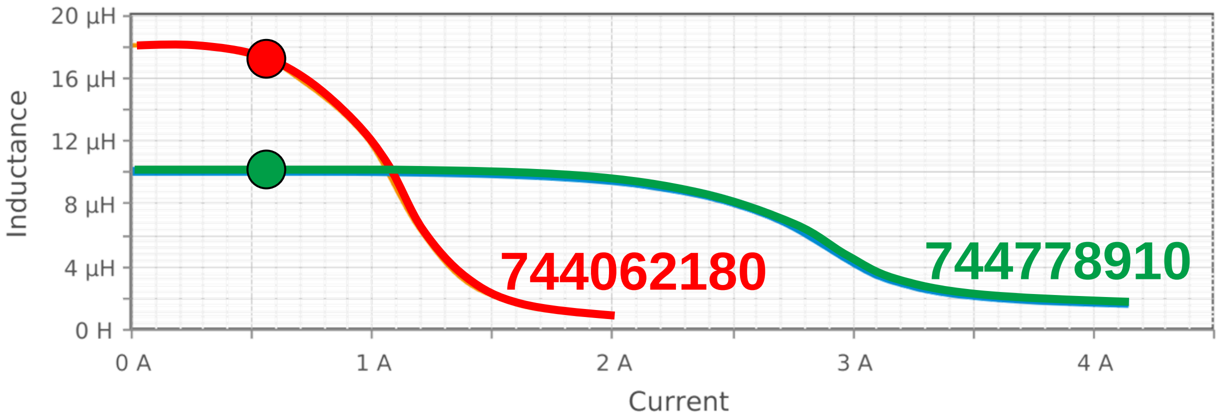

TI-PMLK BOOST: low-current current spectrum

V_{in}10V, V_{out}= 24 V , I_{out}=0.2 A, f_s= 300 kHz

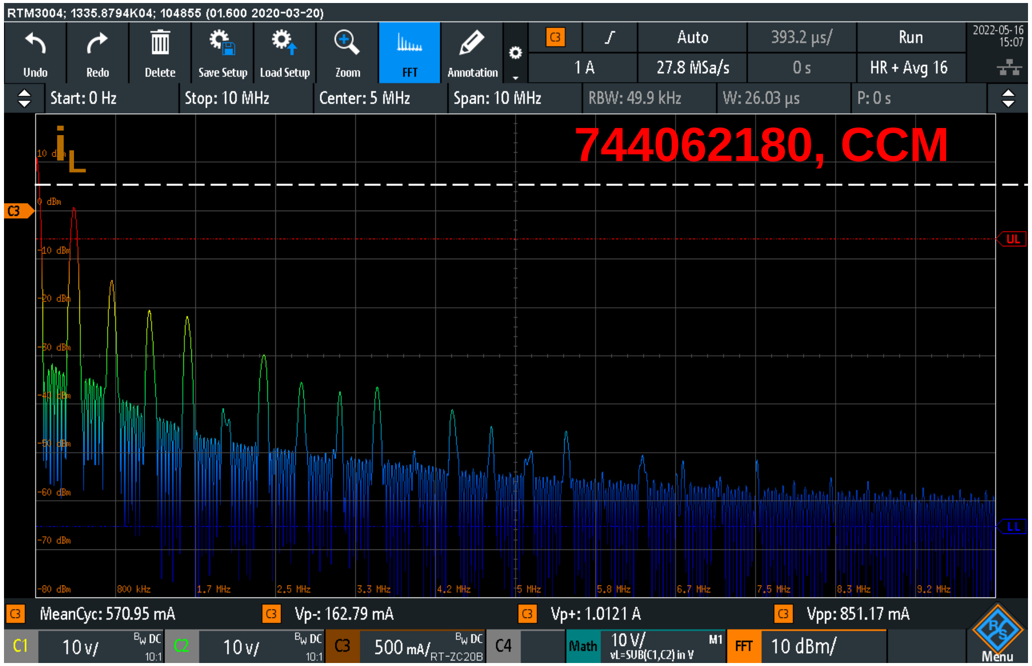

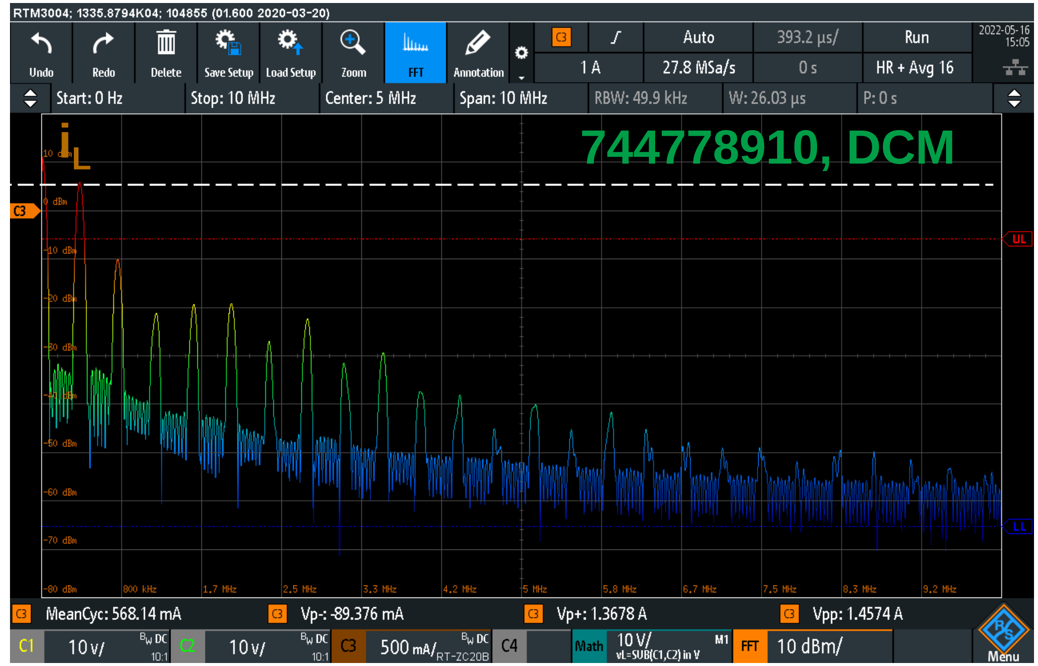

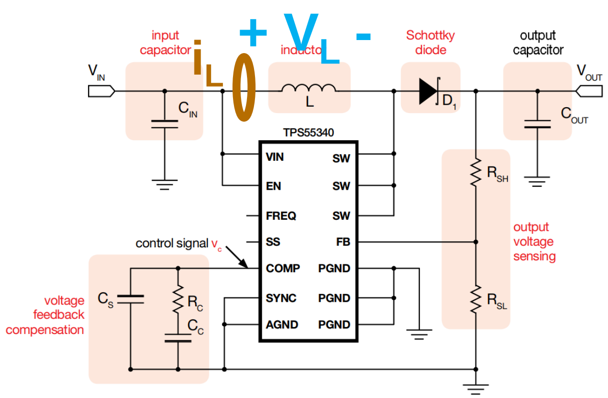

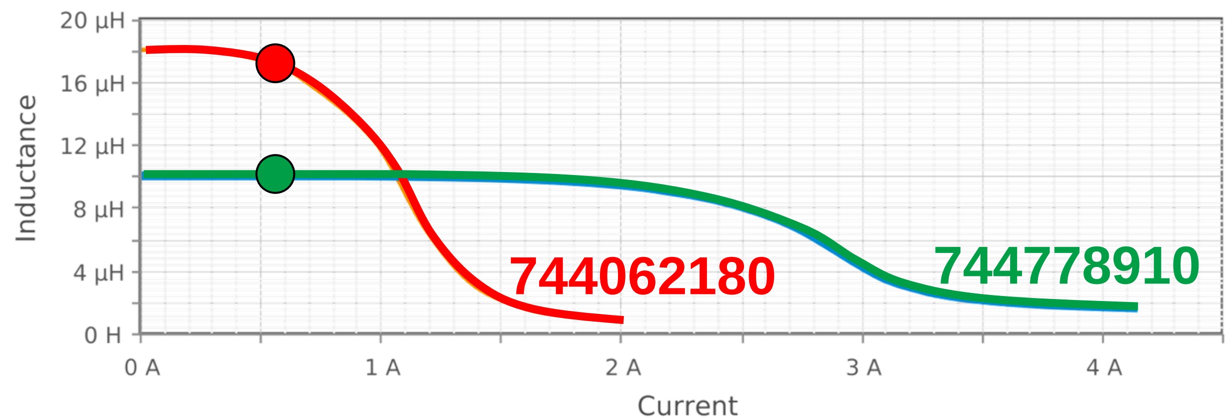

TI-PMLK BOOST: low-current voltage spectrum

V_{in}10V, V_{out}= 24 V , I_{out}=0.2 A, f_s= 300 kHz

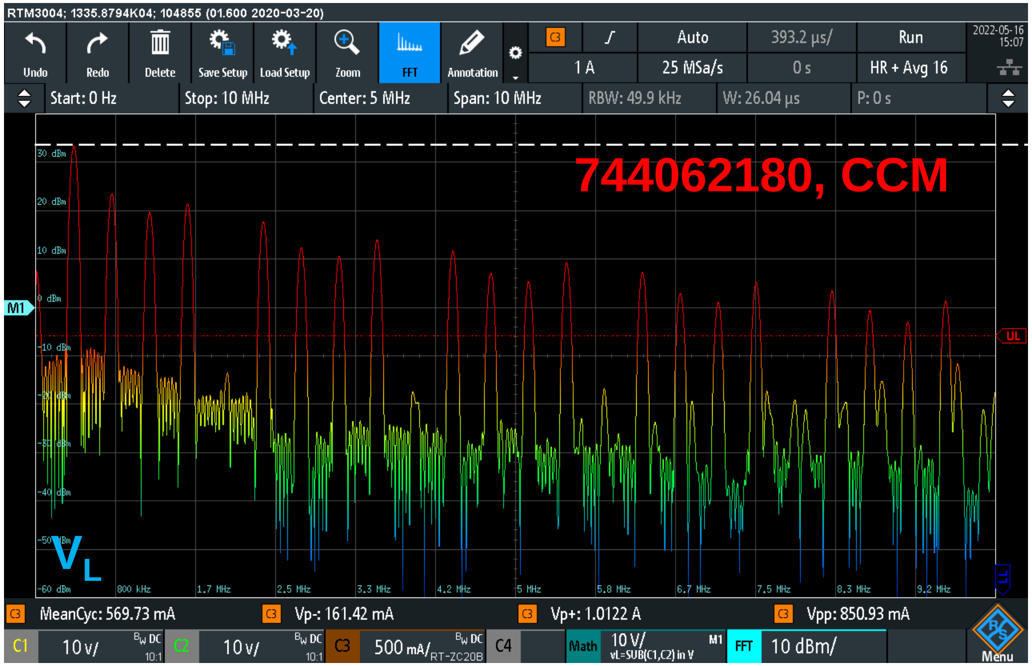

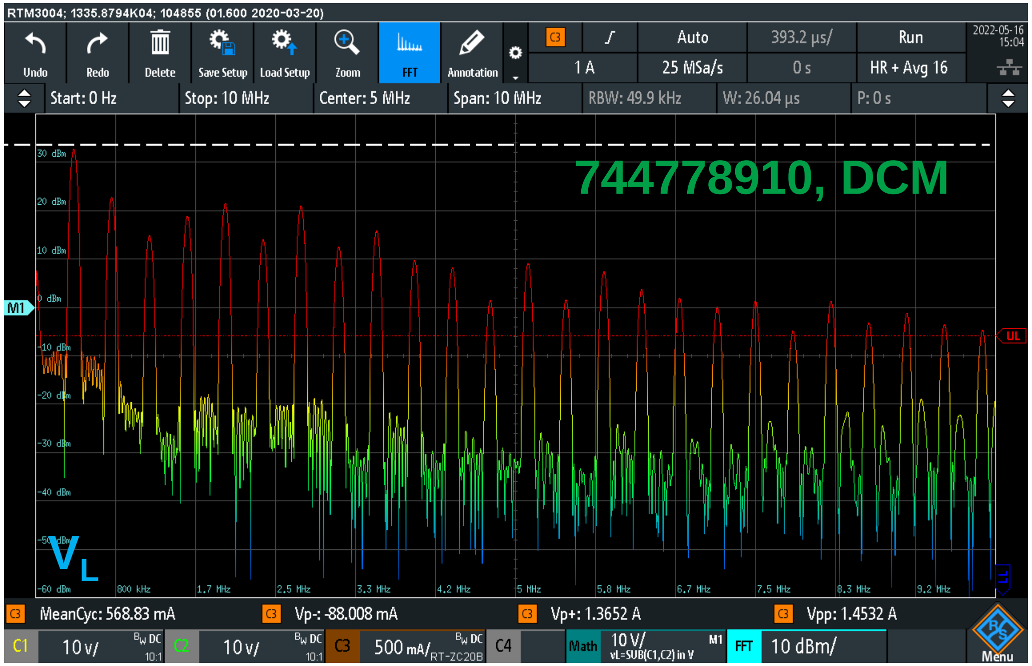

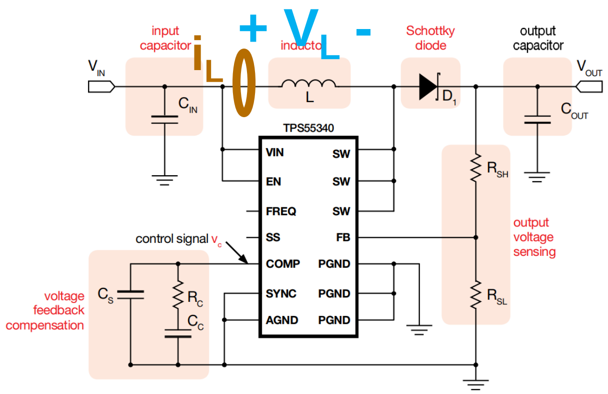

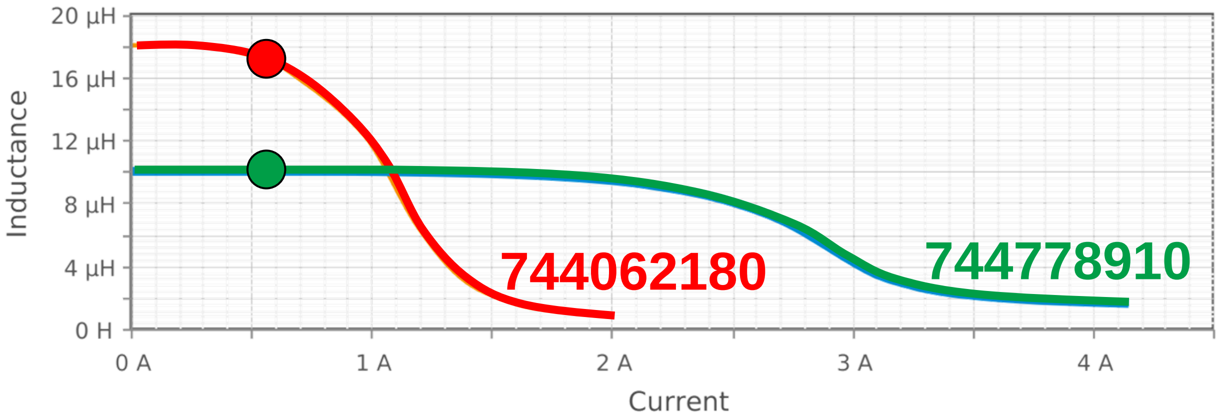

Input Filter

Input filter: coducted EMI limits

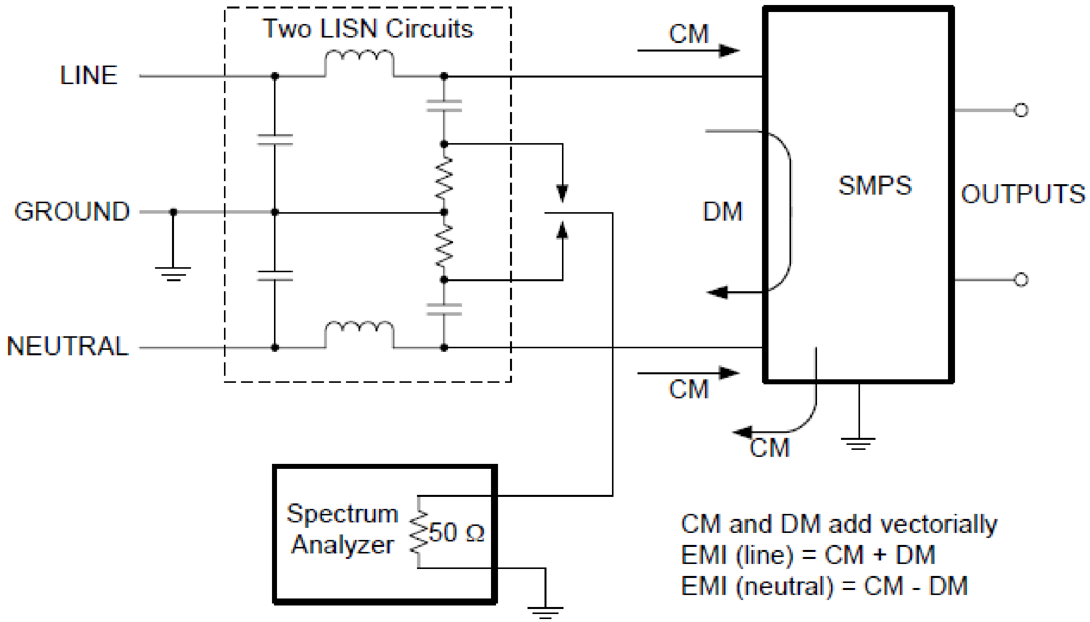

CM and DM add vectorially
EMI (line) = CM + DM
EMI (neutral) = CM - DM

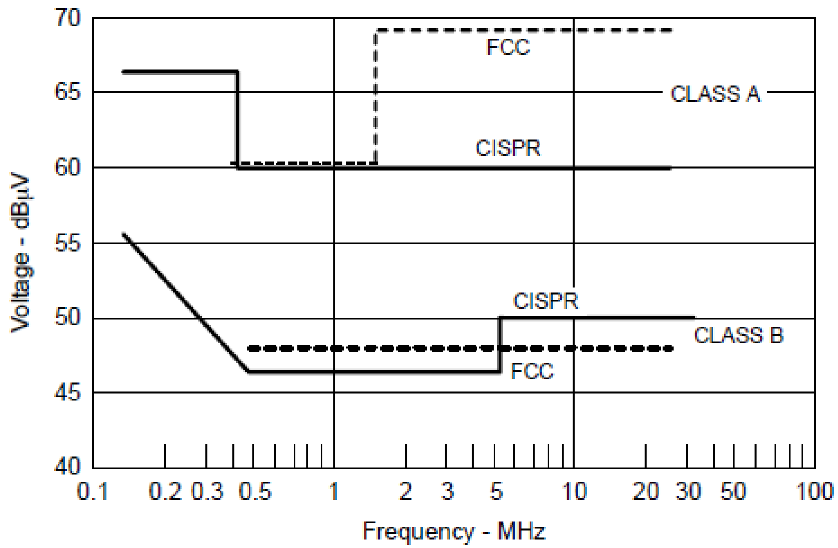

Input filter: buck converter

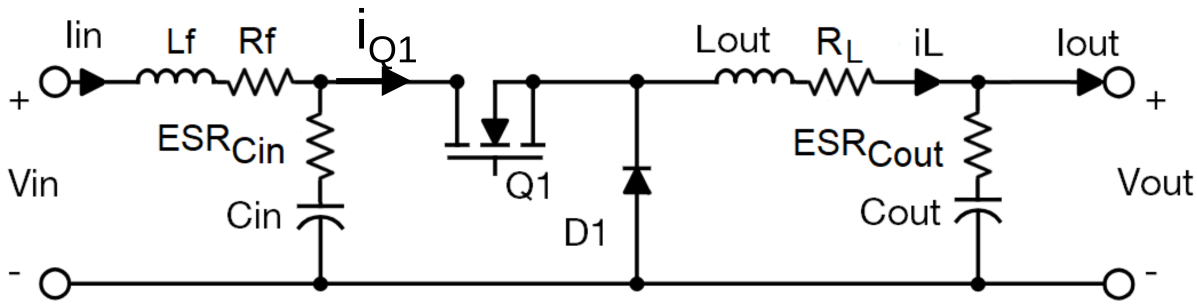

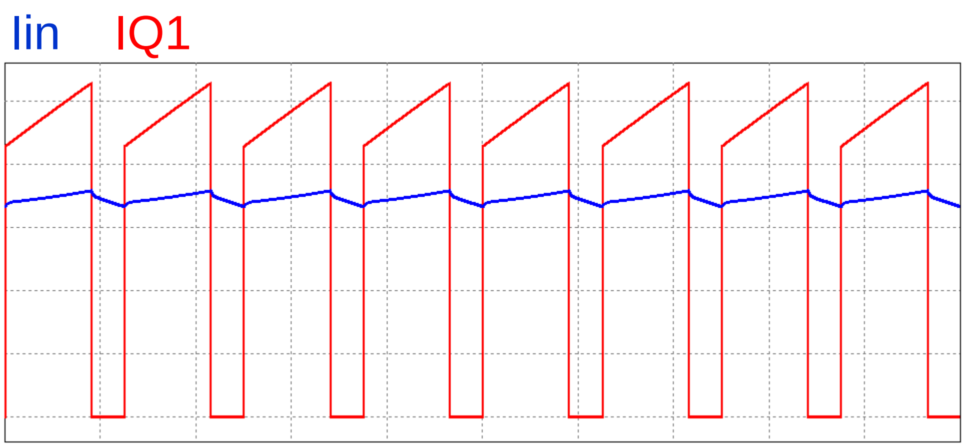

time

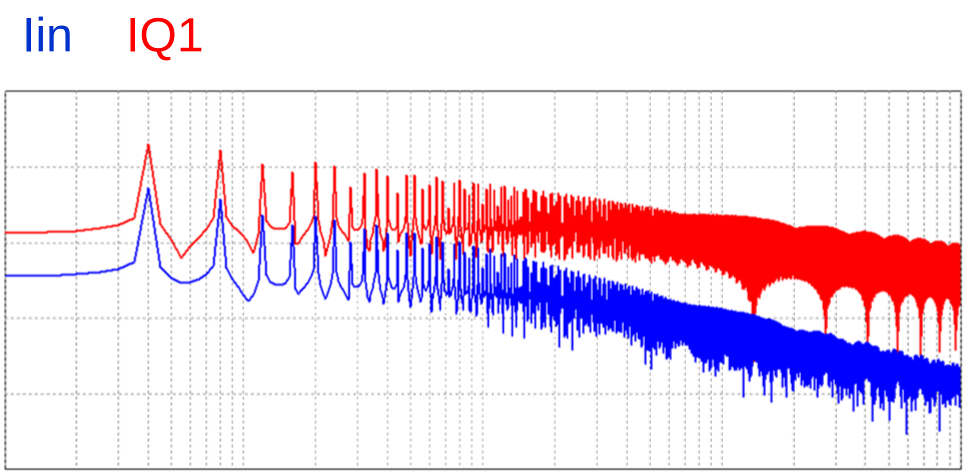

frequency

Input filter: attenuation

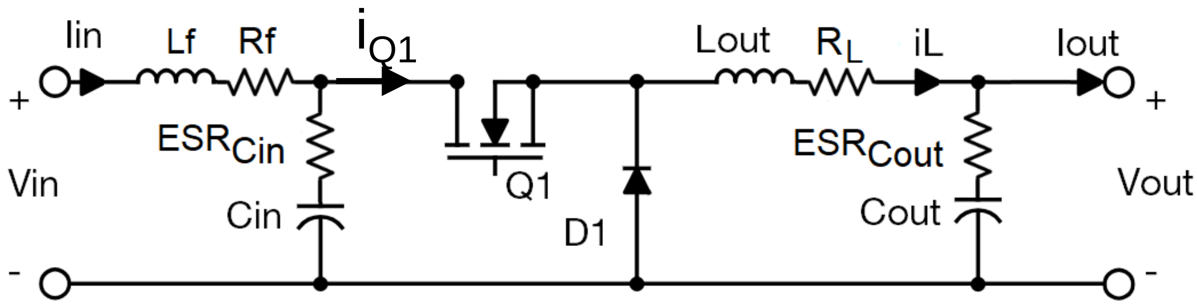

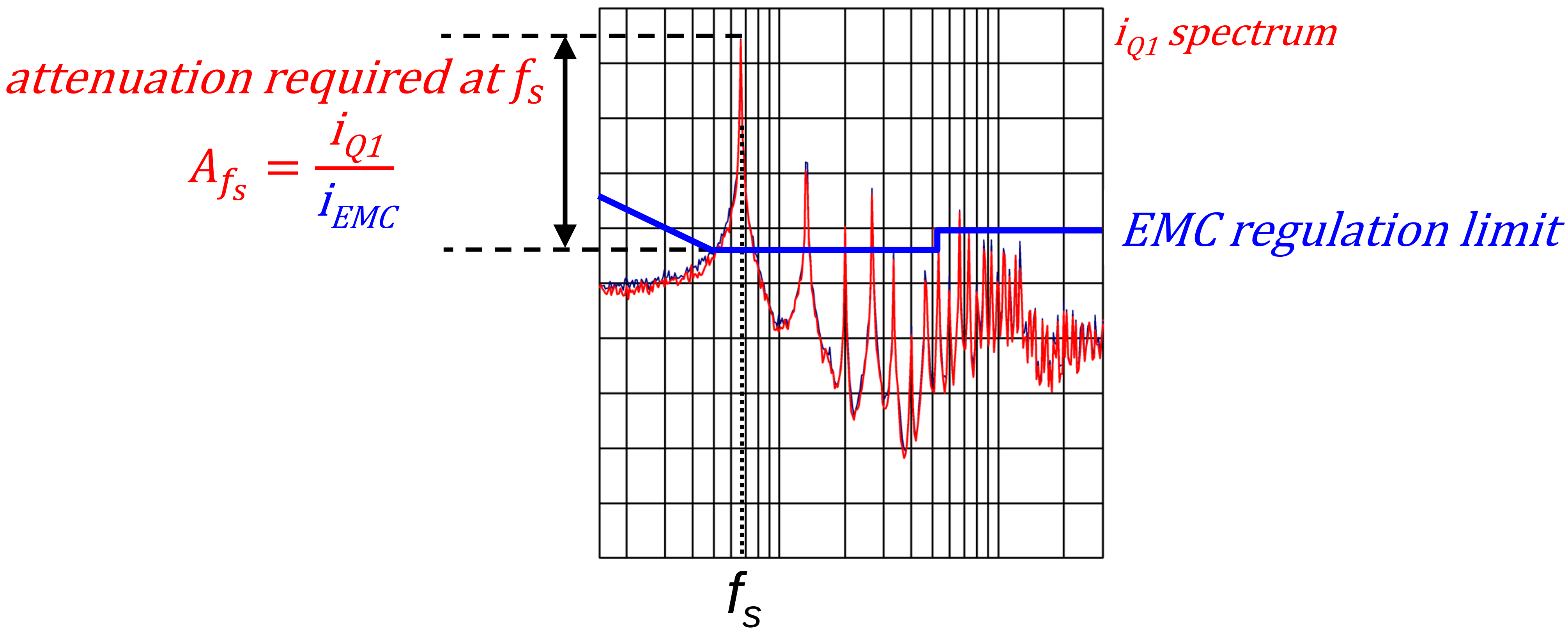

Input filter: resonance frequency

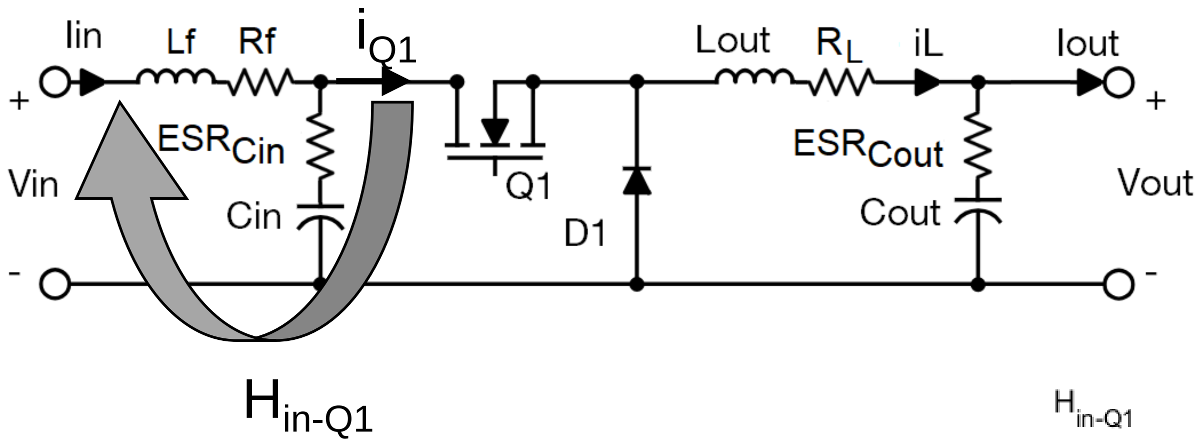

$$A_x \cong \frac{f_s^2}{f_{ox}^2} \quad x = 1,2$$

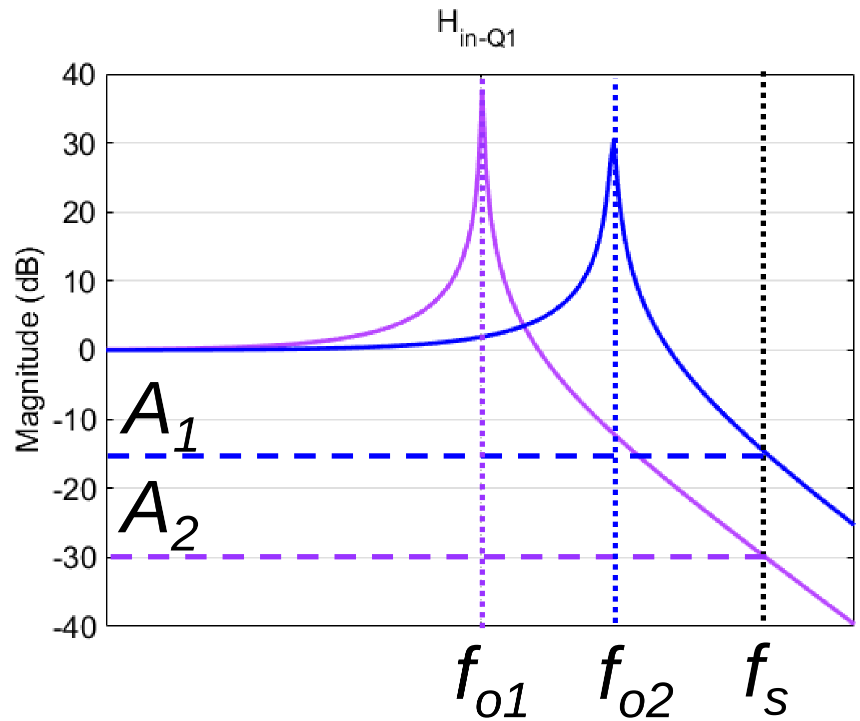

Input filter: inductor constraints

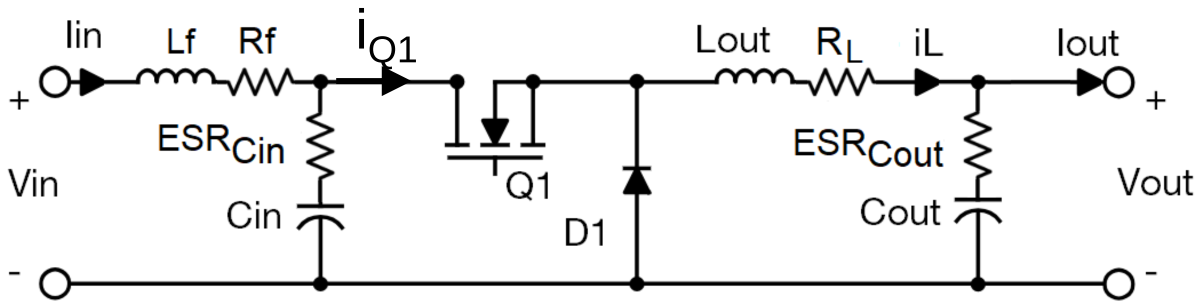

$$f_o = \frac{f_s}{\sqrt{A_{f_s}}}$$

$$L_{f,nom} > \frac{1}{(2\pi f_o)^2 C_{in}}$$

$$R_f < \frac{P_{f,max}}{I^2_{inDC,max}}$$

[v_{noise}=80$dB_{\mu V}$→ $I_{in,ac}$=200μA]

Input filter: impact on loop gain

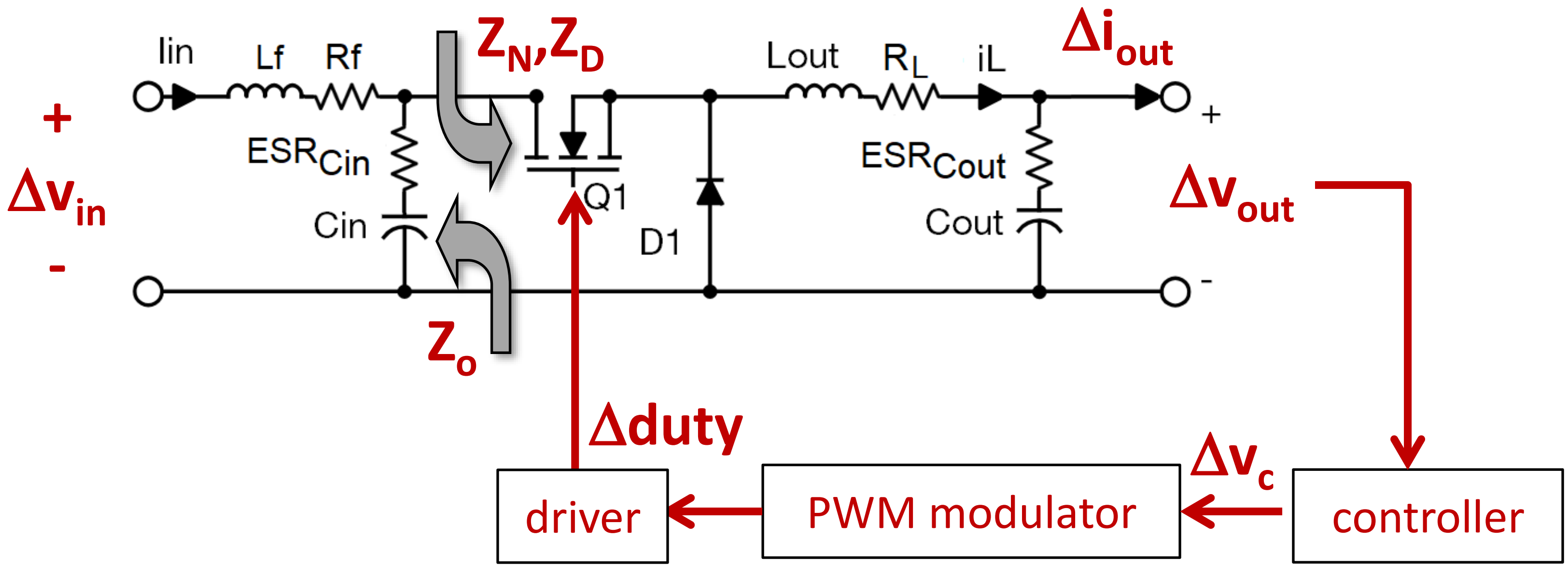

$$G_{vc} = G_{vc,nf}\ H_b \qquad G_{vc,nf} = G_o \frac{1+\dfrac{s}{\omega_r}}{1+\dfrac{s}{Q\omega_n}+\dfrac{s^2}{\omega_n^2}} \qquad H_b = \frac{1+\dfrac{Z_o}{Z_N}}{1+\dfrac{Z_o}{Z_D}}$$

Input filter: converter input impedance

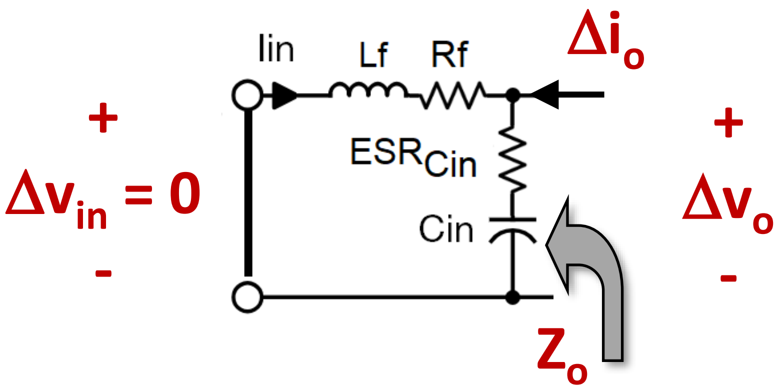

$$Z_o = \left.\frac{\Delta v_o}{\Delta i_o}\right|_{\Delta v_{in}=0}$$

$$Z_N = \left.\frac{\Delta v_o}{\Delta i_o}\right|_{\Delta v_{out}=0}$$

$$Z_D = \left.\frac{\Delta v_o}{\Delta i_o}\right|_{\Delta v_{c}=0}$$

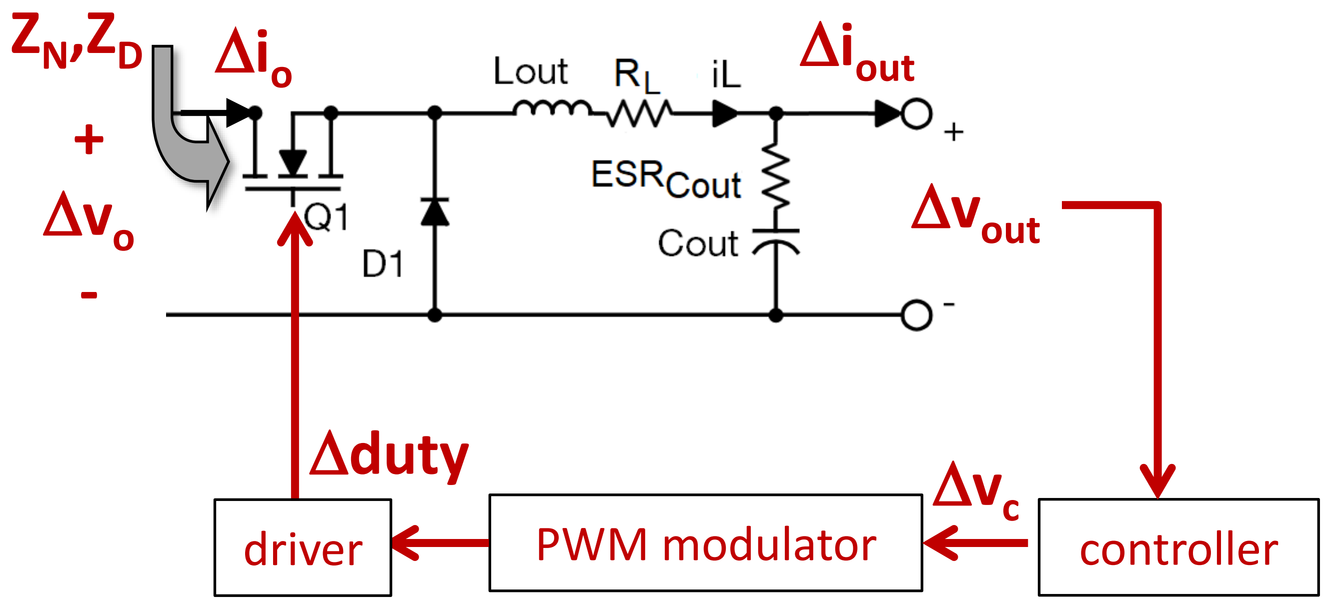

Input filter: filter with low output impedance

$$Z_o \ll Z_N, Z_D$$

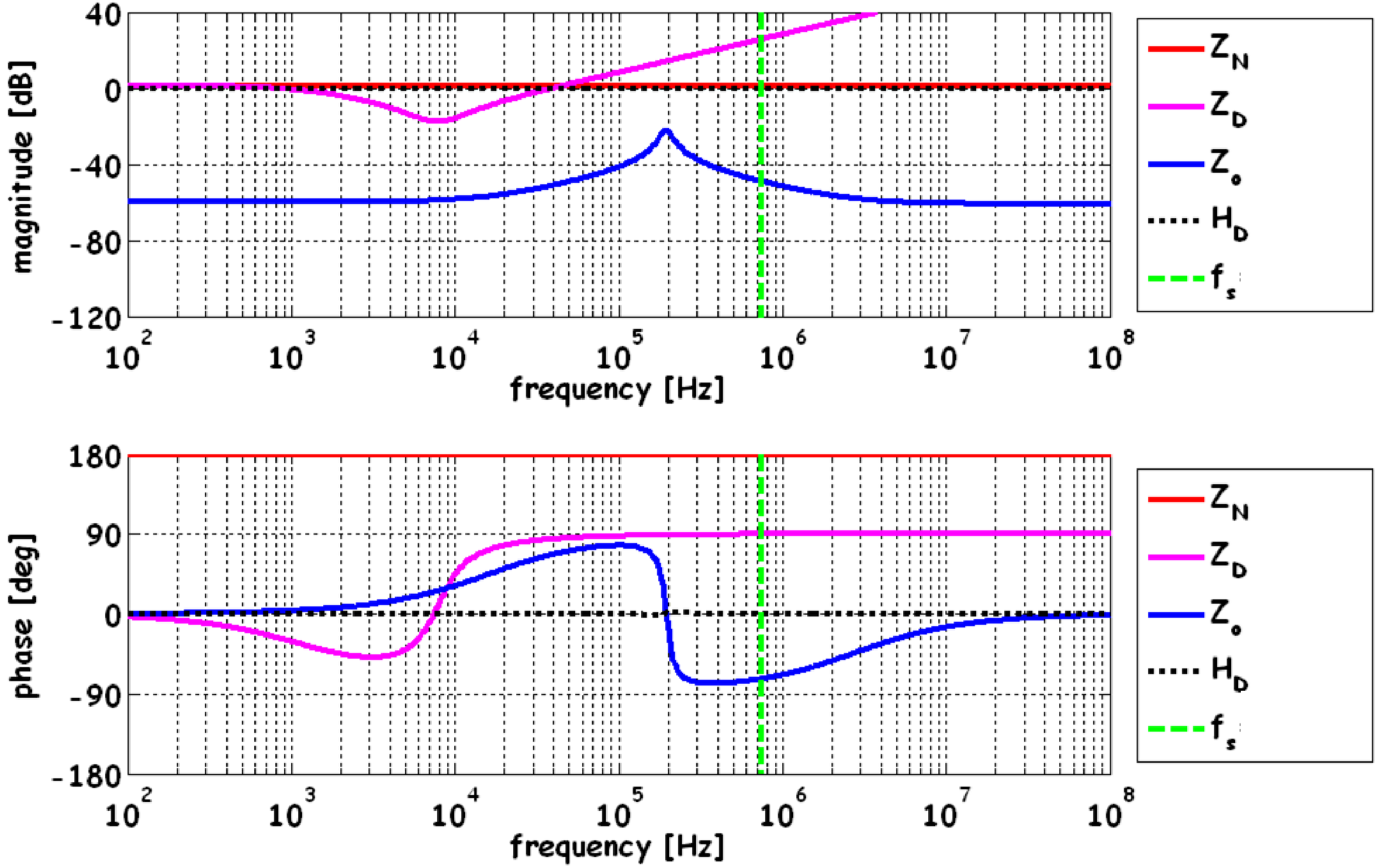

Input filter: resonance-free loop gain

$$Z_o \ll Z_N, Z_D \rightarrow G_{vc} = G_{vc,nf}$$

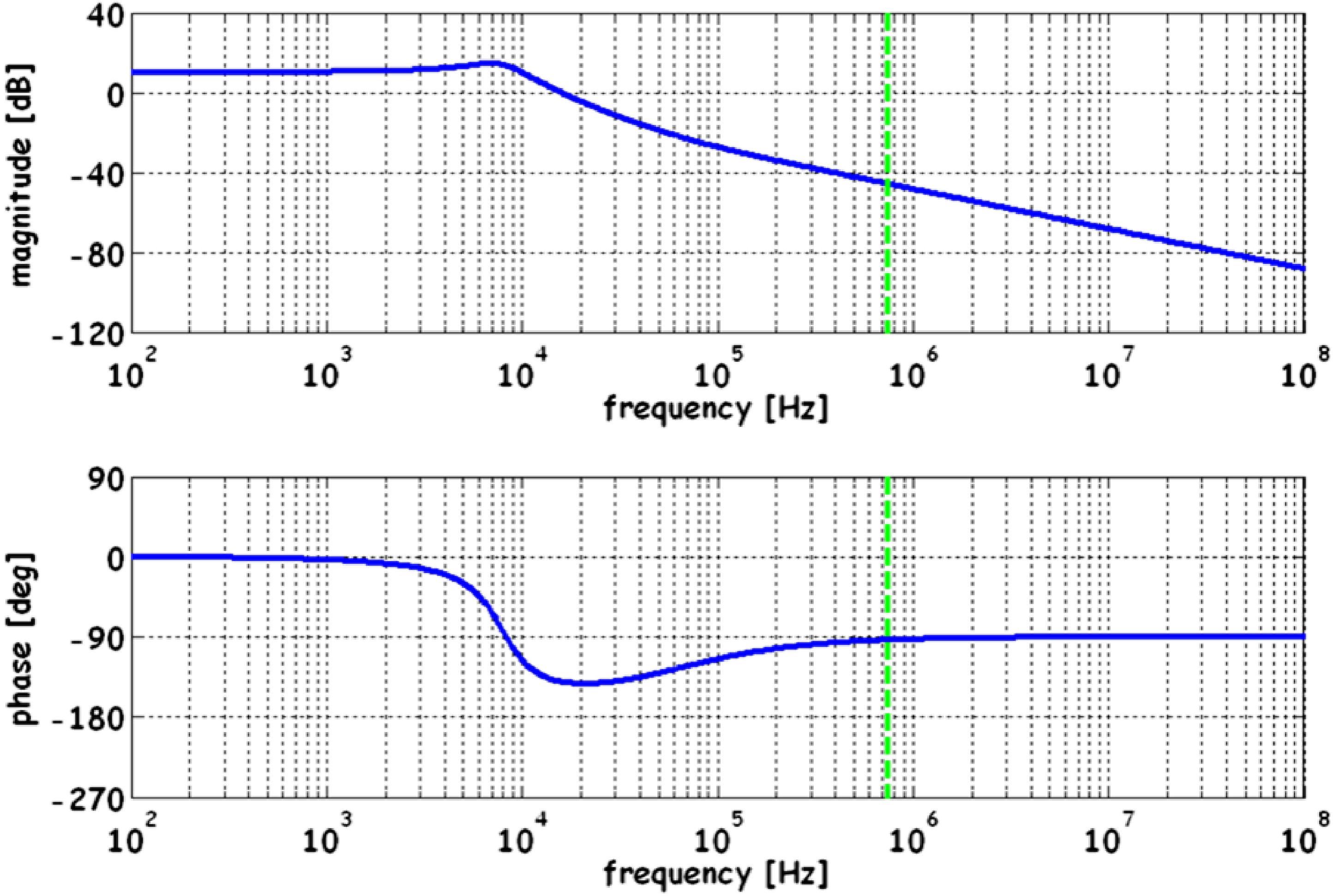

Input filter: filter with large impedance

$$Z_o \approx Z_N, Z_D$$

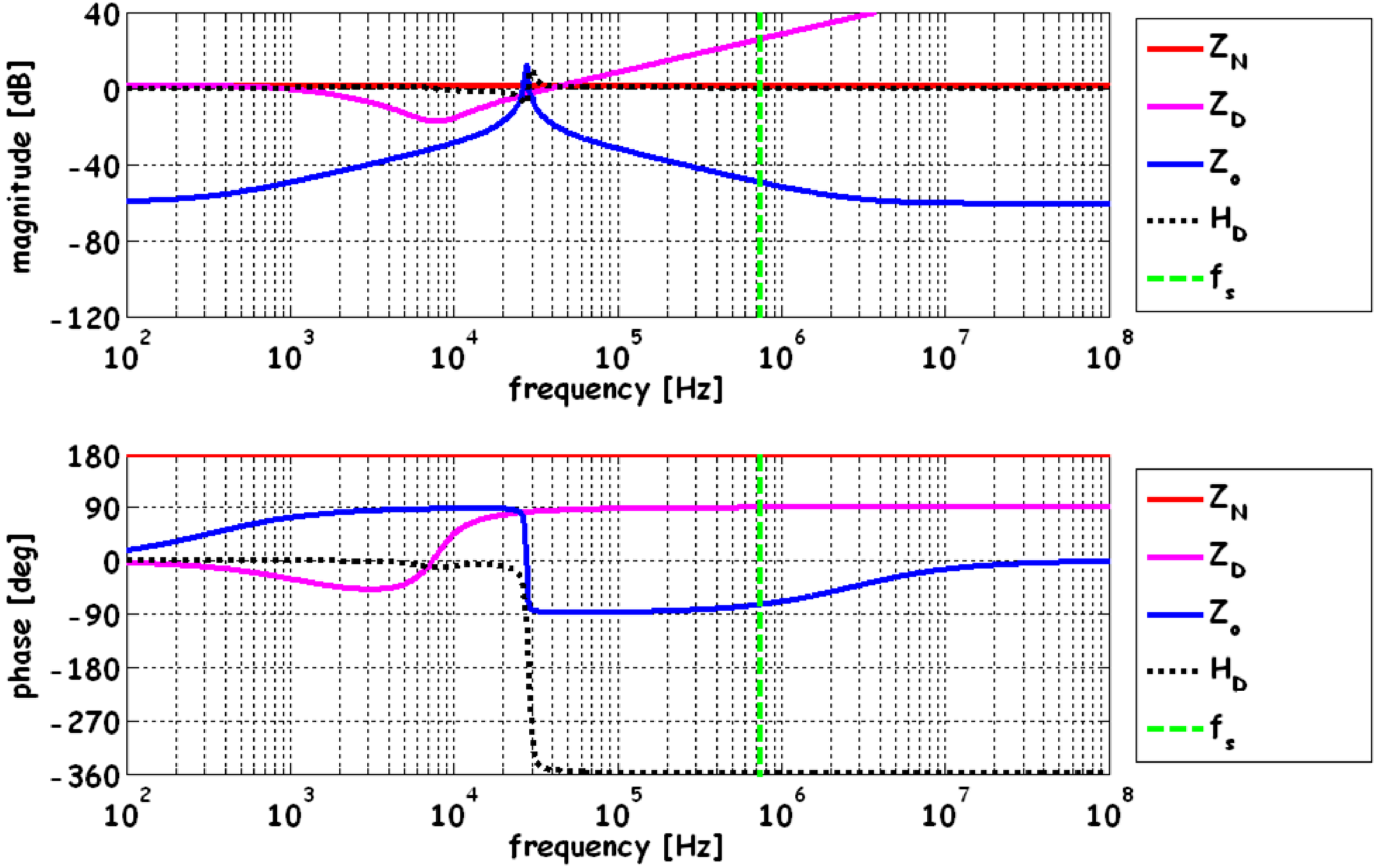

Input filter: resonance-affected loop gain

$$Z_o \approx Z_N, Z_D \rightarrow G_{vc} \neq G_{vc,nf}$$

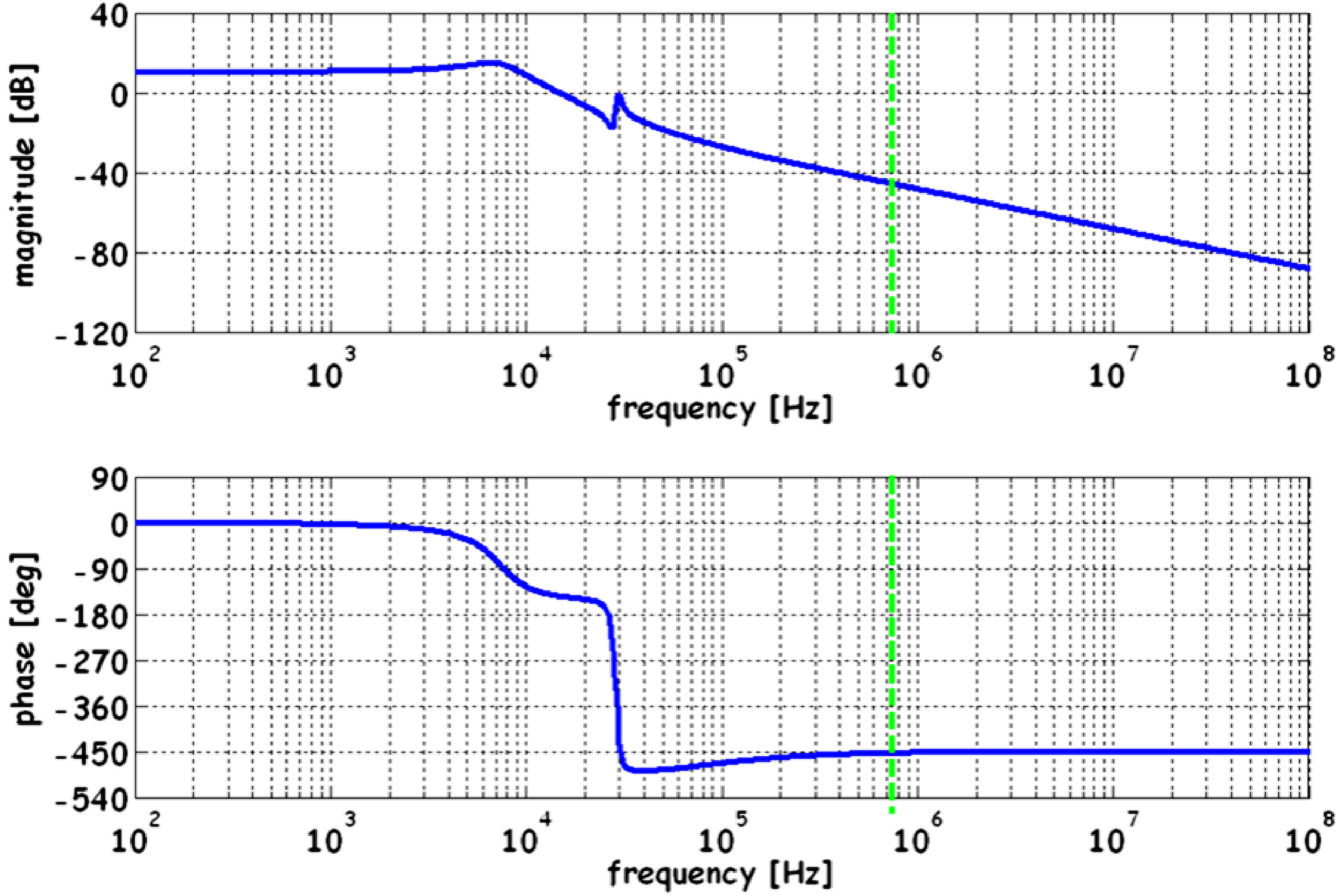

Input filter: damping

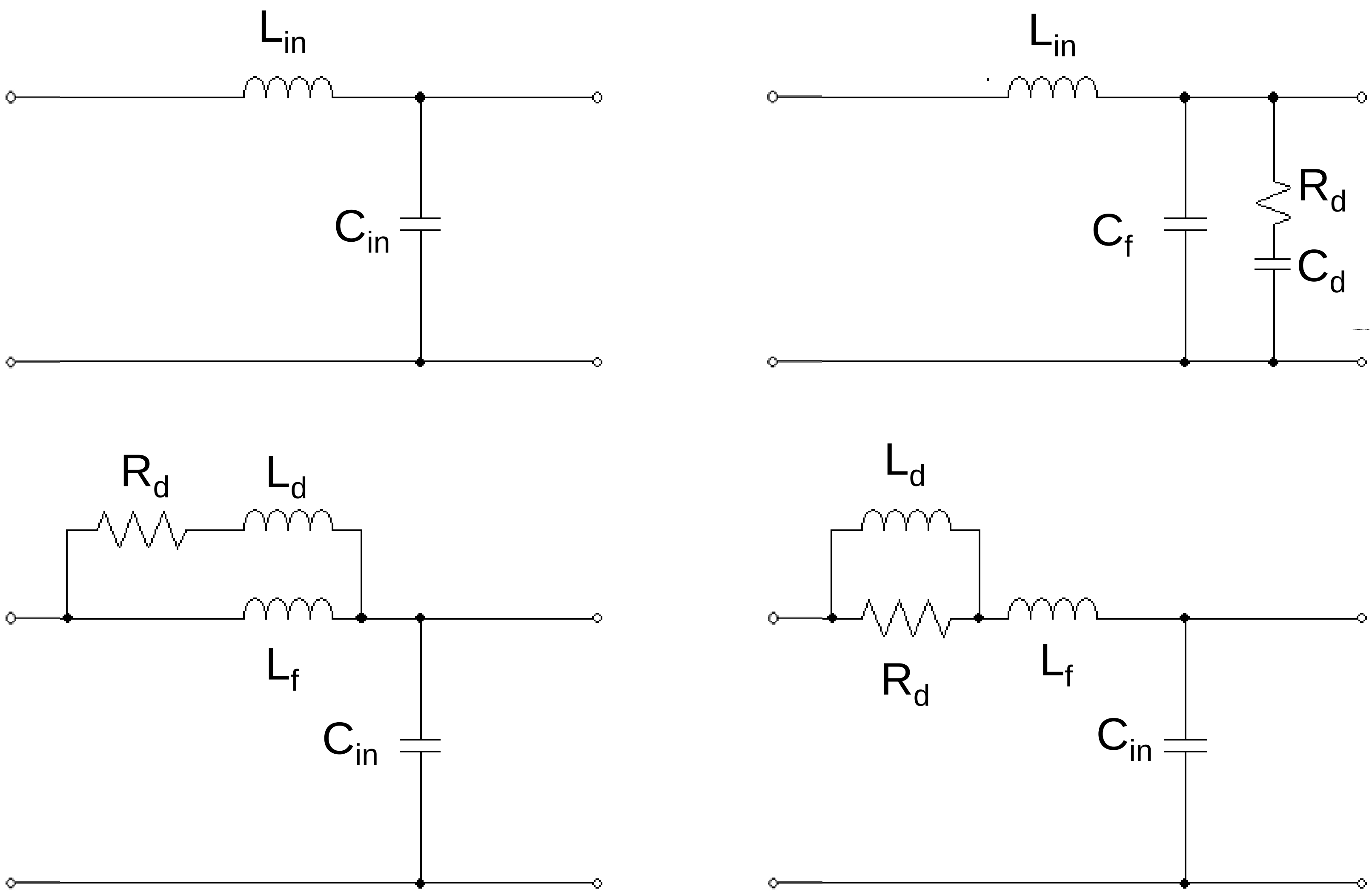

R. W. Erickson, “Optimal single resistors damping of input filters”, *14th Annual Applied Power Electronics Conf. and Expo. (APEC)*, Dallas, March 1999

Input filter: design equations

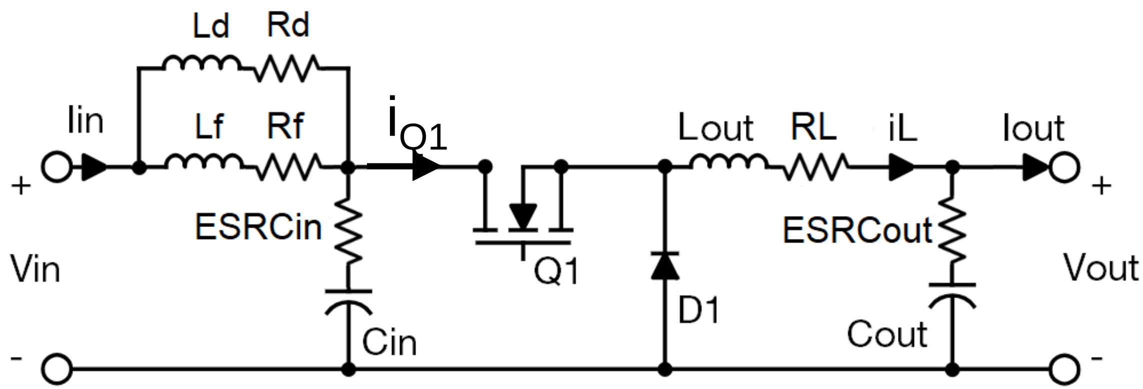

$$f_o = \frac{f_s}{\sqrt{A_{f_s}}}$$

$$L_d = \alpha L_f \quad (\alpha > 1)$$

$$\frac{I_{d,DC}}{I_{f,DC}} = \frac{R_f}{R_d} \ll 1$$

$$L_{eq} > \frac{1}{(2\pi f_o)^2 C_{in}}$$

$$L_f > L_{eq}\left(1 + \frac{1}{\alpha}\right)$$

$$R_f < \frac{P_{f,max}}{I^2_{inDC,max}}$$

$$\frac{1}{L_f} + \frac{1}{L_d} < (2\pi f_o)^2 C_{in}$$

$$L_d > L_{eq}(1 + \alpha)$$

$$R_{d,opt} \cong \frac{1 + \alpha}{2\pi f_o C_{in}}$$

N. Femia, G. Di Capua, "Optimum Design of Differential-Mode Input Filters for DC-DC Switching Regulators," *2021 IEEE Int. Symp. on Circ. and Sys. (ISCAS)*, Daegu, 2021

Input filter: optimal damping

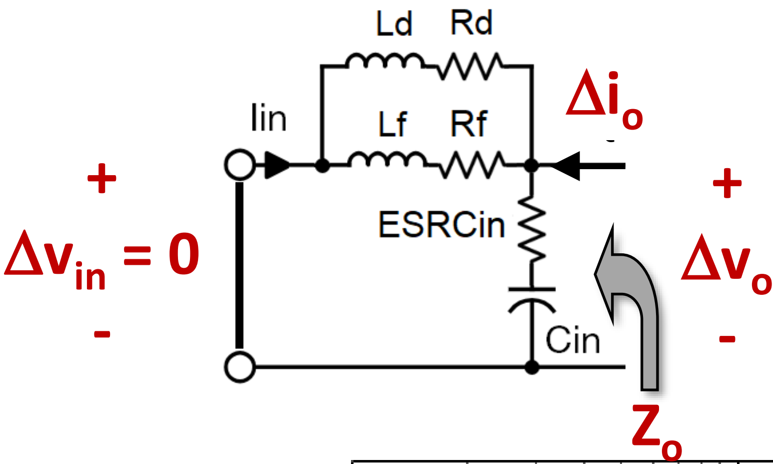

$$Z_o = \left.\frac{\Delta v_o}{\Delta i_o}\right|_{\Delta v_{in}=0}$$

$$Z_{opt} = \frac{\sqrt{2(1+\alpha)(1+2\alpha)}}{2\pi f_o C_{in}}$$

$$f_{opt} = f_o \sqrt{\frac{1+2\alpha}{2(1+\alpha)}}$$

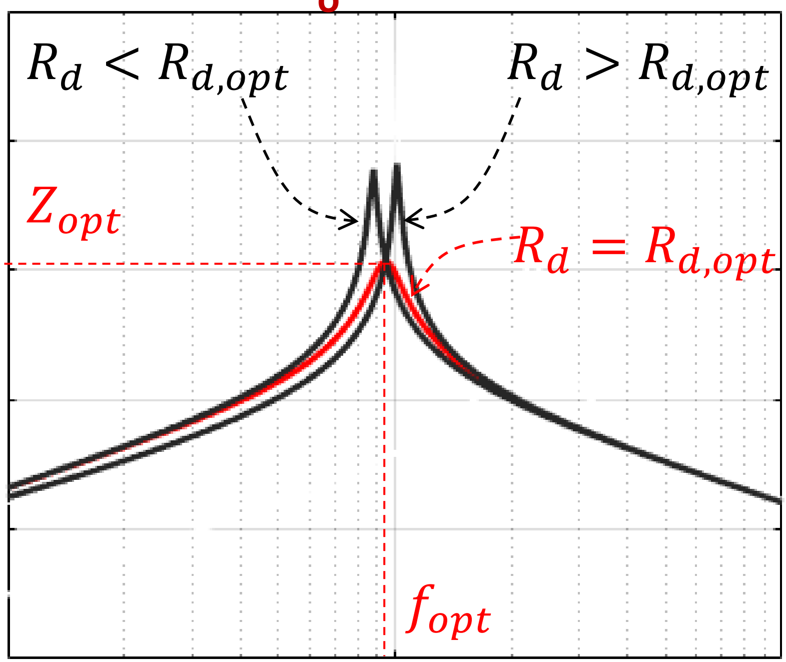

$$L_f > L_{eq}\left(1 + \frac{1}{\alpha}\right)$$

$$L_d > L_{eq}(1+\alpha)$$

$$R_f < \frac{P_{f,max}}{I^2_{inDC,max}}$$

$$R_{d,opt} = \frac{1+\alpha}{2\pi f_o C_{in}}$$

Input filter: design example

V_{in} = 5 V

I_{out} = 1.2 A

V_{out} = 3.3 V

f_{sw}=400 kHz

C_{in}= 50 μF

$ESRC_{in}$= 5 mΩ

Att_{fsw}= 73.4 dBμV

η=90%

P_{loss}=440mW

L_{eq}= 15 μH

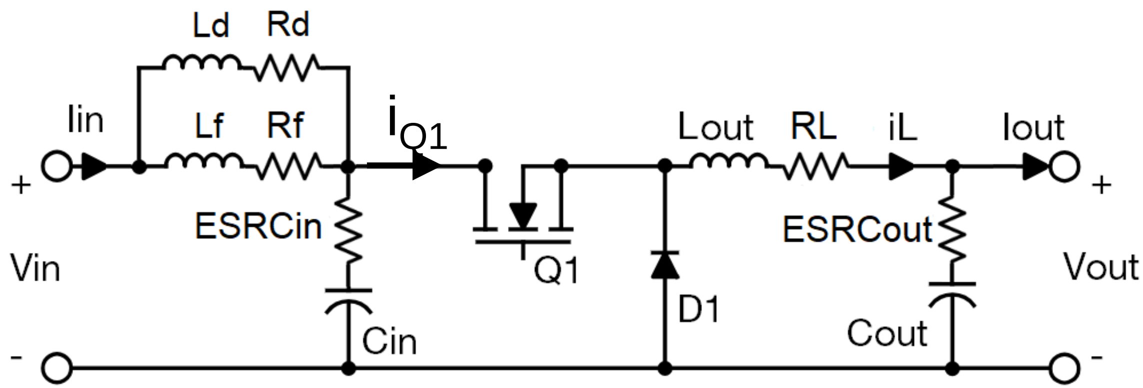

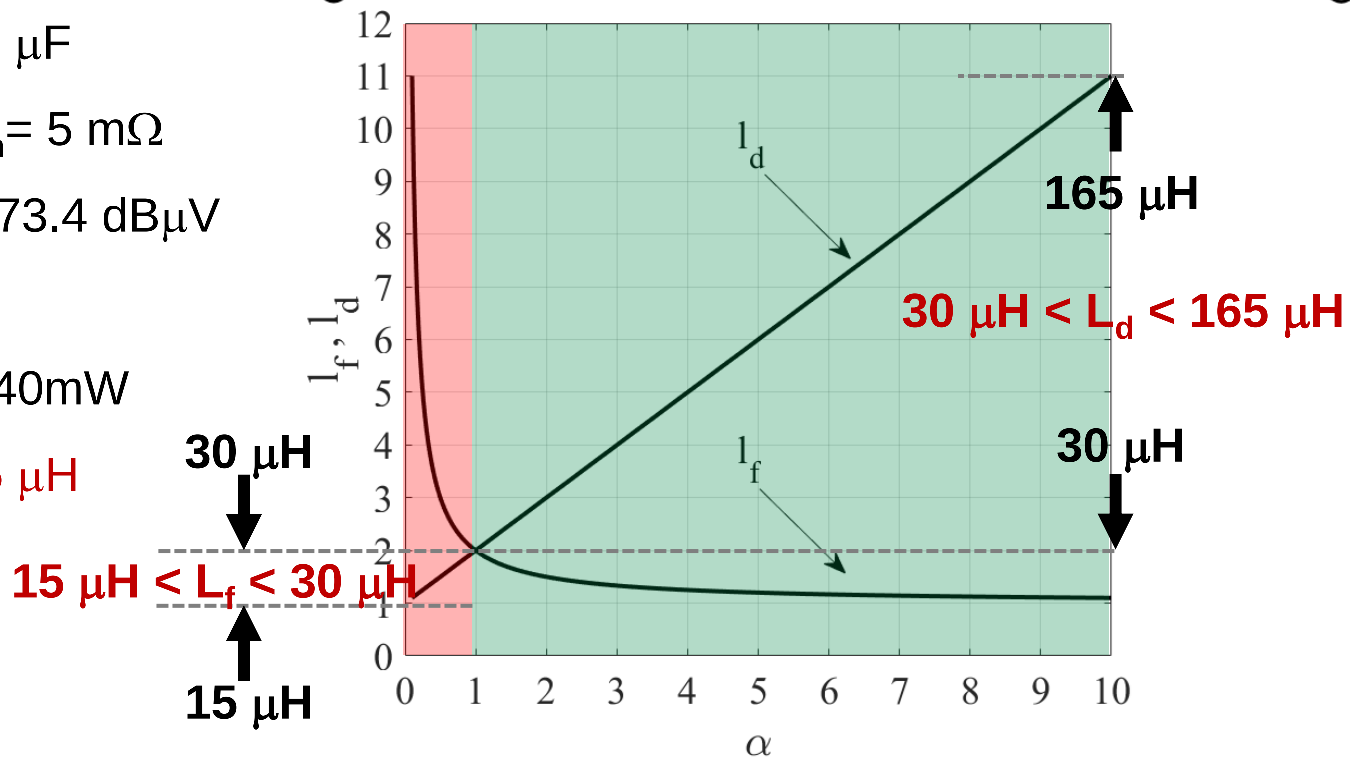

$$l_f = \frac{L_f}{L_{eq}} = 1 + \frac{1}{\alpha}$$

$$l_d = \frac{L_d}{L_{eq}} = 1 + \alpha$$

$$R_f < \frac{P_{f,max}}{I^2_{inDC,max}}$$

$$R_{d,opt} = \frac{1+\alpha}{2\pi f_o C_{in}}$$

Input filter: loss budget allocation

V_{in} = 5 V

I_{out} = 1.2 A

V_{out} = 3.3 V

f_{sw}=400 kHz

C_{in}= 50 μF

$ESRC_{in}$= 5 mΩ

Att_{fsw}= 73.4 dBμV

η=90%

P_{loss}=440mW

$I_{inDC,max}$ = 0.88 A

L_{eq}= 15 μH

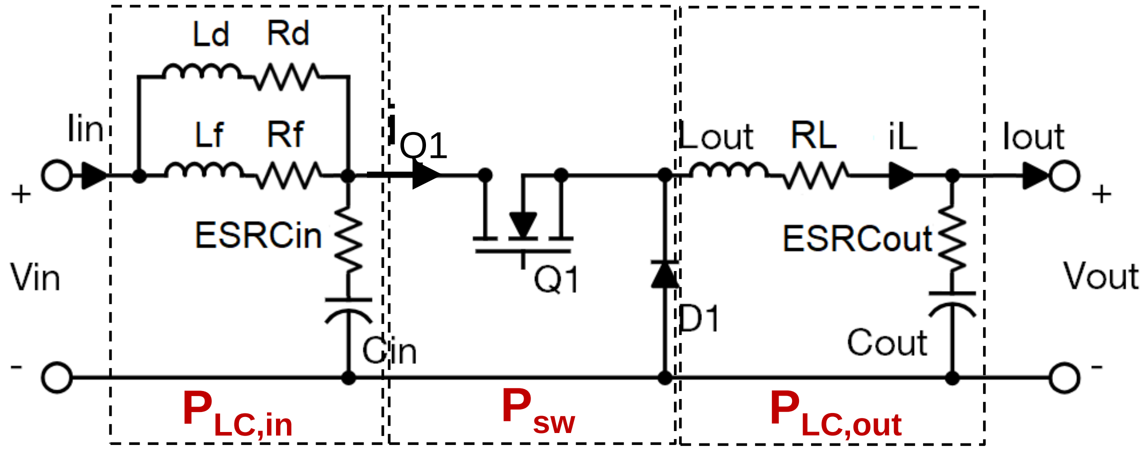

P_f / P_{loss} [%]	$P_{f,max}$ [mW]	$R_{f,max}$ [mΩ]
2	8.8	11.4
5	22	38.5
10	44	57.0
20	88	114.0

$$l_f = \frac{L_f}{L_{eq}} = 1 + \frac{1}{\alpha}$$

$$l_d = \frac{L_d}{L_{eq}} = 1 + \alpha$$

$$R_f < \frac{P_{f,max}}{I^2_{inDC,max}}$$

$$R_{d,opt} = \frac{1+\alpha}{2\pi f_o C_{in}}$$

Input filter: design options

power inductors with 15 µH ≤ L ≤ 33 µH and R_f ≤ 114 mΩ

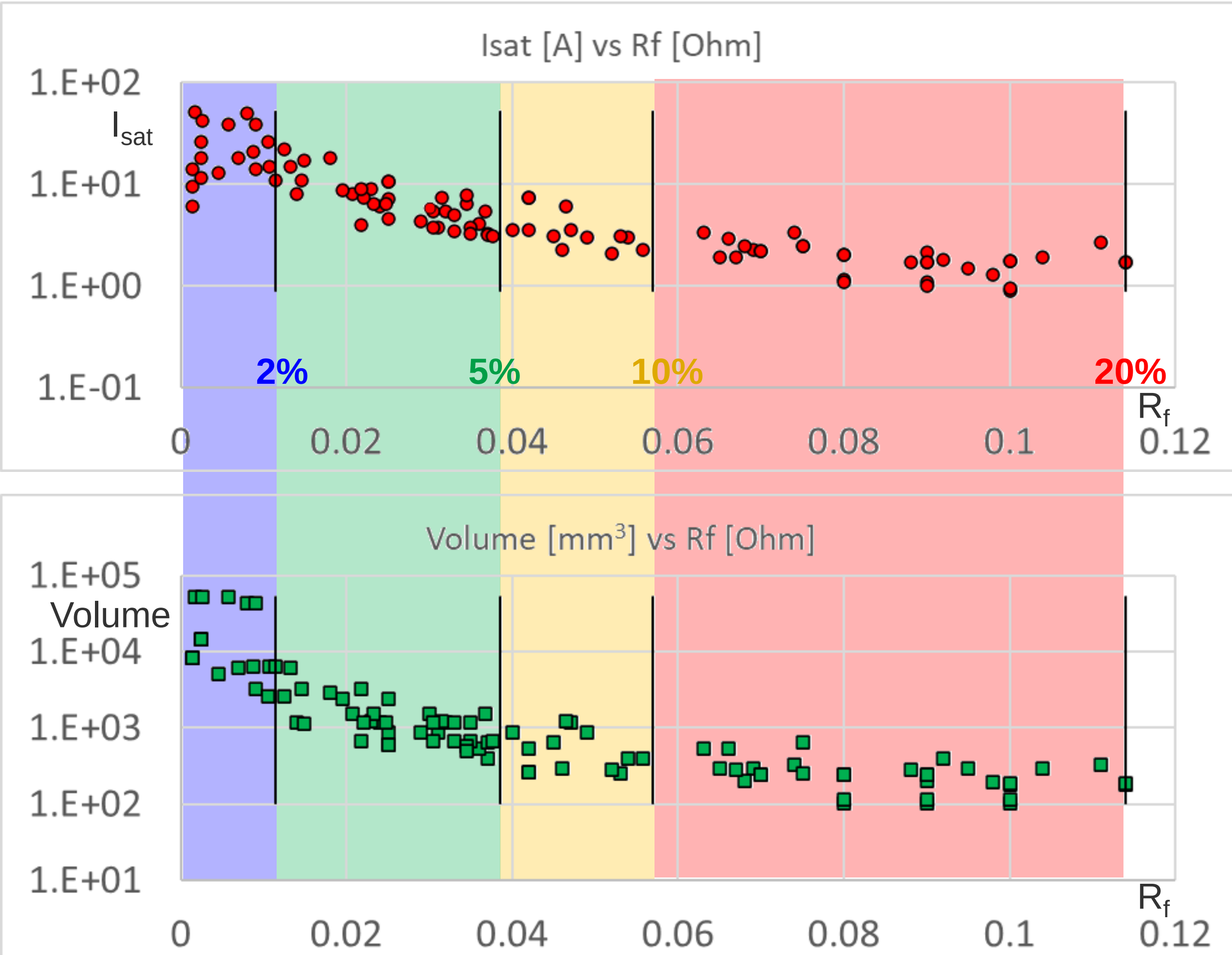

smallest parts with 57.0 mΩ ≤ R_f < 114 mΩ

Part Code	L [µH]	R [mΩ]	Isat [A]	Vol. [mm³]
744062220	22	100.0	0.95	113
744071220	22	65.0	1.9	296
744071330	33	95.0	1.5	296

smallest parts with 38.5 mΩ ≤ R_f < 57.0 mΩ

Part Code	L [µH]	R [mΩ]	Isat [A]	Vol. [mm³]
7447773150	15	53.0	3.1	252
78439346150	15	42.0	7.4	264
74439346150	15	42.0	7.4	264

smallest parts with 11.4 mΩ ≤ R_f < 38.5 mΩ

Part Code	L [µH]	R [mΩ]	Isat [A]	Vol. [mm³]
744066150	15	37.0	3.25	403
784325160	16.7	34.5	7.8	503
7447714150	15	36.0	4.1	541

smallest parts with R_f < 11.4 mΩ

Part Code	L [µH]	R [mΩ]	Isat [A]	Vol. [mm³]
78439370150	15	10.5	26.1	2622
74435571500	15	9.0	14	3212
7443782012150	15	4.6	12.9	5049

[https://www.we-online.com/catalog/en]

Input filter: design with saturating filter inductor

power inductors with 15 µH ≤ L ≤ 33 µH and R_f ≤ 114 mΩ

L_A=18 µH @ $I_{inDC,max}$= 0.9A

P_f≤20%P_{loss}

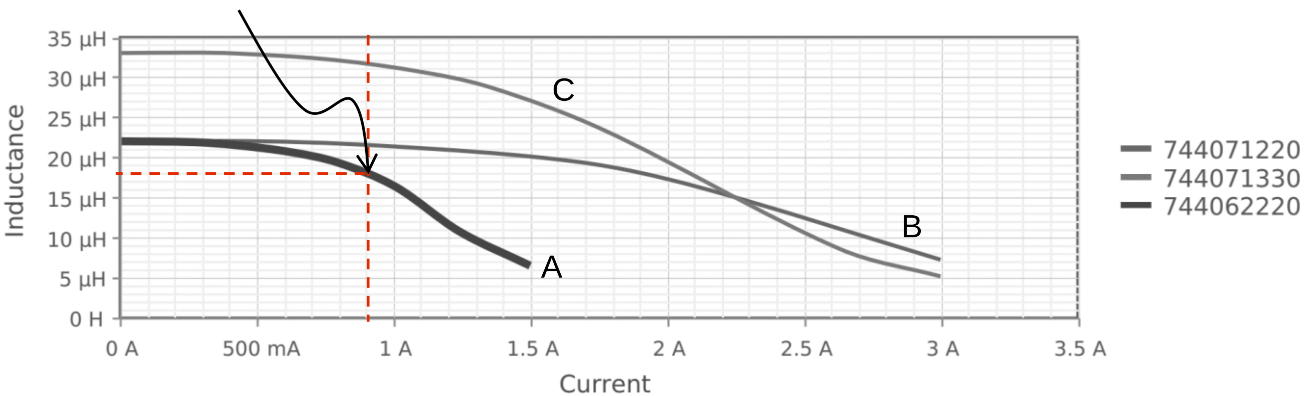

$$L_f = LA \rightarrow l_f = 1.2 \rightarrow \alpha = 5 \rightarrow L_d = 90\mu H, R_{d,opt} = 3.26\Omega$$

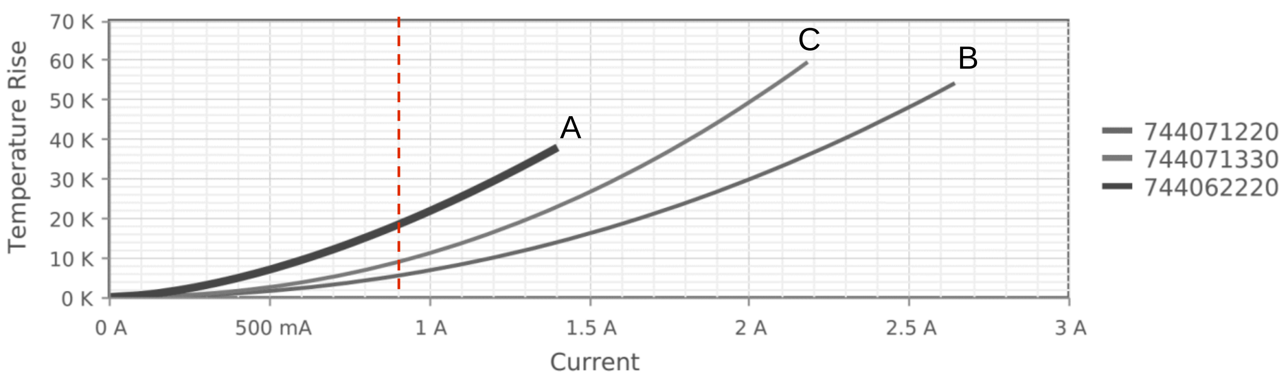

smallest parts with 57.0 mΩ ≤ R_f < 114 mΩ

Part Code	L [µH]	R [mΩ]	Isat [A]	Vol. [mm³]
A - 744062220	**22**	**100.0**	**0.95**	**113**
B - 744071220	22	65.0	1.9	296
C - 744071330	33	95.0	1.5	296

smallest parts with 38.5 mΩ ≤ R_f < 57.0 mΩ

Part Code	L [µH]	R [mΩ]	Isat [A]	Vol. [mm³]
7447773150	15	53.0	3.1	252
78439346150	15	42.0	7.4	264
74439346150	15	42.0	7.4	264

smallest parts with 11.4 mΩ ≤ R_f < 38.5 mΩ

Part Code	L [µH]	R [mΩ]	Isat [A]	Vol. [mm³]
744066150	15	37.0	3.25	403
784325160	16.7	34.5	7.8	503
7447714150	15	36.0	4.1	541

smallest parts with R_f < 11.4 mΩ

Part Code	L [µH]	R [mΩ]	Isat [A]	Vol. [mm³]
78439370150	15	10.5	26.1	2622
74435571500	15	9.0	14	3212
7443782012150	15	4.6	12.9	5049

[https://www.we-online.com/catalog/en]

Input filter: optimal damping inductor

power inductors with 100 µH ≤ L ≤ 150 µH and 2Ω ≤ R_d ≤ 5Ω

$P_f \leq 20\% P_{loss}$

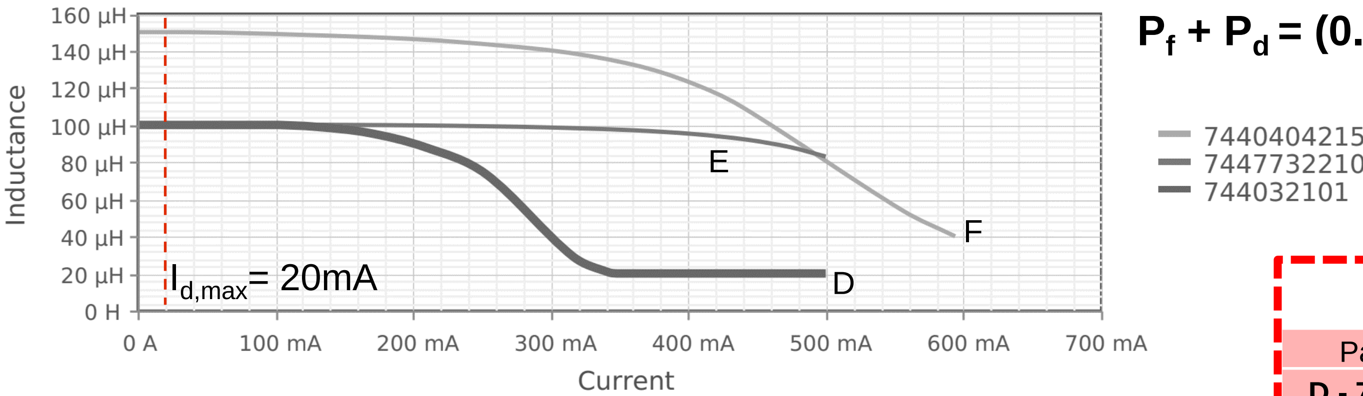

$P_f + P_d = (0.1\Omega//4.25\Omega)0.9^2 = 79mW = 18\% P_{loss}$

$$L_d = LD \rightarrow R_d = 4.25\Omega \rightarrow I_{d,max} = 20mA$$

smallest parts with 2 Ω ≤ R_d < 5 Ω

Part Code	L [µH]	R [mΩ]	Isat [A]	Vol. [mm³]
D - 744032101	**100**	**4.25**	**0.25**	**16**
E - 7447732210	100	2.42	0.41	22
F - 74404042151	150	2.85	0.45	26

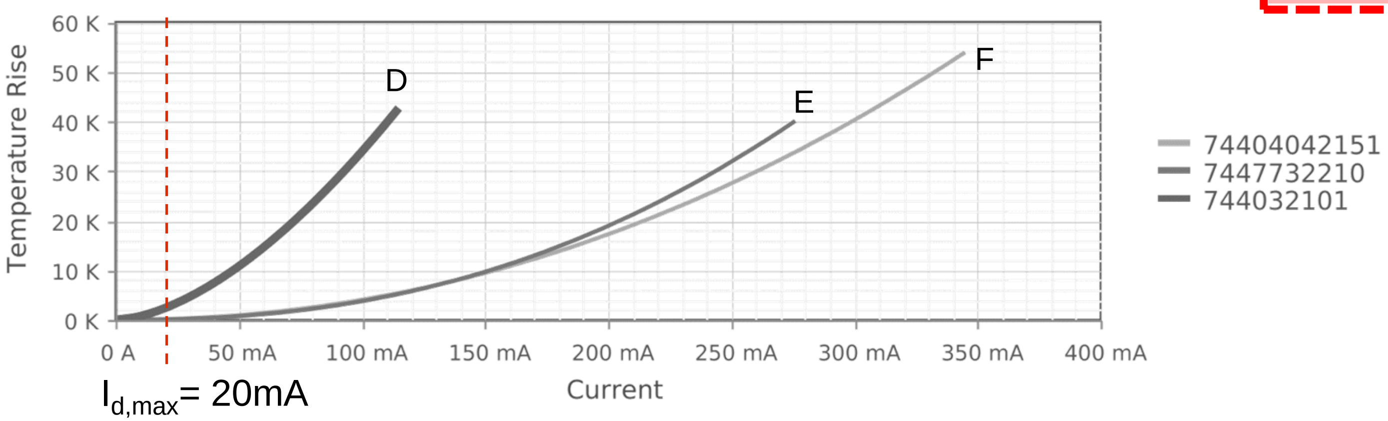

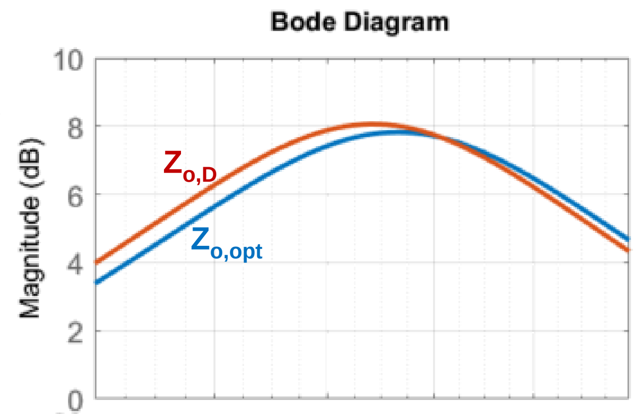

[https://www.we-online.com/catalog/en]

Input filter: design with non-saturating filter inductor (1)

power inductors with 15 µH ≤ L ≤ 33 µH and R_f ≤ 114 mΩ

$P_f \leq 10\% P_{loss}$

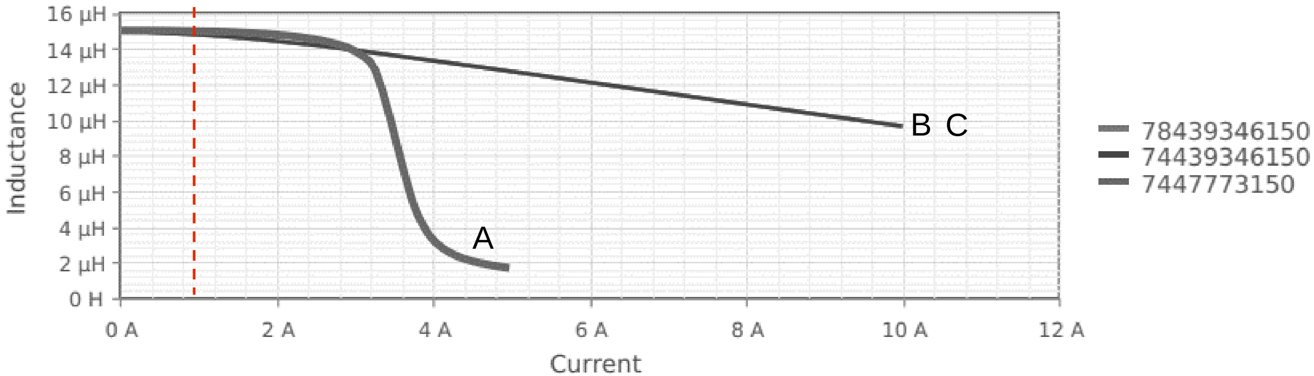

$$l_f \cong 1 \rightarrow \alpha = 11 \rightarrow L_d = 165\mu H, R_{d,opt} = 6.53\Omega$$

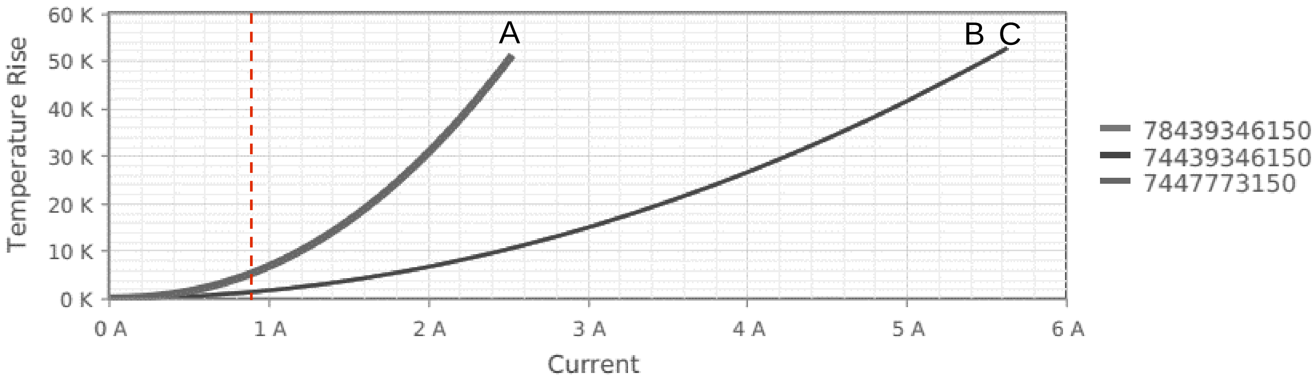

smallest parts with 57.0 mΩ ≤ R_f < 114 mΩ

Part Code	L [µH]	R [mΩ]	Isat [A]	Vol. [mm³]
744062220	**22**	**100.0**	**0.95**	**113**
744071220	22	65.0	1.9	296
744071330	33	95.0	1.5	296

smallest parts with 38.5 mΩ ≤ R_f < 57.0 mΩ

Part Code	L [µH]	R [mΩ]	Isat [A]	Vol. [mm³]
A - 7447773150	**15**	**53.0**	**3.1**	**252 (2.23x)**
B - 78439346150	15	42.0	7.4	264
C - 74439346150	15	42.0	7.4	264

smallest parts with 11.4 mΩ ≤ R_f < 38.5 mΩ

Part Code	L [µH]	R [mΩ]	Isat [A]	Vol. [mm³]
744066150	15	37.0	3.25	403
784325160	16.7	34.5	7.8	503
7447714150	15	36.0	4.1	541

smallest parts with R_f < 11.4 mΩ

Part Code	L [µH]	R [mΩ]	Isat [A]	Vol. [mm³]
78439370150	15	10.5	26.1	2622
74435571500	15	9.0	14	3212
7443782012150	15	4.6	12.9	5049

[https://www.we-online.com/catalog/en]

Input filter: design with non-saturating filter inductor (2)

power inductors with 15 µH ≤ L ≤ 33 µH and R_f ≤ 114 mΩ

$P_f \leq 5\% P_{loss}$

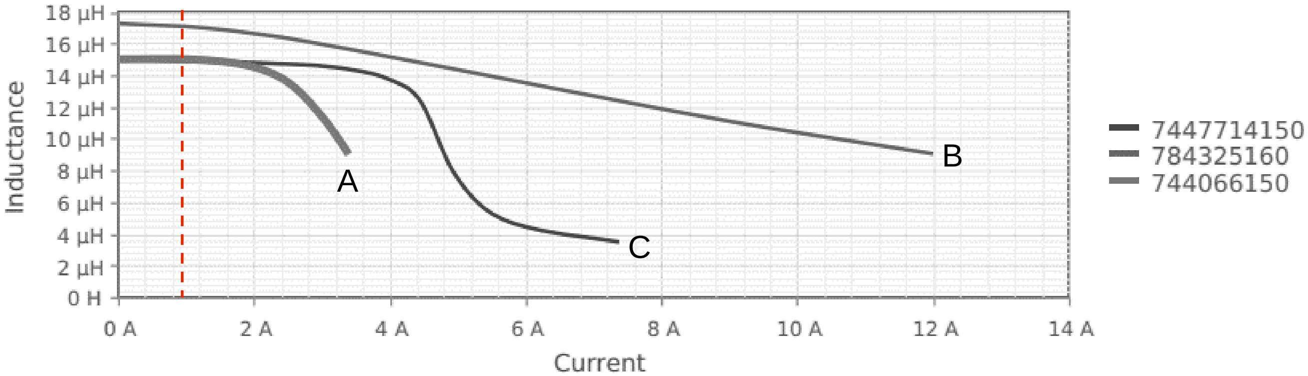

$$l_f \cong 1 \rightarrow \alpha = 11 \rightarrow L_d = 165\mu H, R_{d,opt} = 6.53\Omega$$

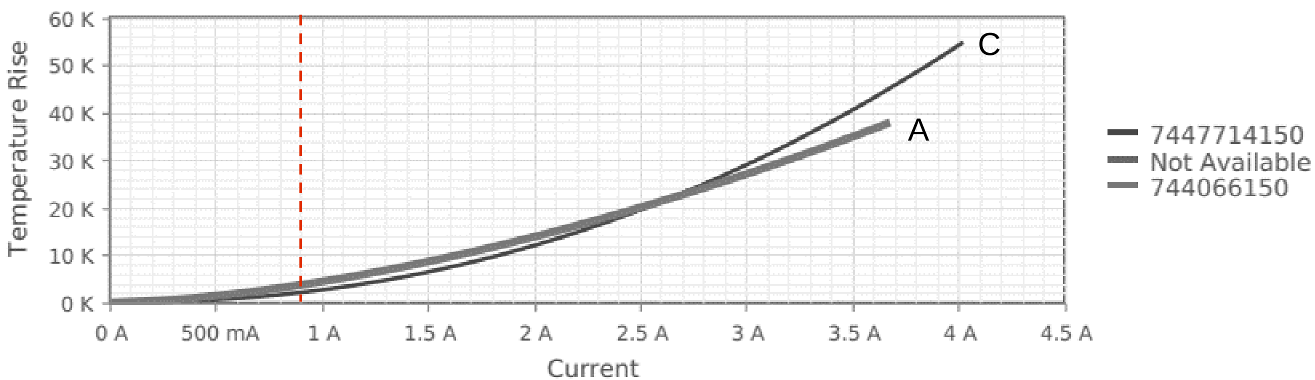

smallest parts with 57.0 mΩ ≤ R_f < 114 mΩ

Part Code	L [µH]	R [mΩ]	Isat [A]	Vol. [mm³]
744062220	**22**	**100.0**	**0.95**	**113**
744071220	22	65.0	1.9	296
744071330	33	95.0	1.5	296

smallest parts with 38.5 mΩ ≤ R_f < 57.0 mΩ

Part Code	L [µH]	R [mΩ]	Isat [A]	Vol. [mm³]
7447773150	15	53.0	3.1	252
78439346150	15	42.0	7.4	264
74439346150	15	42.0	7.4	264

smallest parts with 11.4 mΩ ≤ R_f < 38.5 mΩ

Part Code	L [µH]	R [mΩ]	Isat [A]	Vol. [mm³]
A – 744066150	**15**	**37.0**	**3.25**	**403 (3.57x)**
B - 784325160	16.7	34.5	7.8	503
C - 7447714150	15	36.0	4.1	541

smallest parts with R_f < 11.4 mΩ

Part Code	L [µH]	R [mΩ]	Isat [A]	Vol. [mm³]
78439370150	15	10.5	26.1	2622
74435571500	15	9.0	14	3212
7443782012150	15	4.6	12.9	5049

[https://www.we-online.com/catalog/en]

Input filter: design with non-saturating filter inductor (3)

power inductors with 15 µH ≤ L ≤ 33 µH and R_f ≤ 114 mΩ

$P_f \leq 2\% P_{loss}$

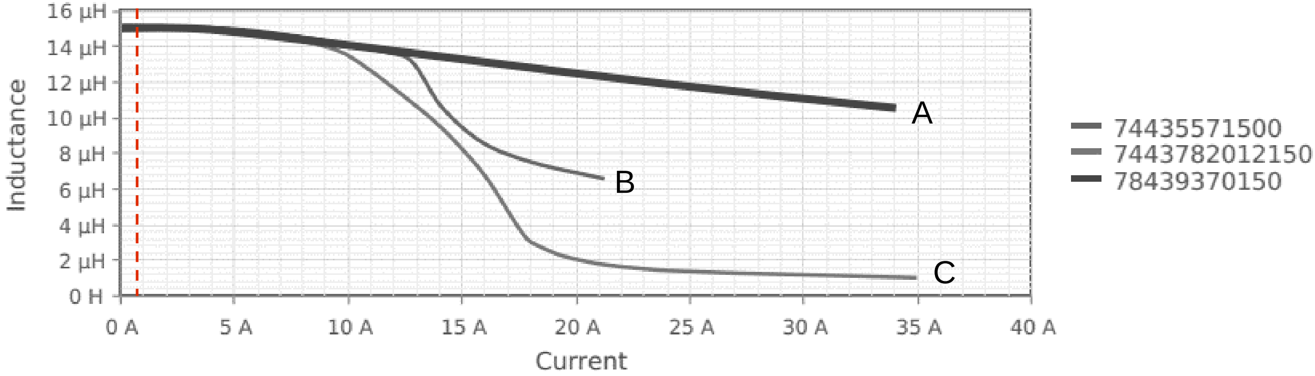

$$l_f \cong 1 \rightarrow \alpha = 11 \rightarrow L_d = 165\mu H, R_{d,opt} = 6.53\Omega$$

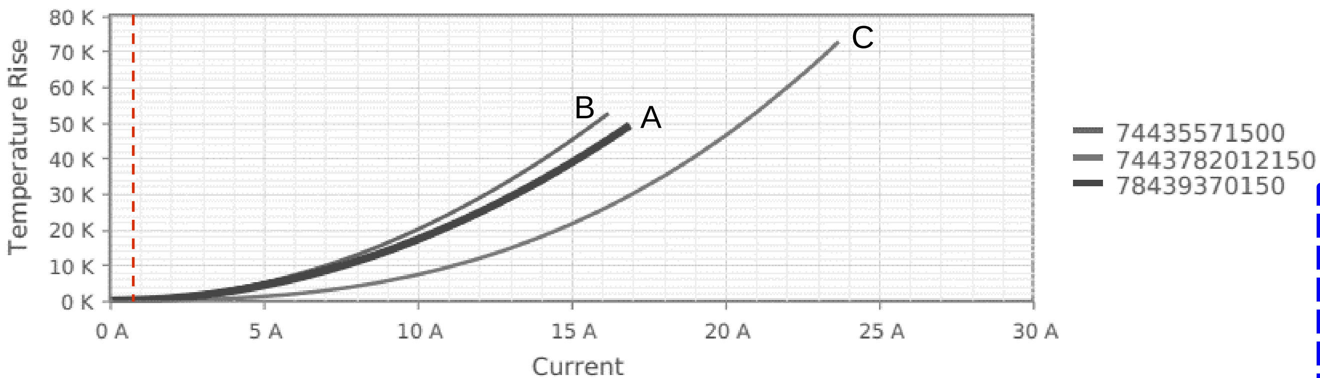

smallest parts with 57.0 mΩ ≤ R_f < 114 mΩ

Part Code	L [µH]	R [mΩ]	Isat [A]	Vol. [mm³]
744062220	**22**	**100.0**	**0.95**	**113**
744071220	22	65.0	1.9	296
744071330	33	95.0	1.5	296

smallest parts with 38.5 mΩ ≤ R_f < 57.0 mΩ

Part Code	L [µH]	R [mΩ]	Isat [A]	Vol. [mm³]
7447773150	15	53.0	3.1	252
78439346150	15	42.0	7.4	264
74439346150	15	42.0	7.4	264

smallest parts with 11.4 mΩ ≤ R_f < 38.5 mΩ

Part Code	L [µH]	R [mΩ]	Isat [A]	Vol. [mm³]
744066150	15	37.0	3.25	403
784325160	16.7	34.5	7.8	503
7447714150	15	36.0	4.1	541

smallest parts with R_f < 11.4 mΩ

Part Code	L[µH]	R[mΩ]	Isat[A]	Vol. [mm³]
A – 78439370150	**15**	**10.5**	**26.1**	**2622 (23.2x)**
B – 74435571500	15	9.0	14	3212
C - 7443782012150	15	4.6	12.9	5049

[https://www.we-online.com/catalog/en]

Input filter: TI-PMLK BUCK WE test board

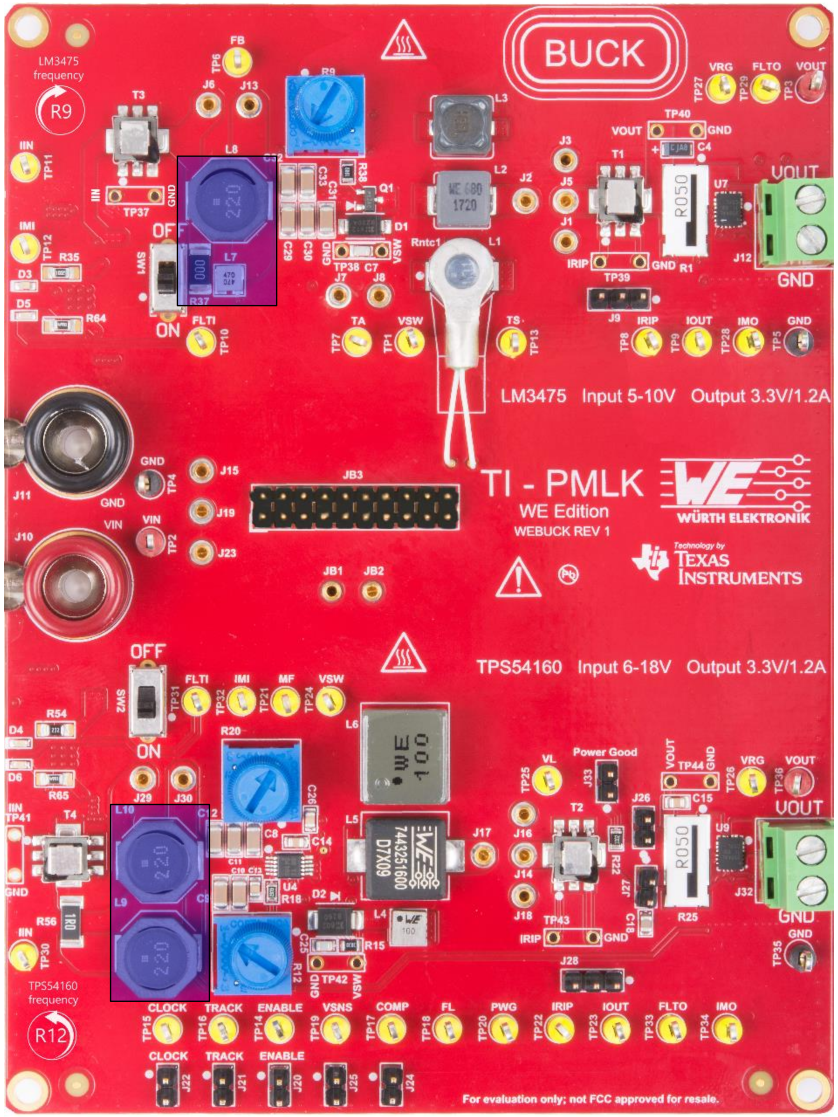

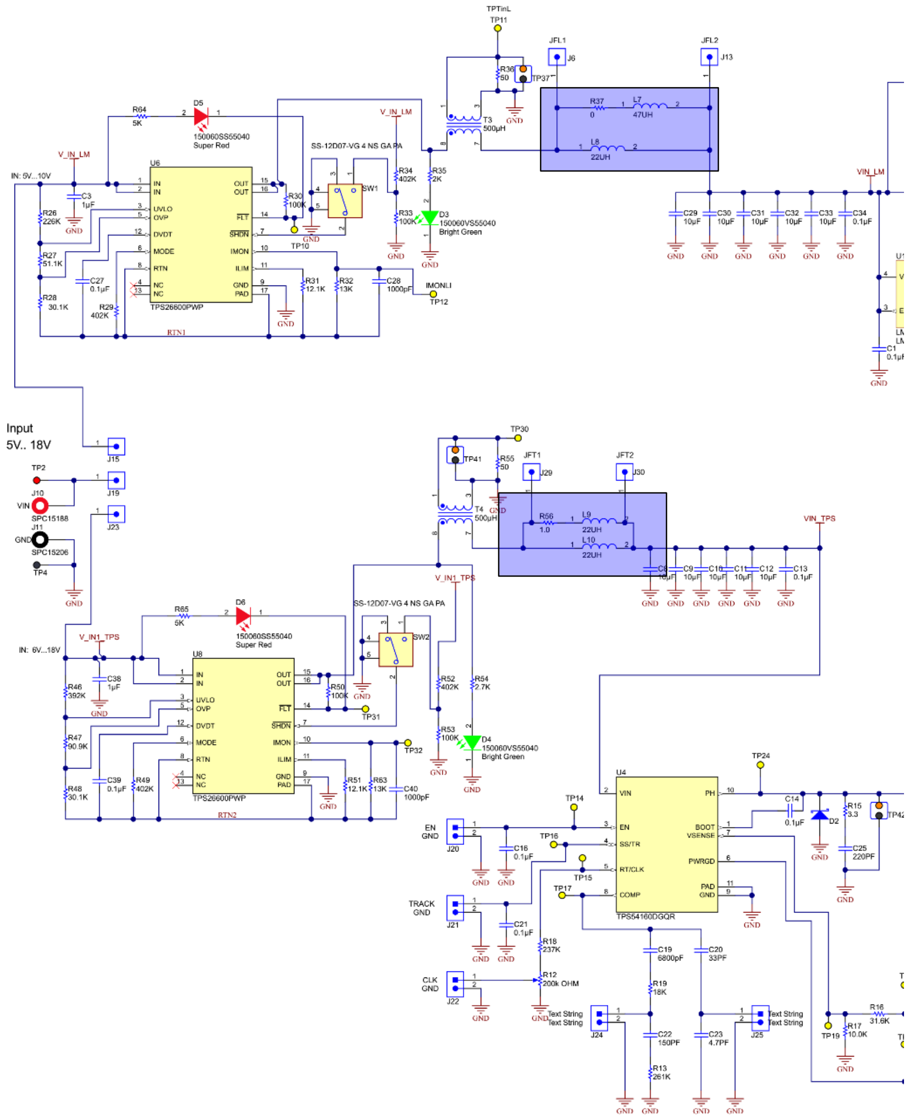

Input filter: experimental test with saturating inductor

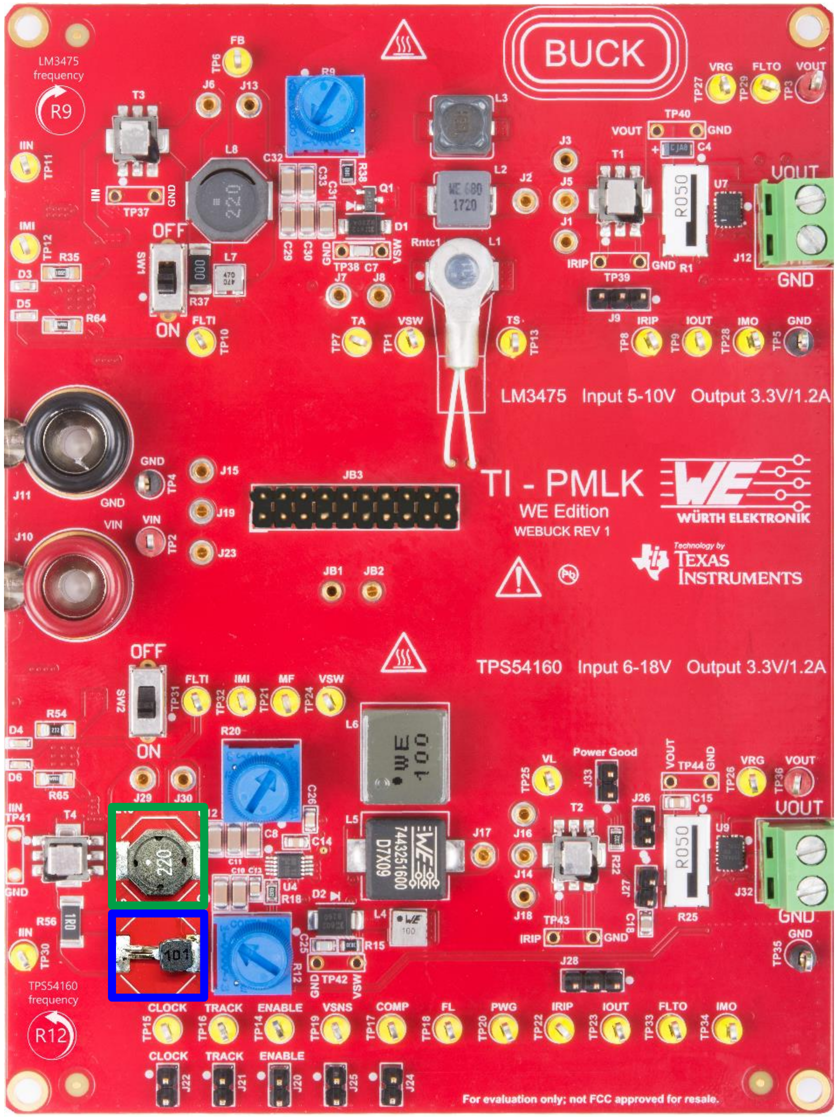

Part Code	L [µH]	R [mΩ]	Isat [A]	Vol. [mm³]
744062220	**22**	**100.0**	**0.95**	**113**

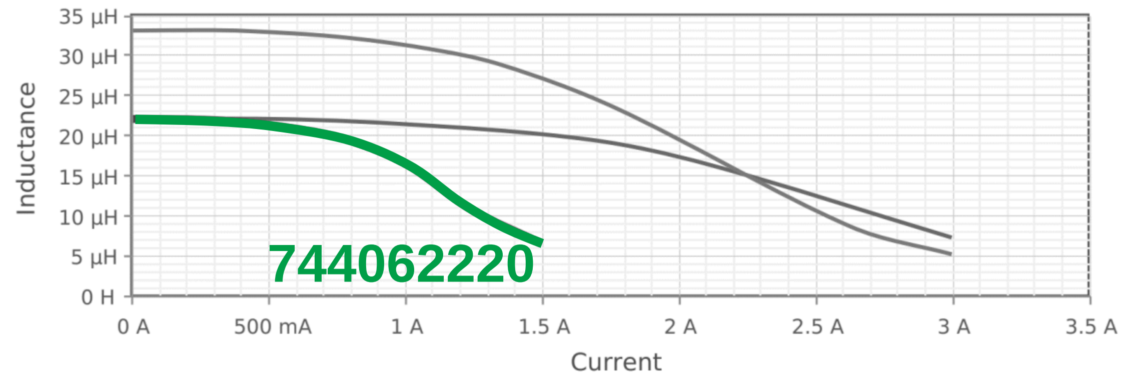

Part Code	L [µH]	R [mΩ]	Isat [A]	Vol. [mm³]
744032101	**100**	**4.25**	**0.25**	**16**

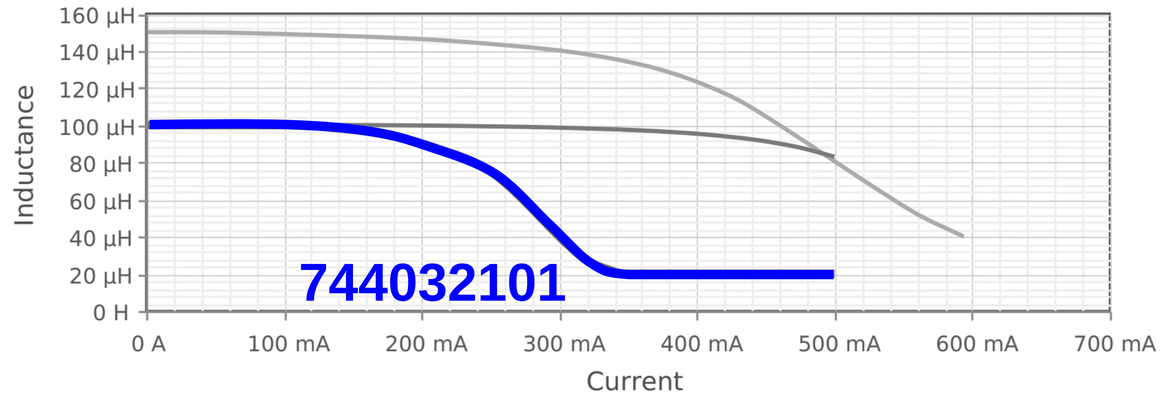

Input filter: test setup

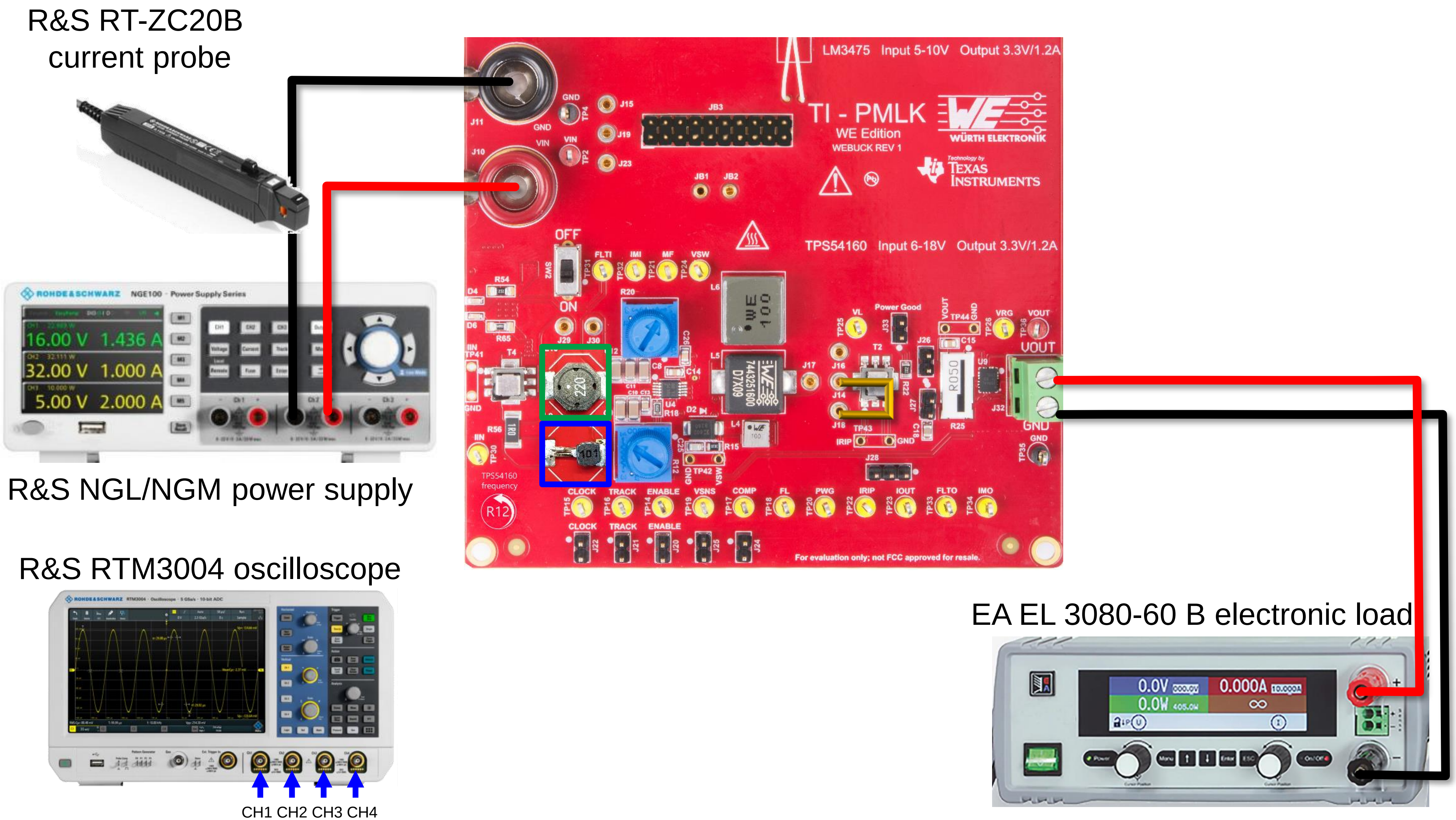

Input filter: experimental input current spectrum

V_{in}=5V, V_{out}= 3.3 V , I_{out}=1.2 A, f_s= 400 kHz

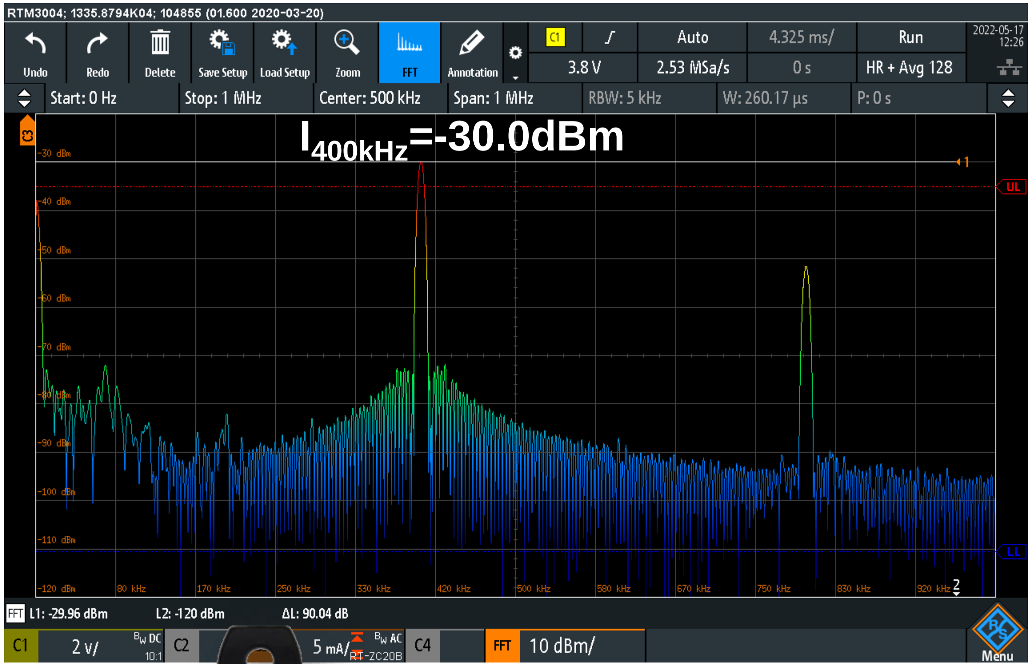

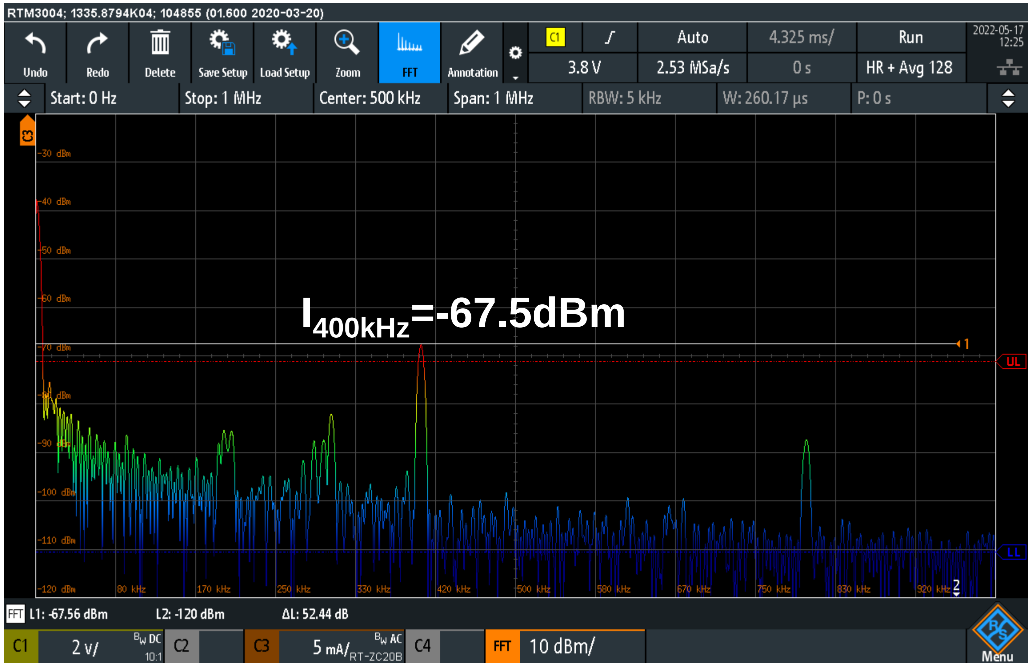

inductors shorted

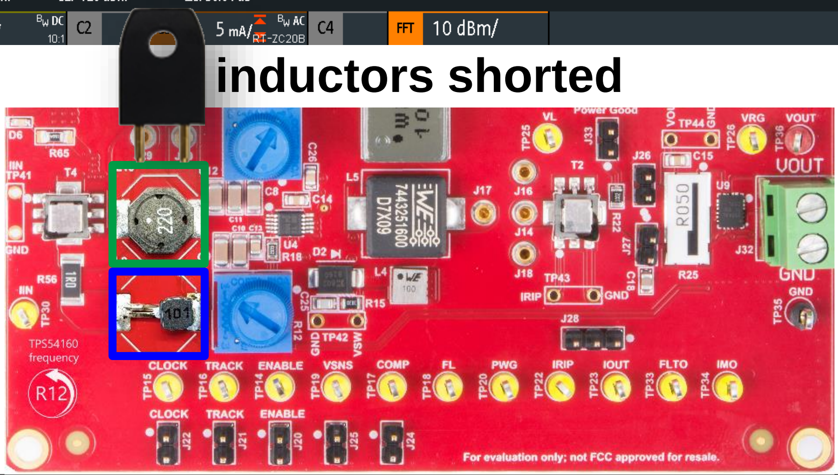

inductors unshorted

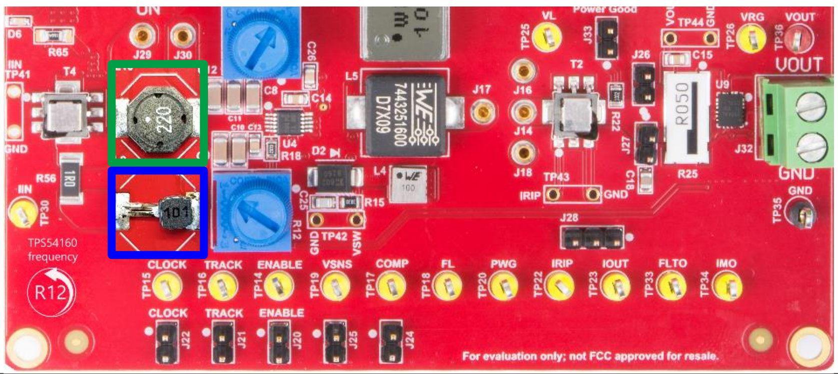

Power-to-Control PCB cross-talk

Crosstalk: SW-to-COMP PCB capacitive coupling

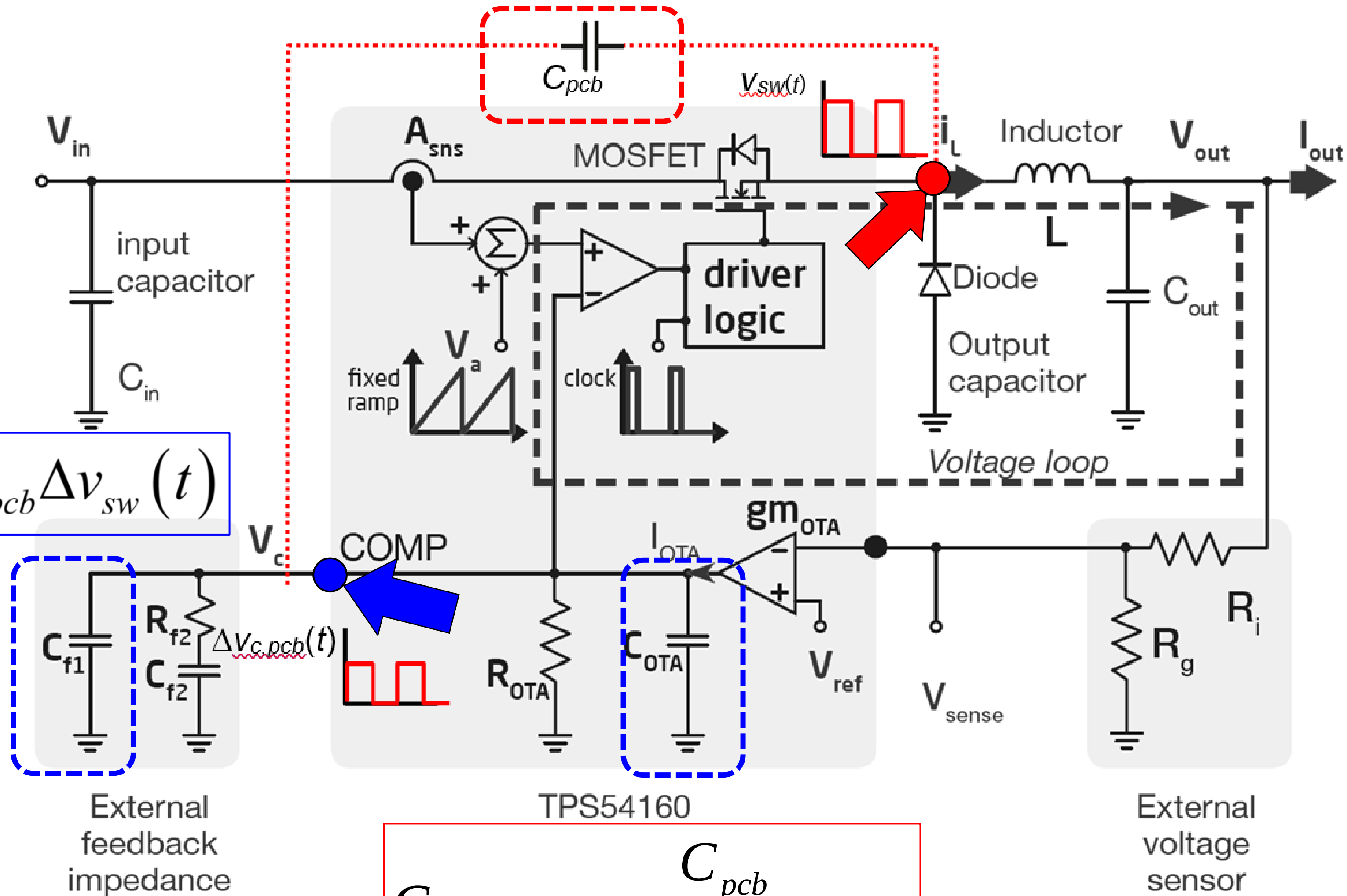

$$\Delta v_{c,pcb}(t) \cong G_{pcb} \Delta v_{sw}(t)$$

$$G_{pcb} = \frac{C_{pcb}}{C_{pcb} + C_{f1} + C_{ota}}$$

Crosstalk: TI-PMLK BUCK experimental example

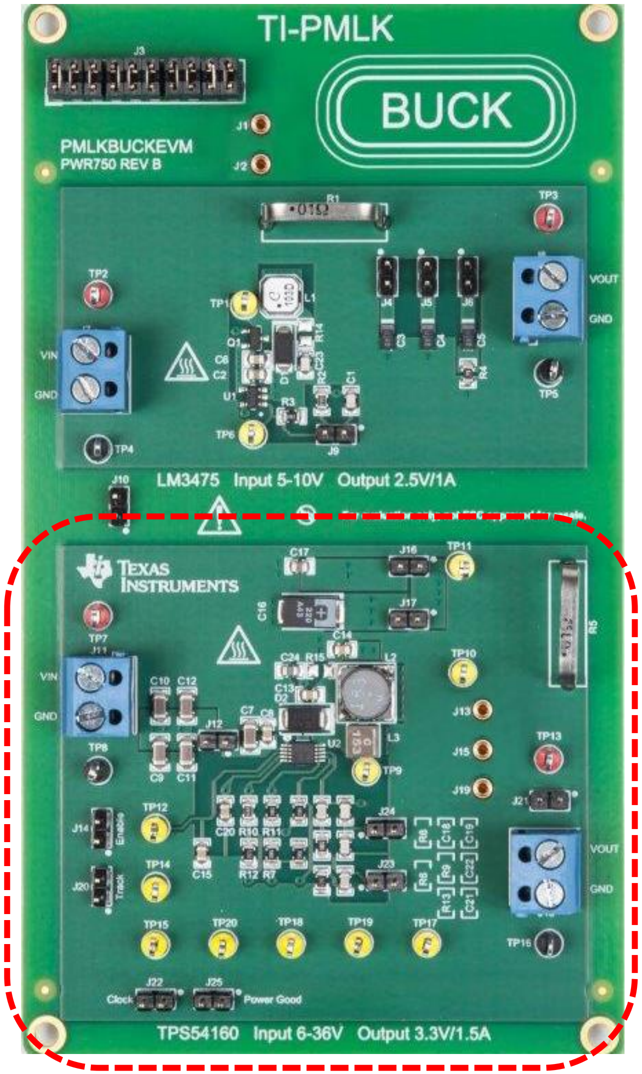

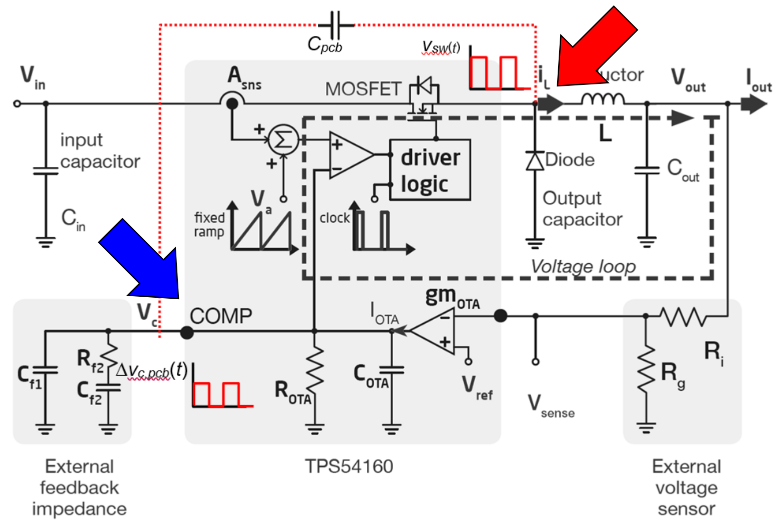

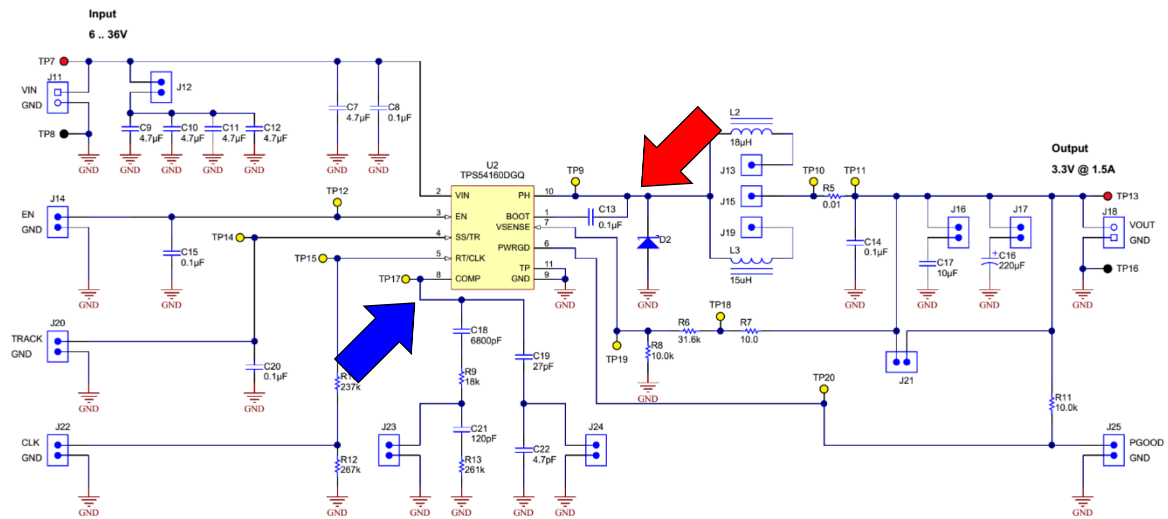

Crosstalk: TI-PMLK BUCK : SW-to-COMP PCB coupling

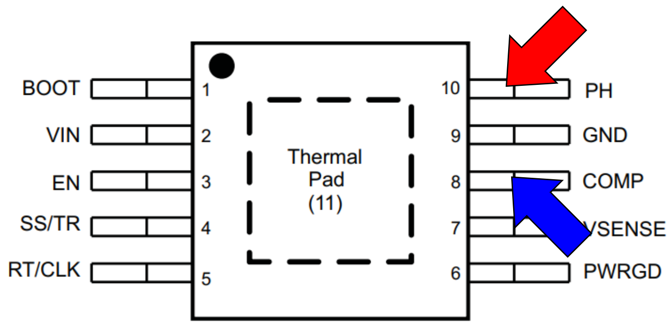

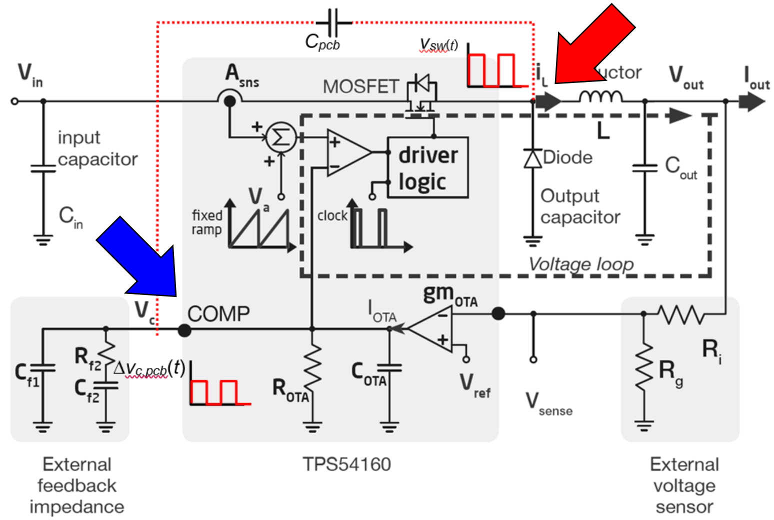

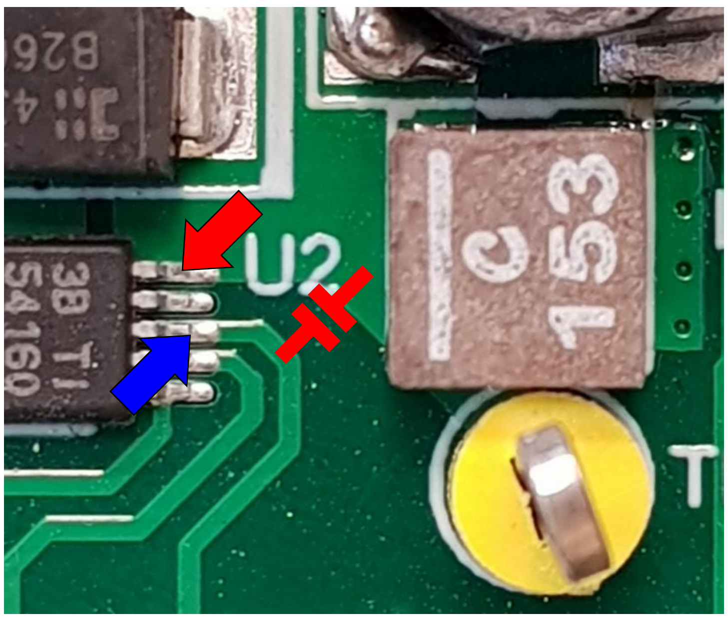

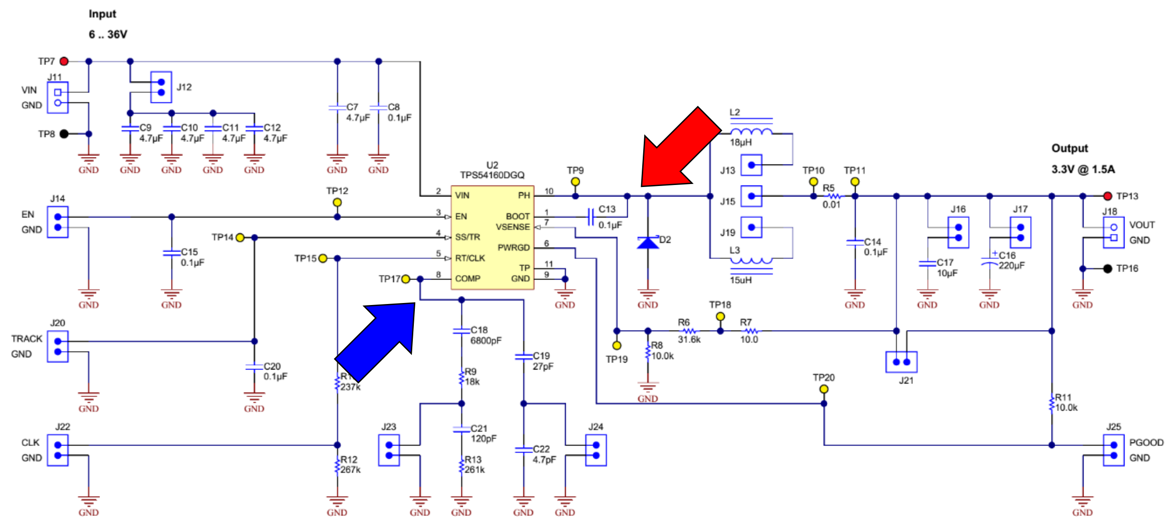

Crosstalk: test setup

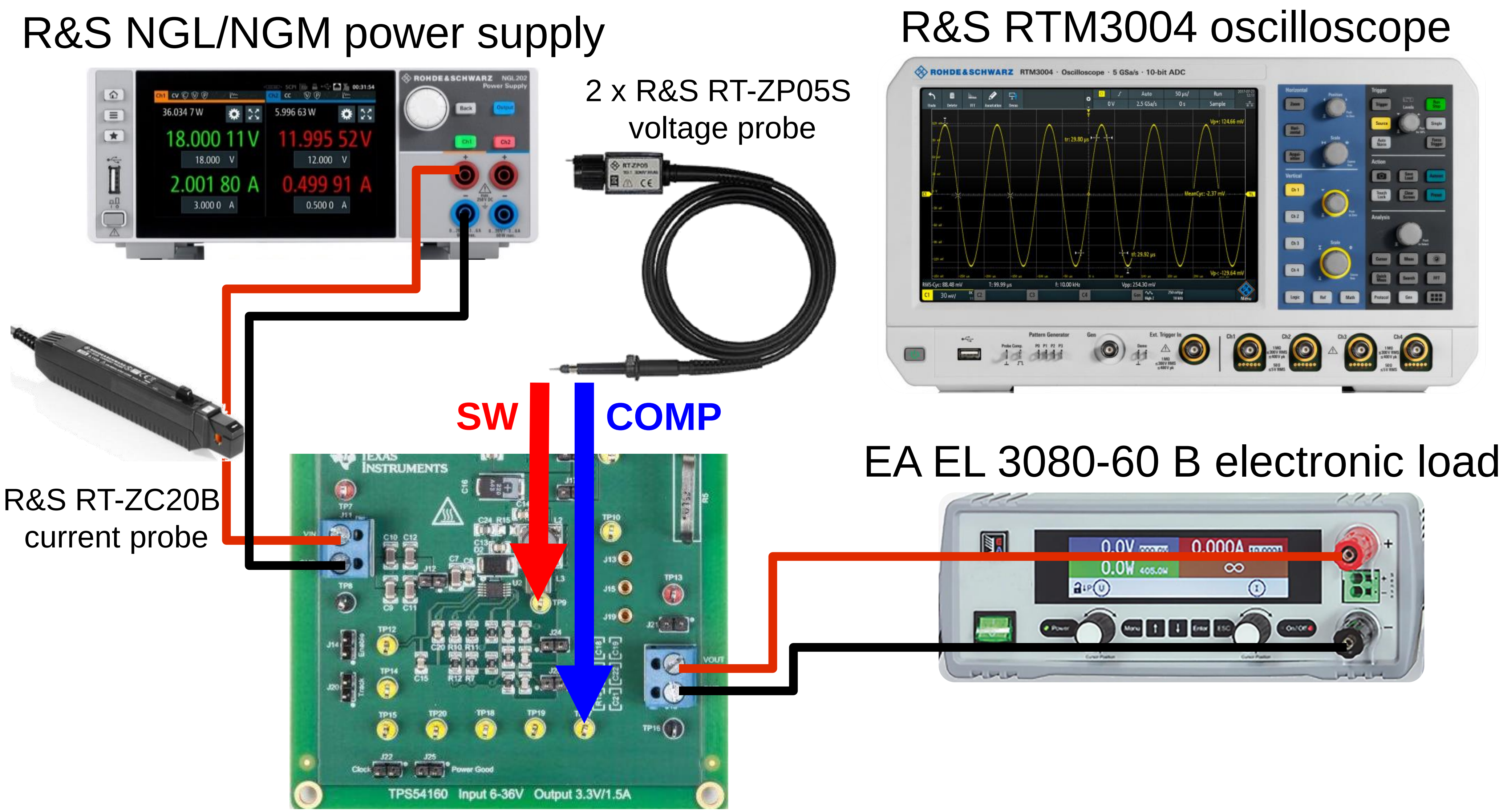

Crosstalk: voltage probe capacitance

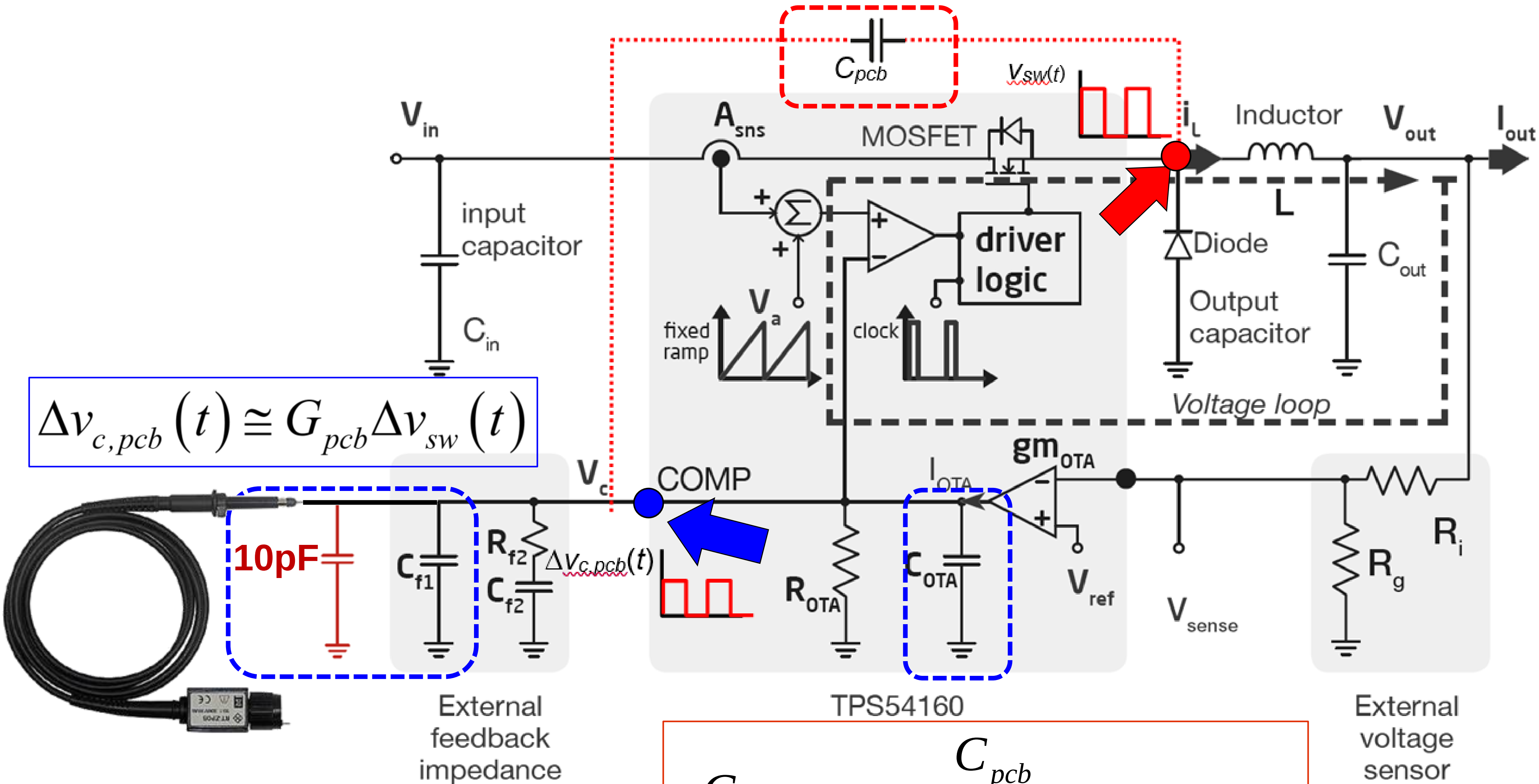

$$\Delta v_{c,pcb}(t) \cong G_{pcb} \Delta v_{sw}(t)$$

$$G_{pcb} = \frac{C_{pcb}}{C_{pcb} + C_{f1} + C_{ota} + 10\text{pF}}$$

Crosstalk: SW-to-COMP gain with narrow BW control

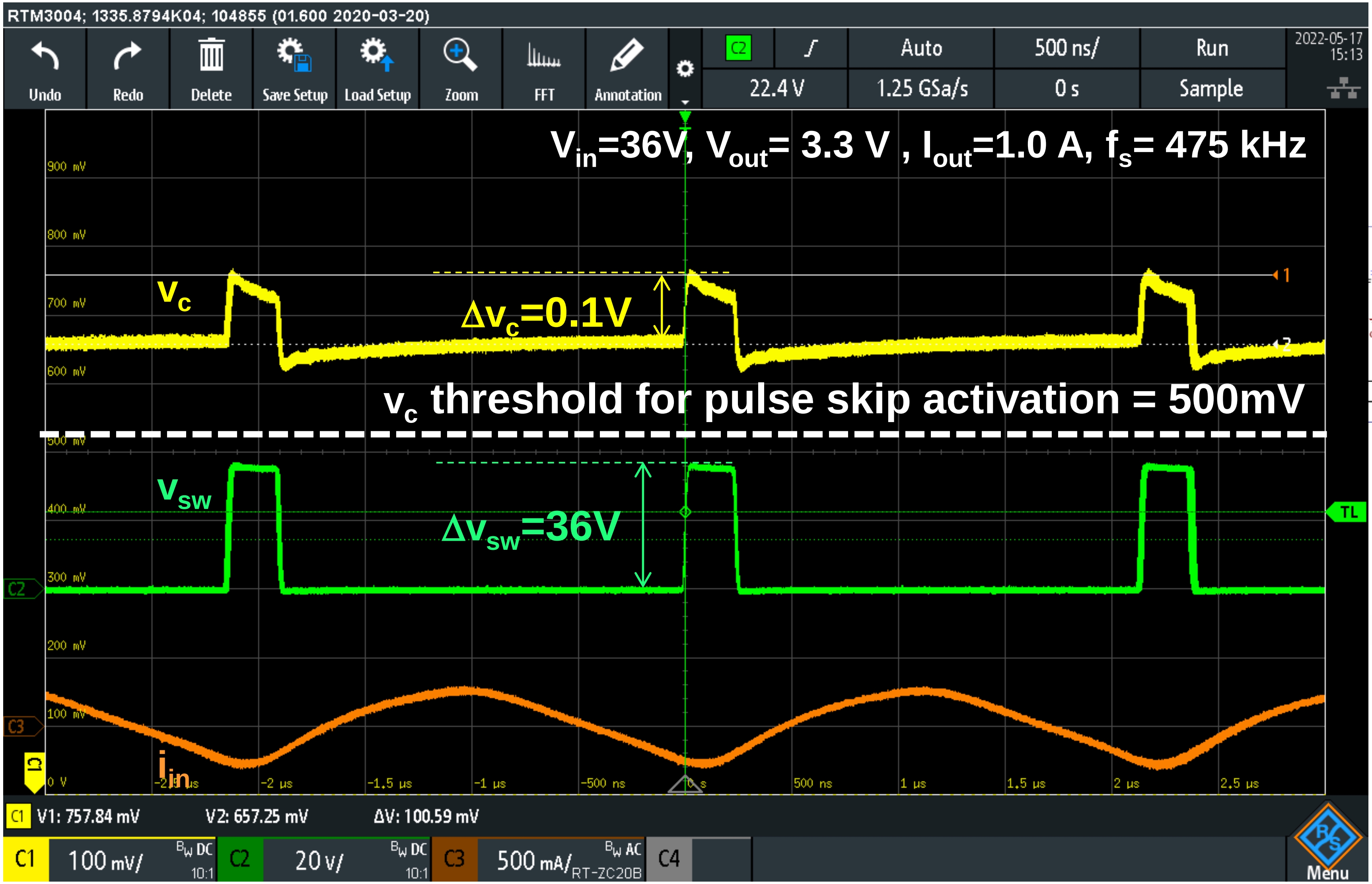

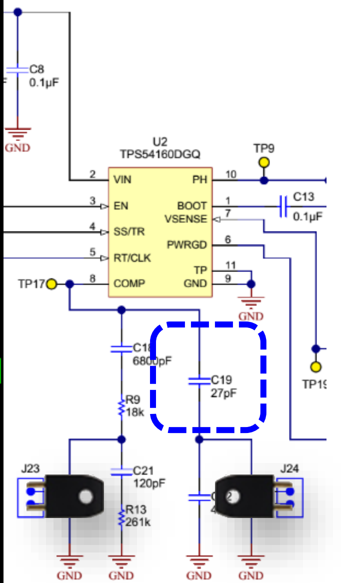

C_{f1} = 27pF

Crosstalk: SW-to-COMP gain with large BW control

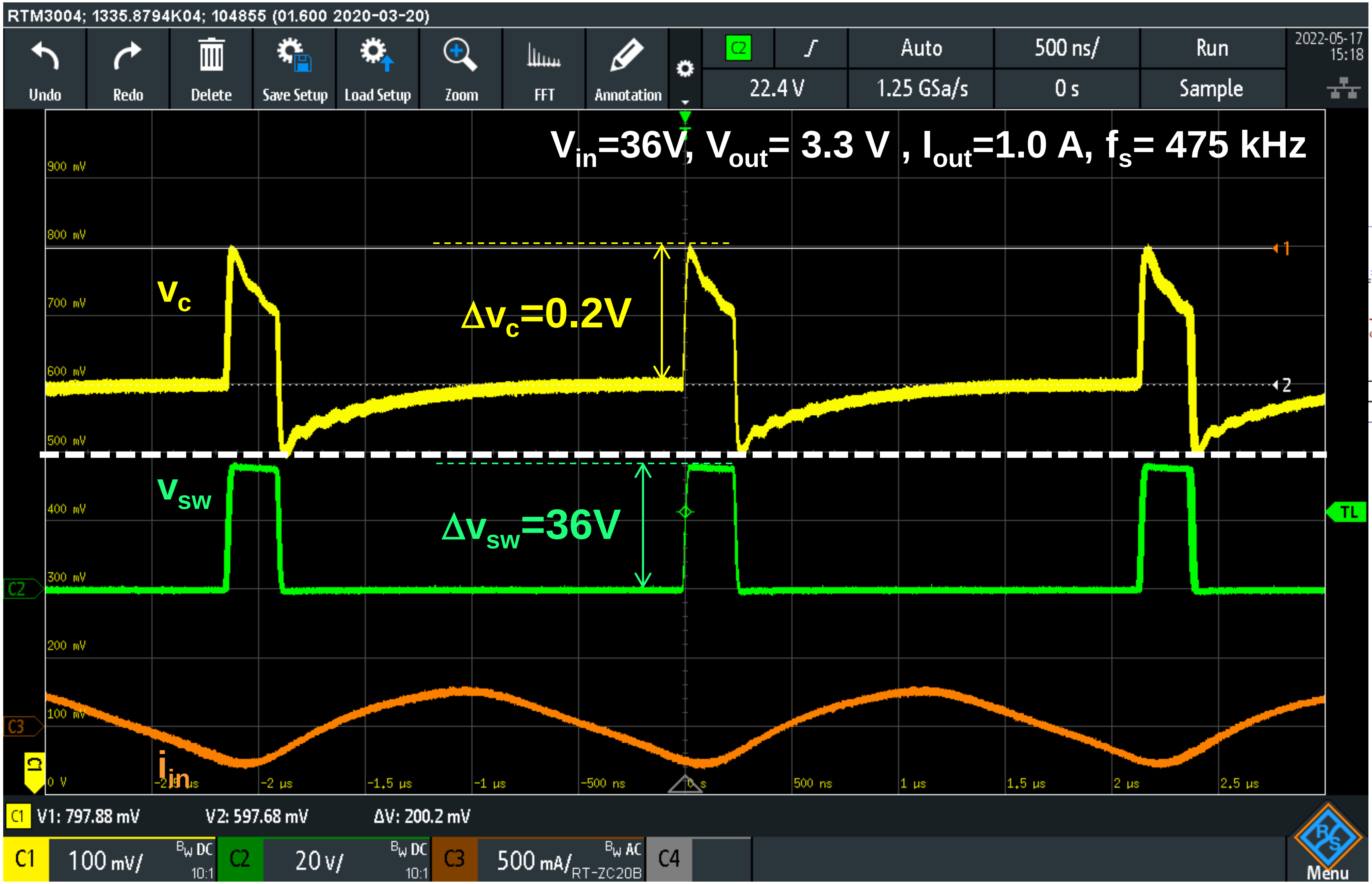

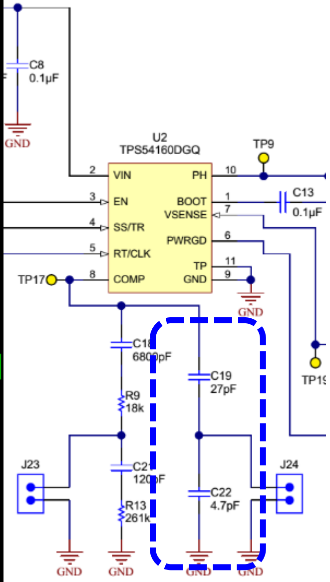

C_{f1} = 4pF

Crosstalk: input current spectrum with voltage probe

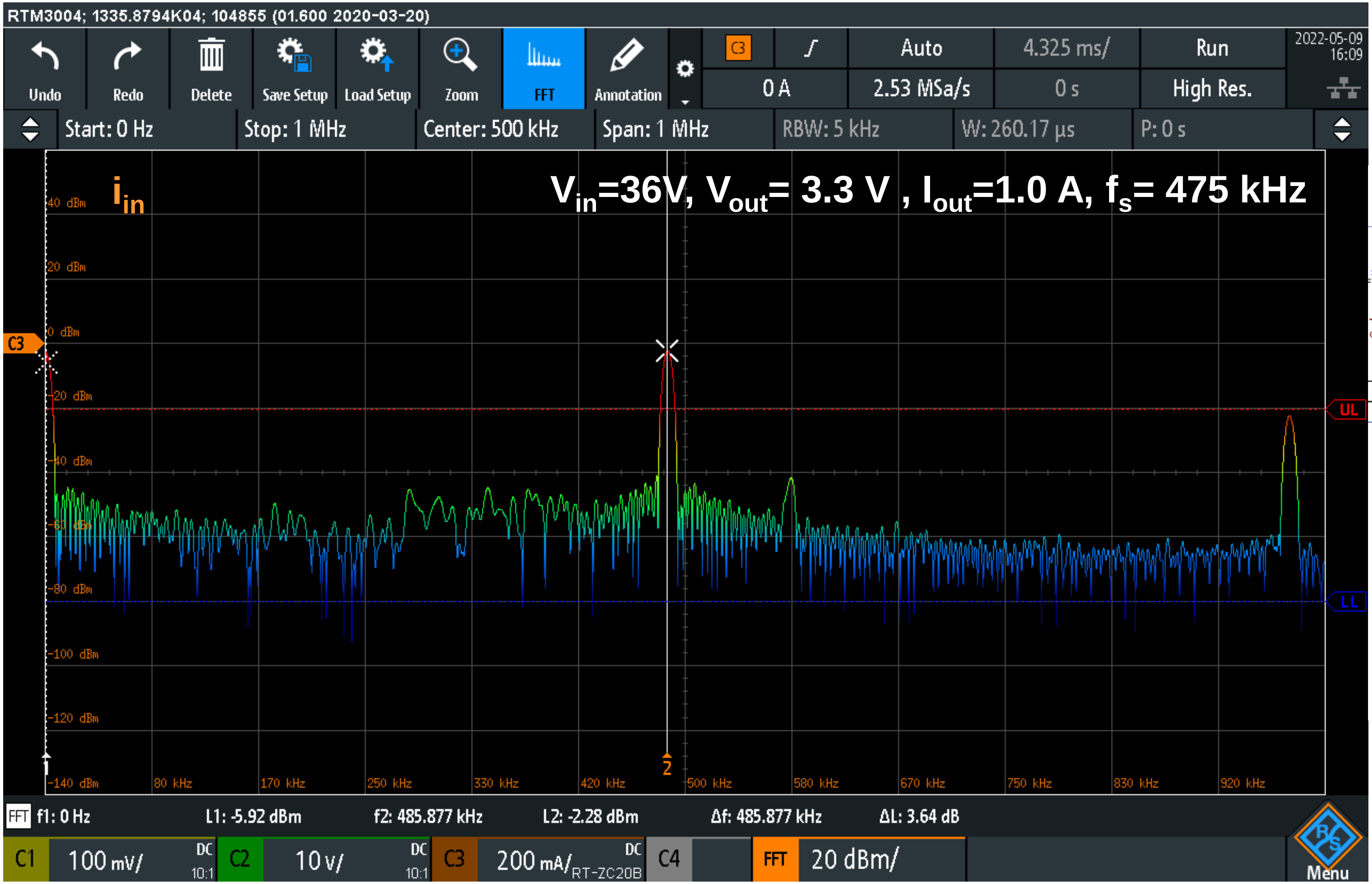

probe on COMP pin (v_c) ⇒ +10pF

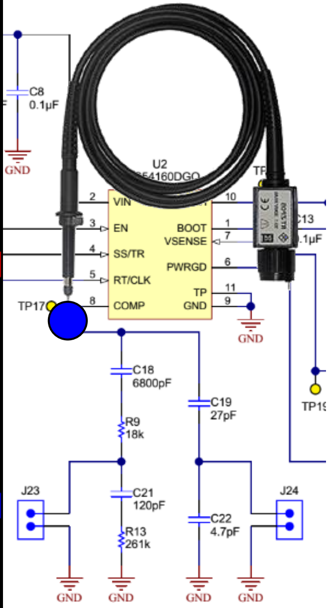

Crosstalk: input current spectrum without voltage probe

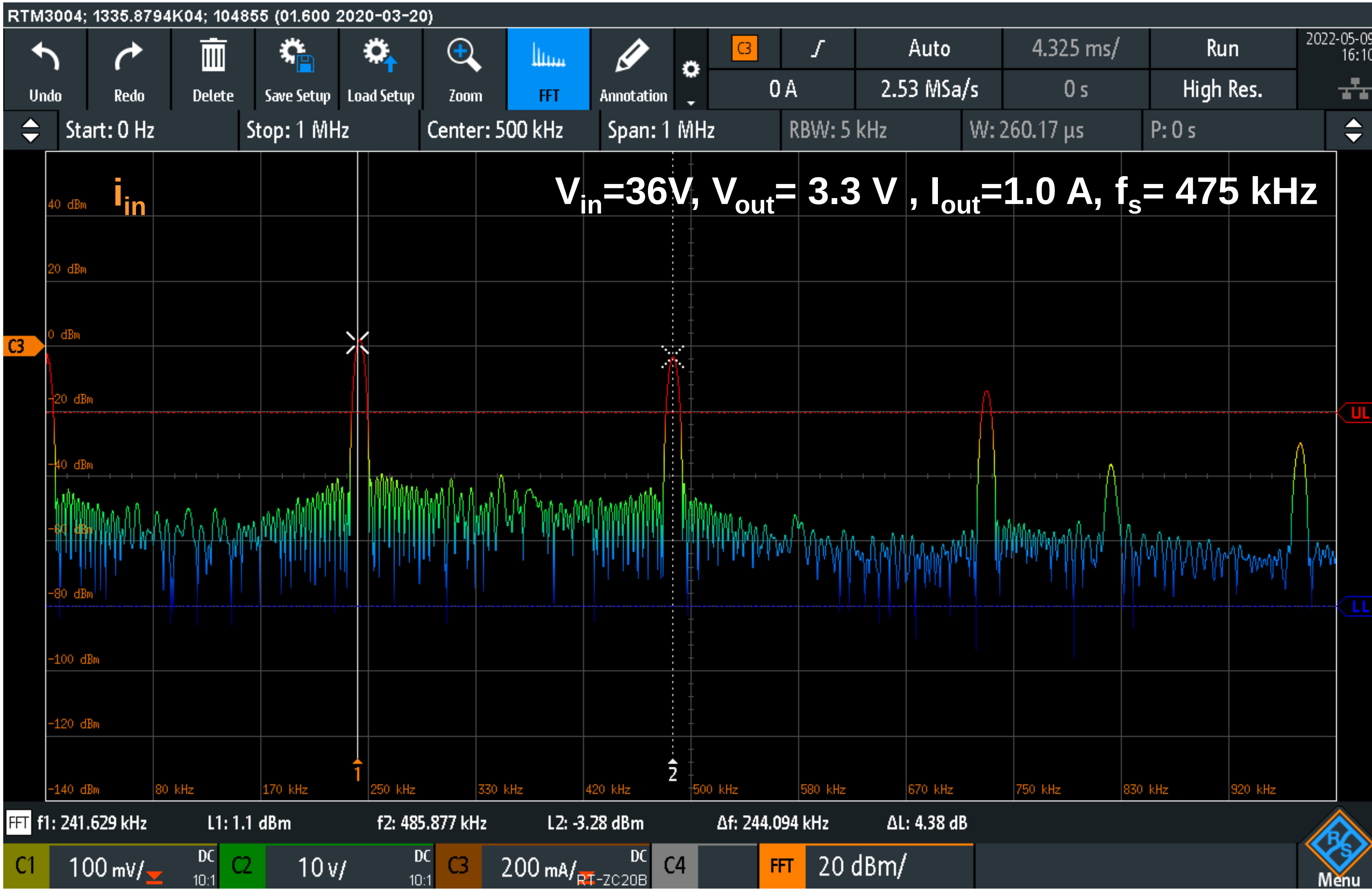

no probe on COMP pin (v_c)

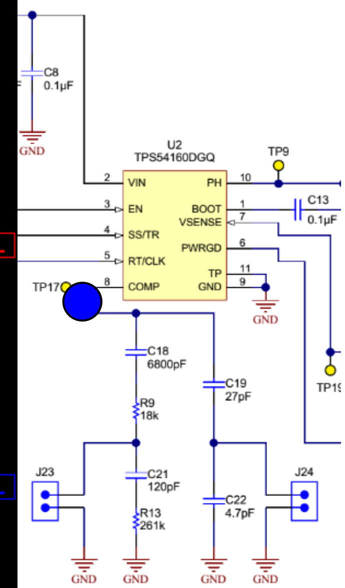

Crosstalk: pulse-skip effects

I_{out}=0.33 A

I_{out}=0.28 A

I_{out}=0.20 A

I_{out}=0.18 A

Crosstalk: impact of de-saturating inductor

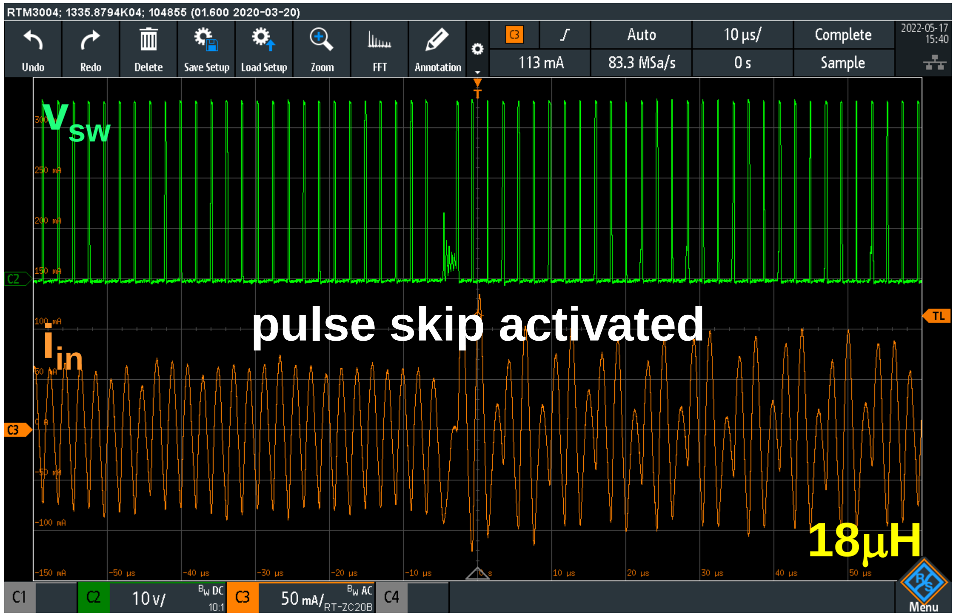

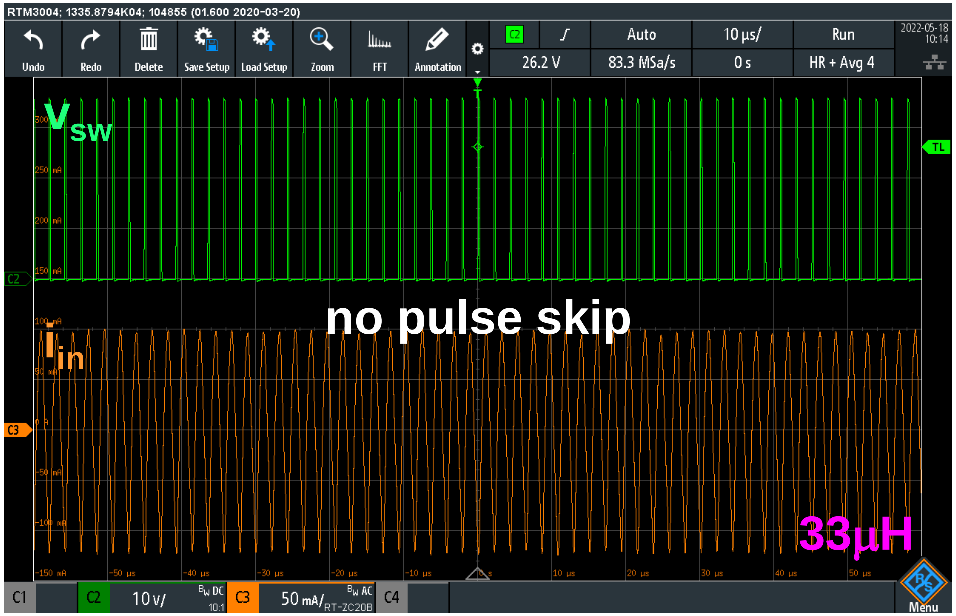

V_{in}=36V
V_{out}= 3.3 V
I_{out}=0.27 A
f_s= 475 kHz

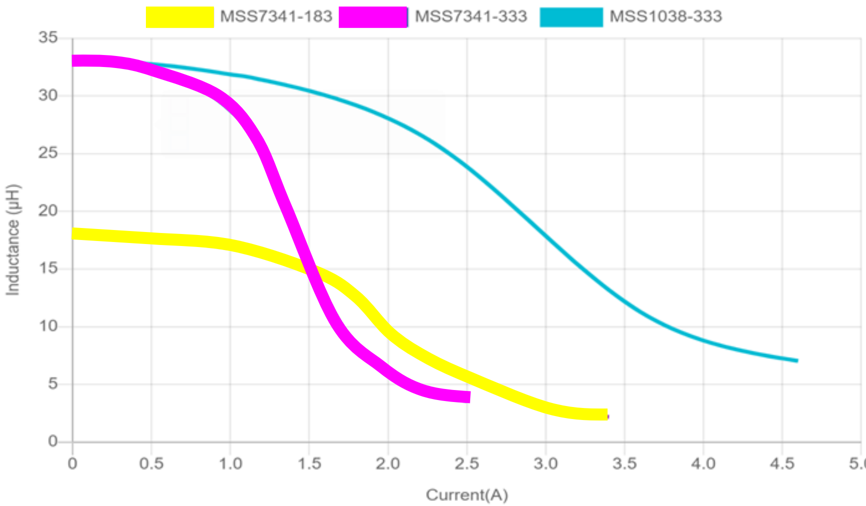

Crosstalk: impact of DCM

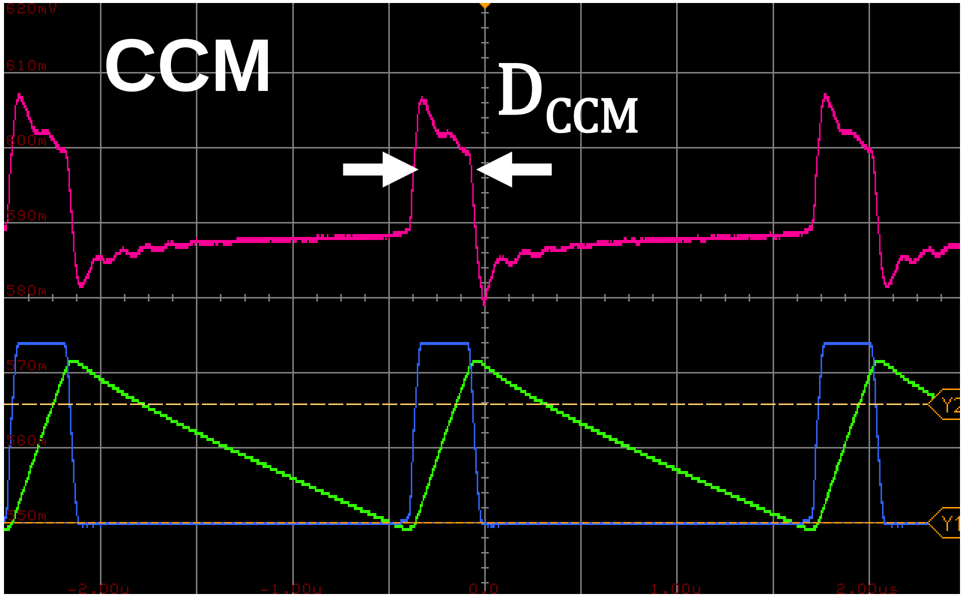

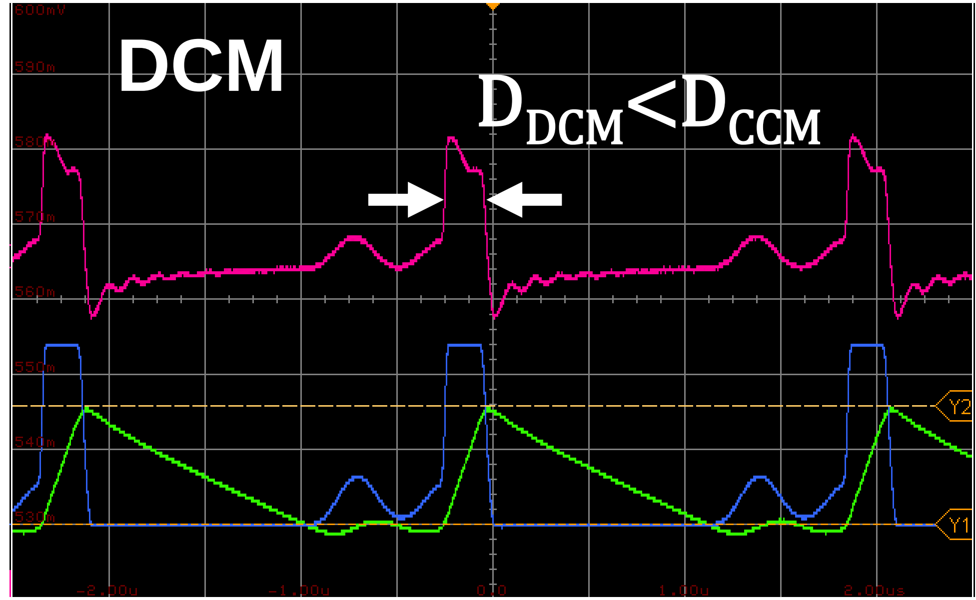

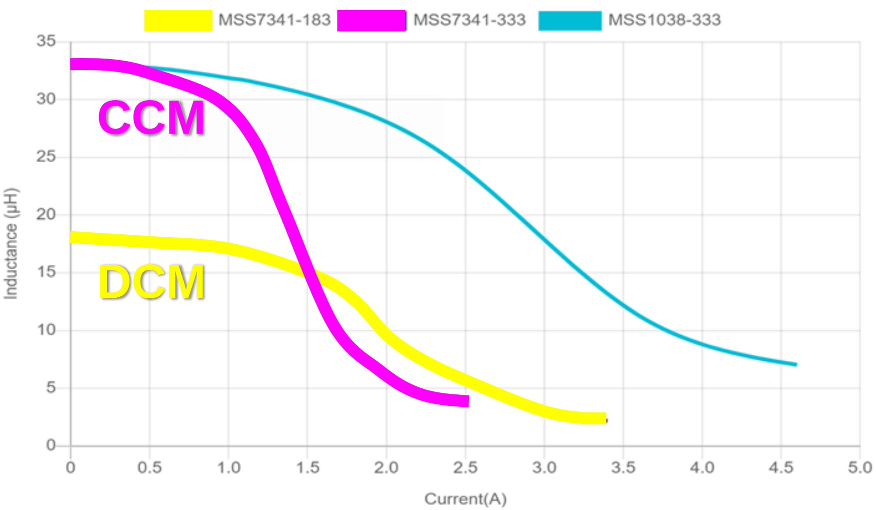

$$v_c = A_s I_o + D\left[V_{ramp} + \frac{A_s(V_i - V_o)}{2Lf_s}\right]$$

$$D_{CCM} = \frac{V_o}{V_i} \qquad D_{DCM} = \frac{V_o}{V_i}\sqrt{\frac{2LI_of_sV_i}{V_o(1-V_o)}}$$

literature

INTERNATIONAL JOURNALS

1. K. Stoyka, N. Femia, G. Di Capua, **Power Inductors Behavioral Modeling Revisited**, IEEE Trans. on Circuits and Systems I: Regular Papers, vol. 0, no. 99, pp. 1-14, 2020 (10.1109/TCSI.2020.3002615).
2. **N. Femia, K. Stoyka, G. Di Capua, Impact of Inductors Saturation on Peak-Current Mode Control Operation, IEEE Trans. on Power Electronics, vol. 0, no. 99, pp. 1-13, 2020 (10.1109/TPEL.2020.2974939).**
3. A. Oliveri, G. Di Capua, K. Stoyka, M. Lodi, M. Storace, N. Femia, **A Power-Loss-Dependent Inductance Model for Ferrite-Core Power Inductors in Switch-Mode Power Supplies**, IEEE Trans. on Circuits and Systems I: Regular Papers, vol. 66, no. 6, pp. 2394-2402, June 2019.
4. **K. Stoyka, G. Di Capua, N. Femia, A Novel AC Power Loss Model for Ferrite Power Inductors, IEEE Trans. on Power Electronics, vol. 34, no. 3, pp. 2680-2692, March 2019.**
5. **G. Di Capua, N. Femia, K. Stoyka, Switching Power Supplies with Ferrite Inductors in Sustainable Saturation Operation, Intern. Journal of Electrical Power and Energy Systems, pp. 494-505, vol. 93, December 2017.**
6. G. Di Capua, N. Femia, K. Stoyka, **A generalized numerical method for ferrite inductors analysis in high current ripple operation**, Integration, the VLSI Journal, vol. 58, pp. 473-484, June 2017.
7. **G. Di Capua, N. Femia, A Novel Method to Predict the Real Operation of Ferrite Inductors with Moderate Saturation in Switching Power Supplies Applications, IEEE Trans. on Power Electronics, vol. 31, no. 3, pp. 2456-2464, March 2016.**

literature

INTERNATIONAL CONFERENCES

1. **G. Di Capua, L. Egiziano, N. Femia, A. Mayhugh, C. Latham, Exploiting the Benefits of Partially Saturating Inductors on Switch-Mode Power Supplies Electro-Magnetic Compatibility and Efficiency, IEEE APEC2022, Houston, TA**
2. K. Stoyka, G. Di Capua and N. Femia, **Coupled Inductors Analysis with Saturation and Thermal Effects**, 2020 27th IEEE International Conference on Electronics, Circuits and Systems (ICECS), Glasgow, UK, 2020, pp. 1-4.
3. **N. Femia, G. Di Capua and K. Stoyka, Saturation and Thermal Stability of Power Inductors, 2020 27th IEEE International Conference on Electronics, Circuits and Systems (ICECS), Glasgow, UK, 2020, pp. 1-4.**
4. K. Stoyka, G. Di Capua, N. Femia, **Normalized inductance modeling for ferrite power inductor families**, 2019 26th IEEE Int. Conference on Electronics, Circuits and Systems (ICECS 2019), Genoa, Italy, 27-29 Nov. 2019.
5. **G. Di Capua, N. Femia K. Stoyka, Impact of Inductors Saturation on DC-DC Switching Regulators, 2019 IEEE 5th Int. forum on Research and Technology for Society and Industry (RTSI 2019), Florence, Italy, 9-12 Sept. 2019.**
6. N. Femia, G. Di Capua, **On Buck-Boost Converter Power Inductor Matching**, 2019 IEEE International Symposium on Circuits and Systems (ISCAS 2019), Sapporo, Japan, 26-29 May 2019.
7. K. Stoyka, G. Di Capua, N. Femia, **Modeling of Stepped Air-Gap Ferrite Inductors in Switching Power Supplies**, IEEE Int. Conf. on Electronics Circuits and Systems (ICECS 2018), Bordeaux, France, 9-12 Dec. 2018.
8. **N. Femia, G. Di Capua, Hysteretic Regulators with Partially-Saturated Inductors, IEEE Int. Conf. on Electronics Circuits and Systems (ICECS 2018), Bordeaux, France, 9-12 Dec. 2018.**
9. G. Di Capua, N. Femia, K. Stoyka, **Loss Behavioral Modeling for Ferrite Inductors**, Int. Conf. on Synthesis, Modeling, Analysis and Simulation Methods and Applications to Circuit Design (SMACD 2018), Prague, Czech Republic, 2-5 July 2018.
10. K. Stoyka, N Femia, G Di Capua, **Optimizing power converters with partially saturated inductors by evolutionary algorithms**, 14th Int. Conf. on Synthesis, Modeling, Analysis and Simulation Methods and Applications to Circuit Design (SMACD 2017), Giardini Naxos, Italy, 12-15 June 2017.

INTERNATIONAL CONFERENCES

11. G Di Capua, N Femia, K. Stoyka, M. Lodi, A. Oliveri, M. Storace, **Ferrite inductor models for switch-mode power supplies analysis and design**, 14th Intern. Conf. on Synthesis, Modeling, Analysis and Simulation Methods and Applications to Circuit Design (SMACD 2017), Giardini Naxos-Taormina, Italy, 12-15 June 2017.
12. **G Di Capua, N Femia, K Stoyka, Validation of inductors sustainable-saturation-operation in switching power supplies design, 2017 IEEE Intern. Conf. on Industrial Technology (ICIT 2017), pp. 242-247, Toronto, Canada, 22-25 March 2017.**
13. G. Di Capua, N. Femia, M. Migliaro, K. Stoyka, **Genetic Programming Approach for Identification of Ferrite Inductors Power Loss Models**, 42nd Annual Conf. of IEEE Industrial Electronics Society (IECON 2016), Florence, Italy, 24-27 October 2016.
14. G. Di Capua, N. Femia, K. Stoyka, **Power Magnetics Volume and Weight Reduction in Aerospace Power Supply Units**, 2016 IEEE 17th Workshop on Control and Modeling for Power Electronics (COMPEL 2016), Trondheim, Norway, 27-30 June 2016.
15. G. Di Capua, N. Femia, K. Stoyka, **An Improved Algorithm for the Analysis of Partially Saturated Ferrite Inductors in Switching Power Supplies**, Intern. Conf. on Synthesis, Modeling, Analysis and Simulation Methods and Applications to Circuit Design (SMACD 2016), Lisbon, Portugal, 27-30 June 2016.
16. G. Di Capua, N. Femia, K. Stoyka, **Differential Evolution Algorithm-based Identification of Ferrite Core Inductors Saturation Curves**, 2015 IEEE Intern. Conf. on Industrial Informatics (INDIN 2015), pp. 1636-1641, Cambridge, UK, 22-24 July 2015.
17. K. Stoyka, G. Di Capua, A. Della Cioppa, N. Femia, G. Spagnuolo, **Identification of Ferrite Core Inductors Parameters by Evolutionary Algorithms**, 2015 IEEE Intern. Conf. on Industrial Informatics (INDIN 2015), pp. 1648-1653, Cambridge, UK, 22-24 July 2015.
18. G. Di Capua, N. Femia, **Switching Power Supplies operating with partially Saturated Inductors**, 2015 IEEE Intern. Conf. on Industrial Technology (ICIT 2015), pp. 1205-1210, Seville, Spain, 17-19 March 2015.

concluding remarks

- inductors saturation does not yield negative effects on EMI, provided that the inductors are selected based on good practice fundamentals of power-design
- an intelligent power loss distribution in combination with saturating inductors enables reducing SMPS EMI filters size
- (de)saturating inductors help mitigating the noise generated by the combination of control chip special features, large BW feedback compensation and PCB crosstalk

next events and new tools

- Power Design Hands-on Courses
  - high power density SMPS design based on semiconductor-to-passive devices optimal tuning
  - high dynamic performance SMPS design based on power-to-control optimal tayloring
  - EMC compliant SMPS design based on power-control-PCB optimal trading
- Low-Cost Inductors Testing Equipment
- Power Design Software